Title	Tin whisker growth mechanism and mitigation for lead-free electronics
Author(s)	Jo, Jung-Lae
Citation	大阪大学, 2013, 博士論文
Version Type	VoR
URL	https://doi.org/10.18910/26202
rights	
Note	

Doctoral Dissertation

Tin whisker growth mechanism and mitigation for lead-free electronics

Jung-Lae Jo

July 2013

Department of Adaptive Machine System

Graduate School of Engineering,

Osaka University

Ph.D. Dissertation

Tin whisker growth mechanism and mitigation for lead-free electronics

by

Jung-Lae Jo

Department of Adaptive Machine System

Graduate School of Engineering

Osaka University

September 2013

Approved by

Professor Katsuaki Suganuma

Professor Yoritoshi Minamino

Associate Professor Masaya Nogi

Associate Professor Shijo Nagao

Tin whisker growth mechanism and mitigation for lead-free electronics

Preface

Tin whisker growth has remained a serious problem in electronics for many decades. The problem has been avoided temporary by alloying Pb into Sn without understanding the whisker growth and elimination mechanisms. With the movement of banning Pb usage in electronics like RoHS directive, and also with increasing demand for electronics miniaturization, the incorrigible whisker problem is coming back to the field of contemporary electronics packaging. Although many efforts were made for understanding tin whiskers, their growth-mechanisms and mitigation methods have not been clarified yet.

The present doctoral thesis aims to provide metallurgical approach to understand the whisker growth mechanism on electroplated tin surfaces, and propose a further mitigation method.

At first, a small amount of Pb addition is approached to understand whisker-growth mechanism. The pure Sn and Sn-xPb ($1 \leq x \leq 10$ wt. %) electroplating have been investigated under ambient temperature. No whisker has been observed on all Sn-xPb samples. The mitigation mechanism by such a trace amount of Pb is not caused by the grain texture control, but is due to the less inter-metallic composite (IMC) growth.

Furthermore, a special and high reliability electronics application such as a satellite in a space, the vacuum whisker has been studied by thermal cycling with comparing air whisker. The effect of plating thickness also investigated for understanding of stress relaxation mechanism. The grain structure of whisker root, particularly grain boundary cracks oxidized in air, determines the stress concentration to drive the whisker growth. Cracking caused by oxidation was rarely observed in vacuum hence causes thin and straight whiskers even from thick plating. These investigations indicate that the stress concentration at whisker root rolls the whisker growth shape and density.

Finally, this thesis establishes the Sn whisker mitigation by least Bi addition. The four different environment tests were performed for verifying of Sn whisker elimination. The results confirmed that adding Bi into Sn refines the grain size of the as-plated films, and alter the columnar structure to equiaxed grains which is excellent for reliving of compressive stress. The refined and equiaxed grains alter the growth pattern of IMC to uniform on the interface between Cu substrate and the plating layer. These microstructure improvements by Bi addition effectively release the internal stress of Sn plating, and hence mitigate whisker growth on the electro-plated surface under various extreme environments.

Table of Contents

Chapter 1

Introduction

Chapter 1

Introduction

Chapter 1

Introduction

1.1 Sn whisker failure in electronics

Sn whisker was firstly reported in 1951 by Compton et al [1]. Sn whiskers mainly grow by compressive stress from internal or / and external stress. Sn whisker formation has been remained one of the most serious problems in electronic devices for more than six decades as they cause short circuits and device malfunctions. This old problem has once solved by alloying Pb with Sn electroplating, but is coming back nowadays because of the RoHS (Restriction of Hazardous Substances) directive banning Pb in electronics packaging. Electro or electro-less plating has been also developed without lead following the recent movement for lead-free packaging of electronics devices [2-3]. Lead-free plating of pure Sn, Sn-Bi, Sn-Ag and Sn-Cu have replaced the conventional Sn-Pb electro plating. However, such lead-free plating faces a risk of Sn whisker growth. Sn whiskers that can grow up to a few millimeters often cause a short circuit failure in electronic components. Fig. 1 shows a representative long tin whisker on Sn plating surface of 42 alloy lead-frame. Due to the miniaturization trend of electronic devices, a few ten micrometers length of whisker is enough to make a short circuit in fine-pitch packaging [3-5]. In particular, the electronics for aerospace have to be faced extreme situations without maintenance. For instance, the satellite needs high reliability to accomplish the given mission for a long time. Recently, the whisker failures have been reported in auto vehicles and satellites by National Aeronautics and Space Administration (NASA) [6-7]. The main reason for the tin whisker growth is driven by compressive stress from internal or external stress under various environments. The tin whisker growth mechanism by internal or external mechanical stress has been reported frequently during the past decades. These reports have focused on: (i) the expansion of intermetallic compound (IMC) volume, (ii) Sn grain growth at room temperature by recrystallization or by grain migration, (iii) thermal stress caused by thermal expansion mismatch between the plated layers and substrates, (iv) oxidation on plating surface accelerated by high temperature and humidity [8-9].

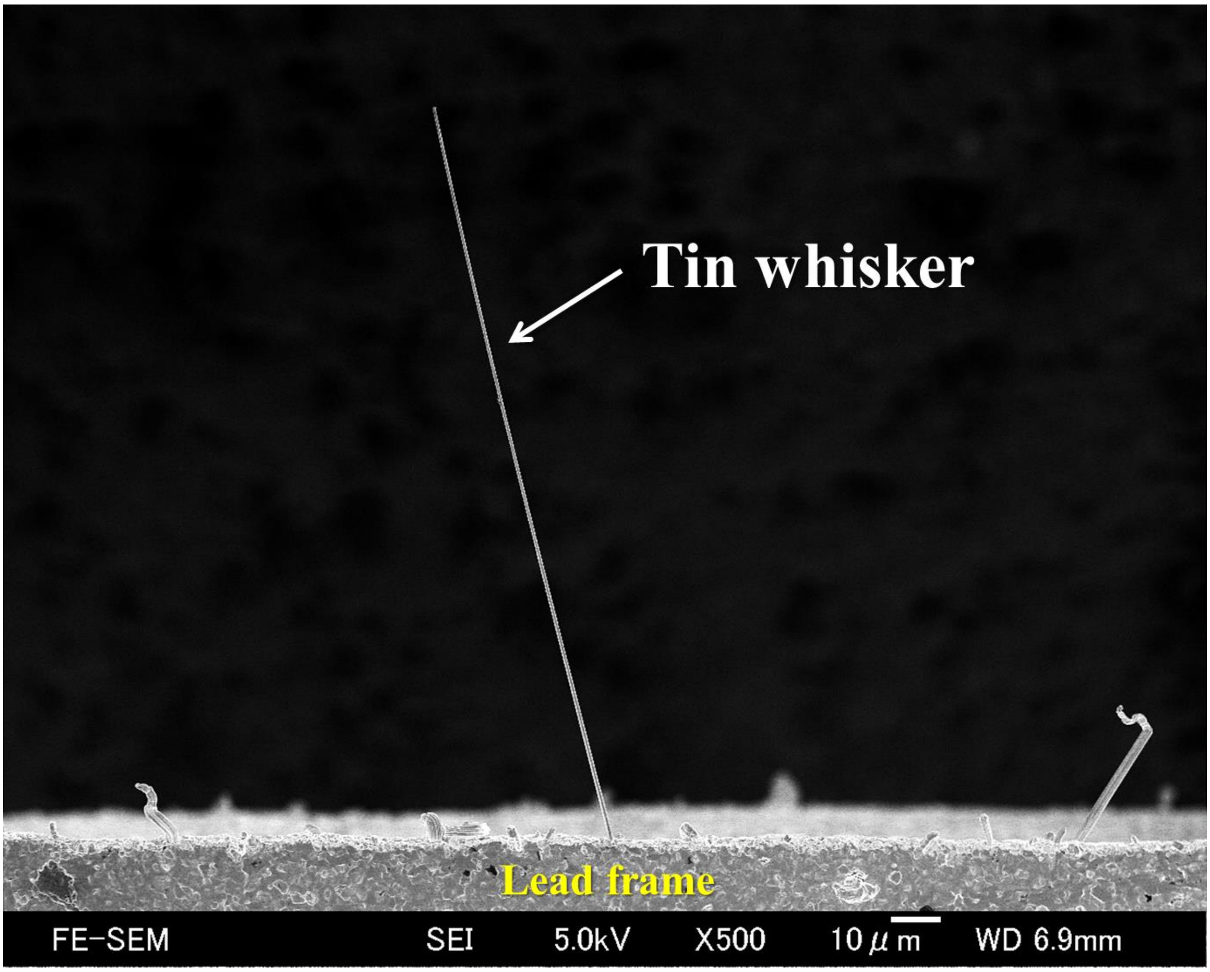

Fig. 1 Whiskers on tin surface after 500 thermal cycling under vacuum condition.

1.2 Causes of whisker growth

1.2.1 Room temperature

The main driving source of tin whisker is compressive stress from internal / external stress. The tin whisker growth mechanisms have been widely reported through various investigations. The intermetallic compound (IMC) between the electro plated layer and copper substrate has grown even under room temperature. In particular, the IMC growth concentrates along the grain boundaries. Thus, compressive stress has increased as growth of IMC on the boundaries. Whisker grows for reliving the accumulated stress by IMC growth called room temperature whisker (see Fig.2) [10-16].

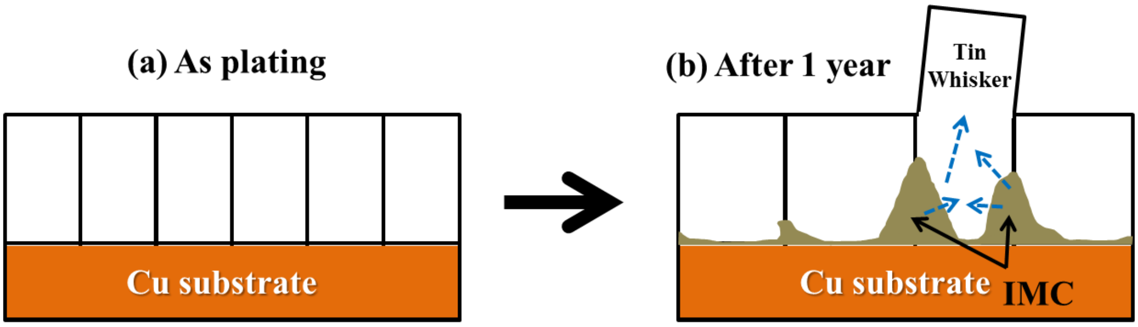

Fig. 2 Schematic of whisker growth under room temperature [10].

1.2.2 Oxidation and corrosion

Oxidation and corrosion of the metal induces a volume expansion into Sn plating layer during high humidity storage, and whiskers grow to relieve the accumulated compressive stresses from the volume expansion [8-9]. The whisker growth by oxidation displays in Fig. 3.

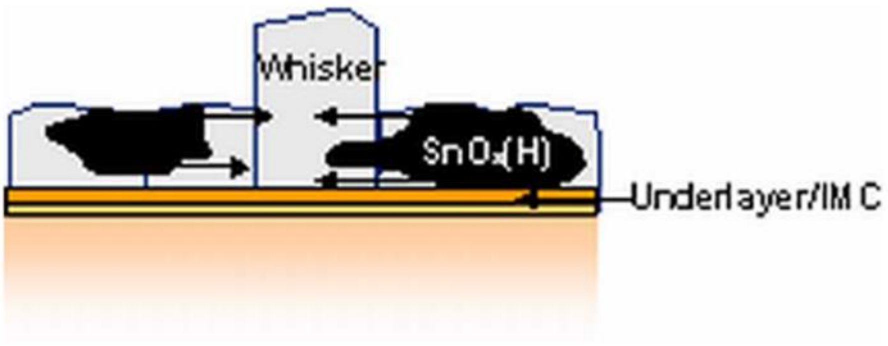

(a)

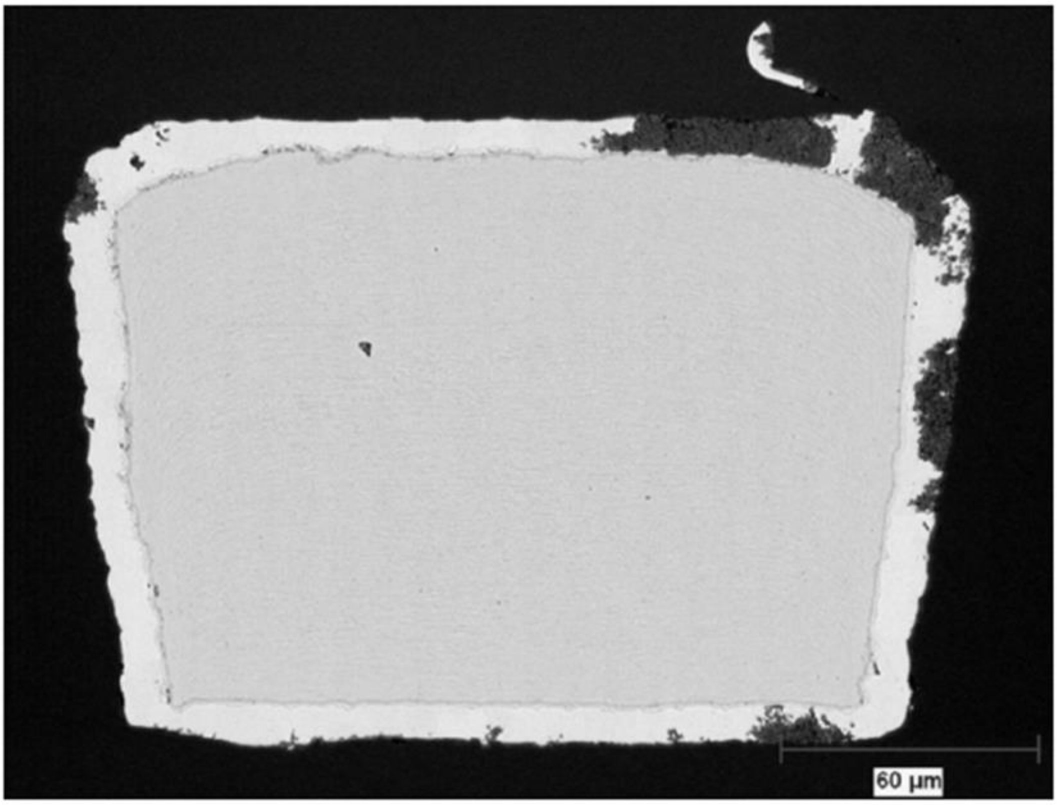

(b)

Fig.3 (a) The mechanism schematic of whisker growth with corrosion/oxidation. (b) Optical micrograph of cross section of lead after prolonged exposure to 60 C/93% RH. Black spots are corroded. Note part of the whisker emanating from the top [8].

1.2.3 Mechanically induced stress

The stress induced by directional load or pressure from the external pressure. For instance, the connectors used in electronics are easily getting a mechanical stress. These mechanical stresses also increase compressive stress in the internal grain also, on the surface of electro plated layer. The stress reliving comes from the whisker growth on the surface as similar manners with the above whisker growth under room temperature and by the oxidation. Mechanically induced whiskers show higher growth rate than that of the whiskers induced by IMC [17-22]. Y. Mizuguchi et al. have observed mechanically induced whiskers over 200 μm length just a few days (see Fig. 4.). The recrystallization and/or grain growth makes volume expansion of Sn grains when the surface induced by the application of mechanical stress. These volume expansion result whisker growth to reliving accumulated stresses. In addition, the Sn whisker growth by the mechanical stress is deeply related with the grain orientation. Mechanical inducing make twined grains and large grains, and Sn whiskers grow mainly a twined grain as shown in Fig.5 [22].

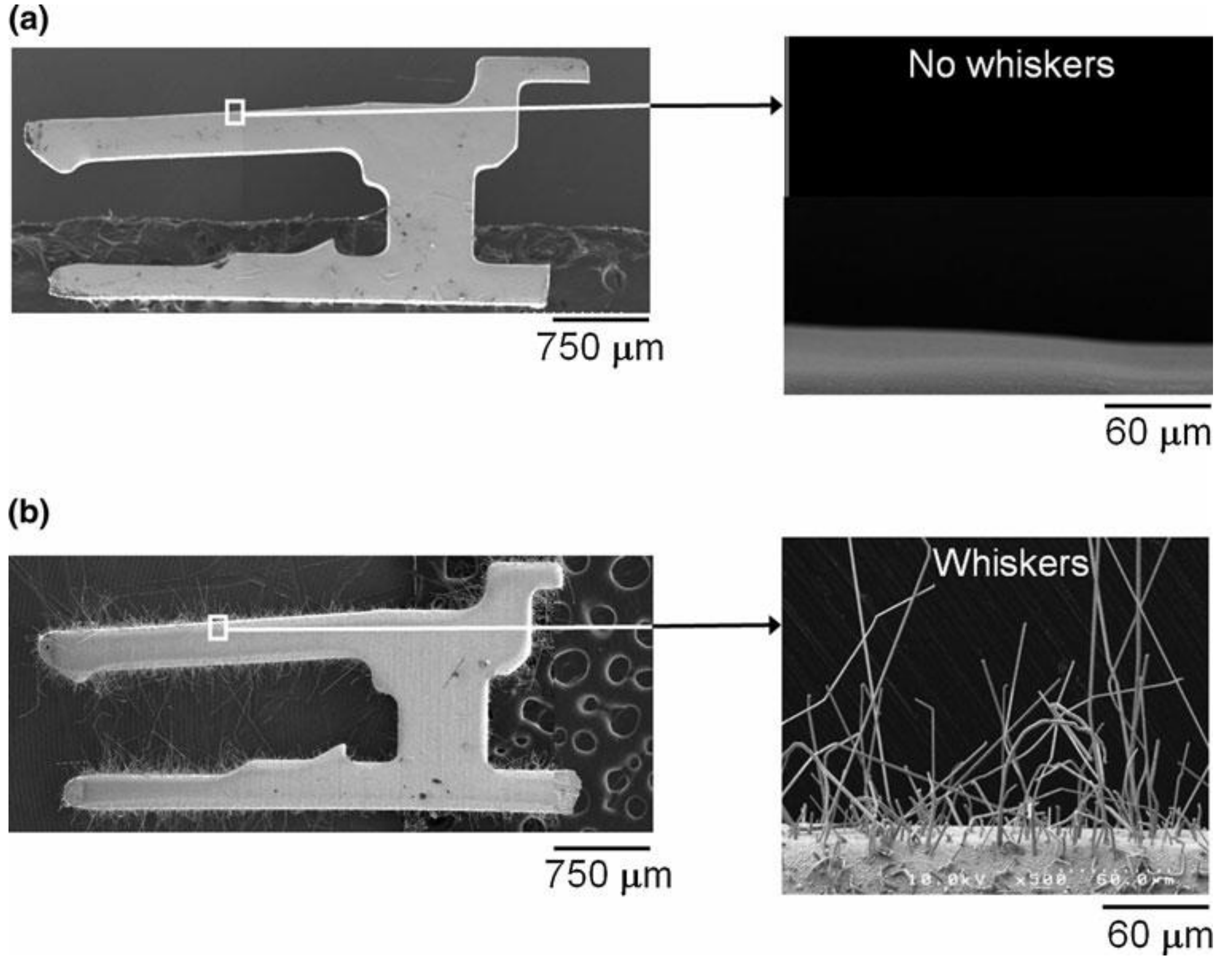

Fig. 4. Mechanically induced connector samples: (a) as plated of Sn, and (b) mechanical stress had been indented for 3 days [22].

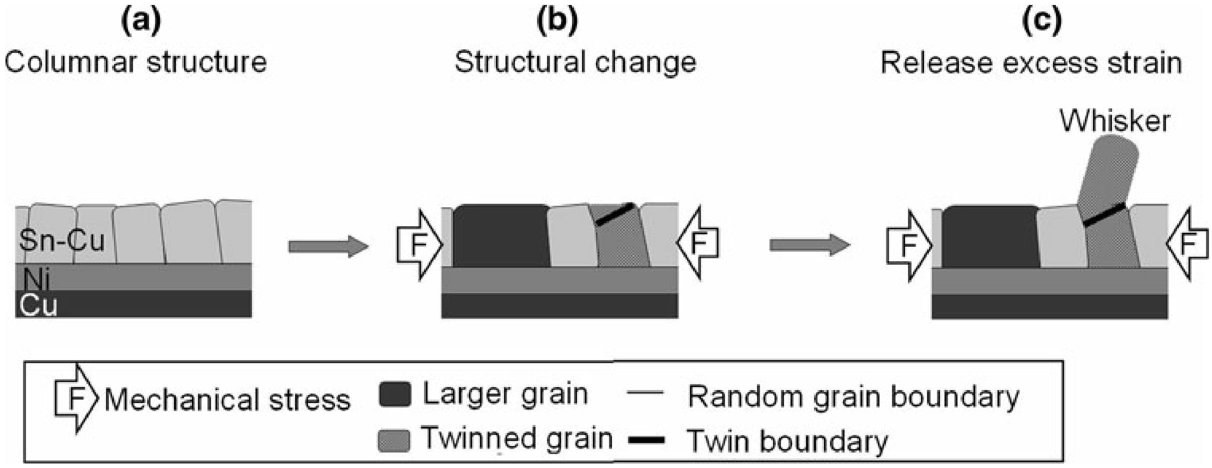

Fig. 5. Schematics of whisker growth by mechanical stress [22].

1.2.4 Thermo-mechanical stress driven by thermal cycling

Thermal stress is one of the main causes of Sn whisker growth. Thermal cycling is a typical factor of thermal stress by inducing a thermo-mechanical stress to plating layer. The difference in coefficient of thermal expansions (CTEs) between plating layer and substrate causes compressive and tensile stress to plating layer repeatedly during thermal cycling. Fig. 6 indicates the schematic of thermal stress progress during thermal cycling. Thermal cycling whisker have been widely reported because electronic components frequently are suffered that environment [23-24]. In the air, thermal cycling induces boundary cracking on the electro plating surface with progress of the surface oxidation. The repeatedly compressive and tensile stress accelerates the grain boundary cracking on plating layer with whisker growth to relax the accumulated the compressive stress. In case of vacuum, though, the same stress relaxation has been arises, the characteristic of whisker growth is different with that of in air. Thick and bended type of whisker mainly have been observed in air, but thin and straight like a filament type of whisker mainly have been observed in vacuum. These variations come from the existence of oxidation during thermal cycling [23, 25].

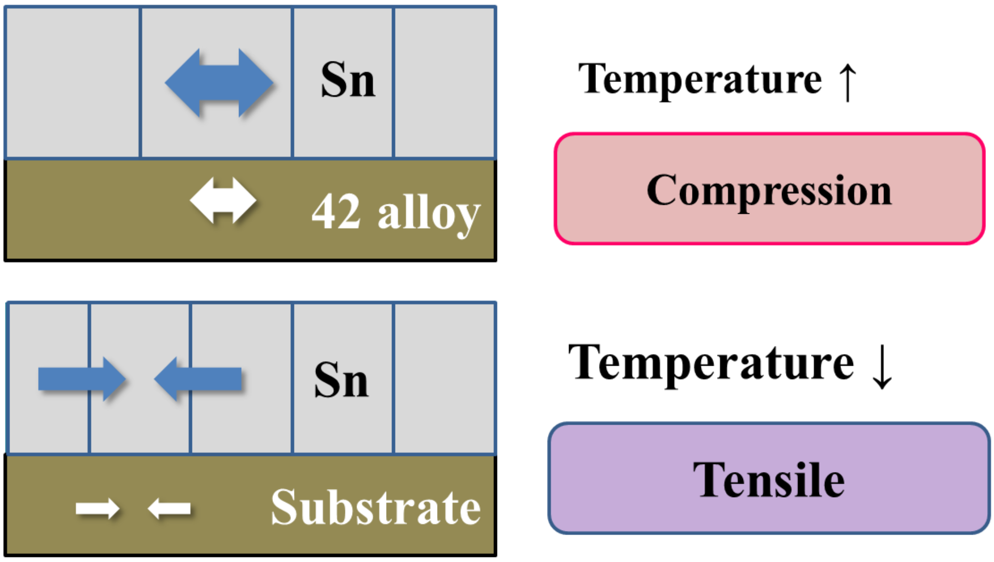

Fig. 6 The schematic of induced thermal stress during thermal cycling.

1.2.5 Electro migration

Electro migration (EM) drives metal whisker by current stress and/or electrical potential [26-27]. Fig.7 shows whisker and hillock growth on the Sn-Bi solder induced by electro migration. The molten Sn-Bi solder during EM overflows and spread on the top surface of the Cu substrate. And then, the overflowed solder film makes IMC (Cu_6Sn_5), which causes the whisker and hillock growth for relieving compressive stress [27]. Q.S. ZHU et al. suggest a model of stress generation by EM (see Fig. 8). They also, show the tin hillock induced by EM as shown in Fig. 9. These Sn hillocks indicated in Fig. 9 can explain by the schematic diagram in Fig.10, explaining hillocks induced by the compressive stress from Cu_6Sn_5 segregation. Furthermore, as increasing EM time, the hillocks have grown larger [26]. As mentioned above, the compressive stress from IMC growth drives the Sn whiskers. It is basically similar driving source of Sn whisker i.e. the compressive stress during EM and room temperature storage.

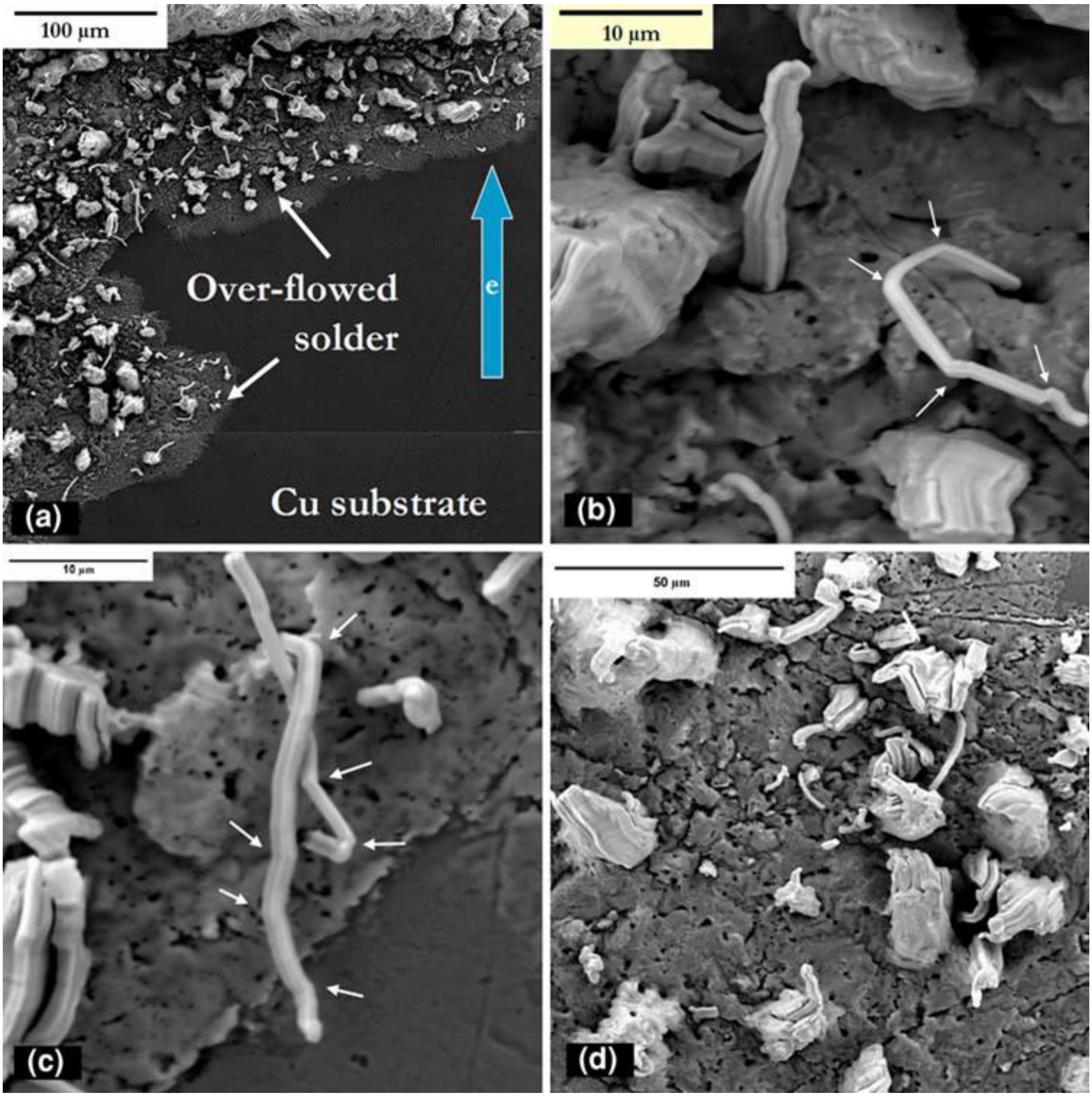

Fig. 7. Whisker growth on solder joints after 48 h of current stressing: (a) formation of whiskers and hillocks on the overflowed solder film, (b) morphology of the whiskers, (c) morphology of two twisting whiskers, and (d) morphology of the hillocks [27].

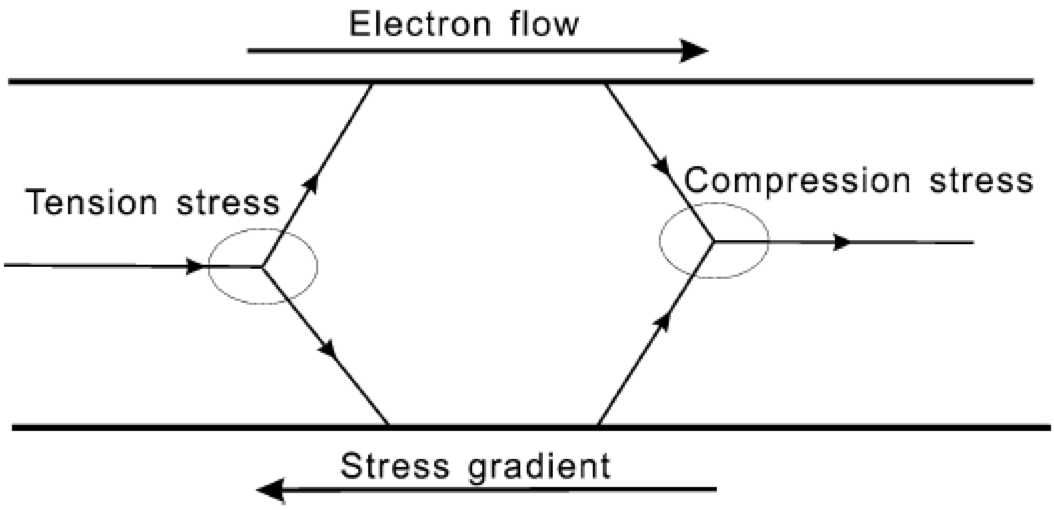

Fig. 8 Schematic diagram of stress generation at a trigeminal grain boundary by electromigration [26].

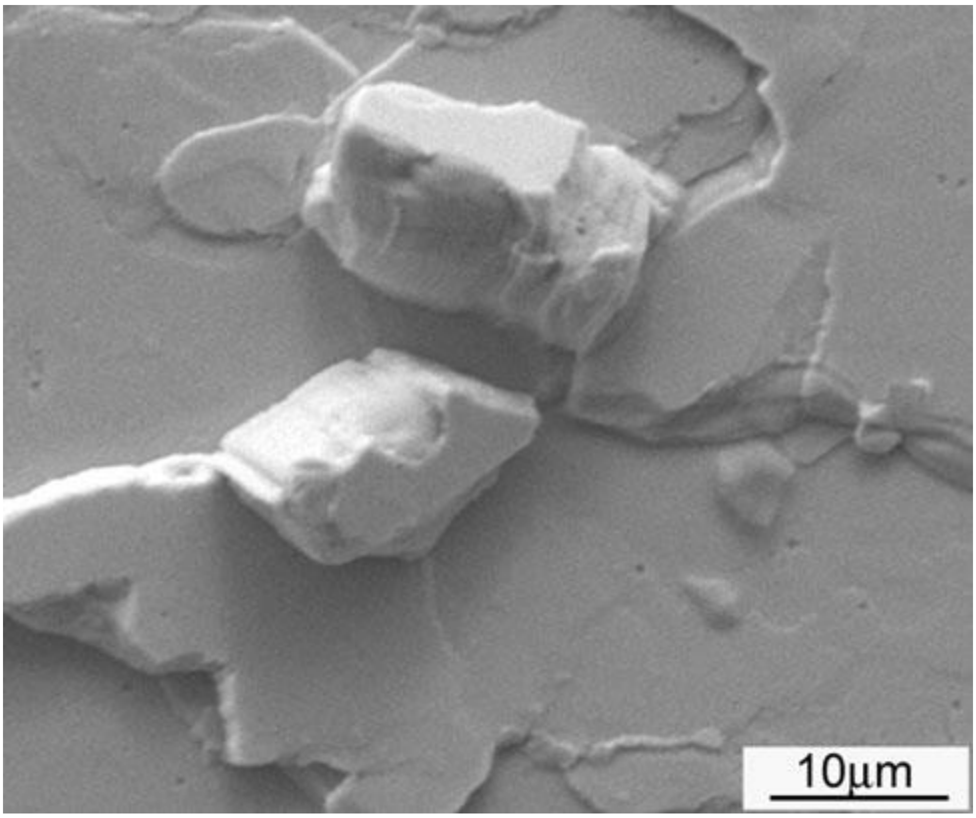

Fig.9 Sn hillocks induced by electro migration [26].

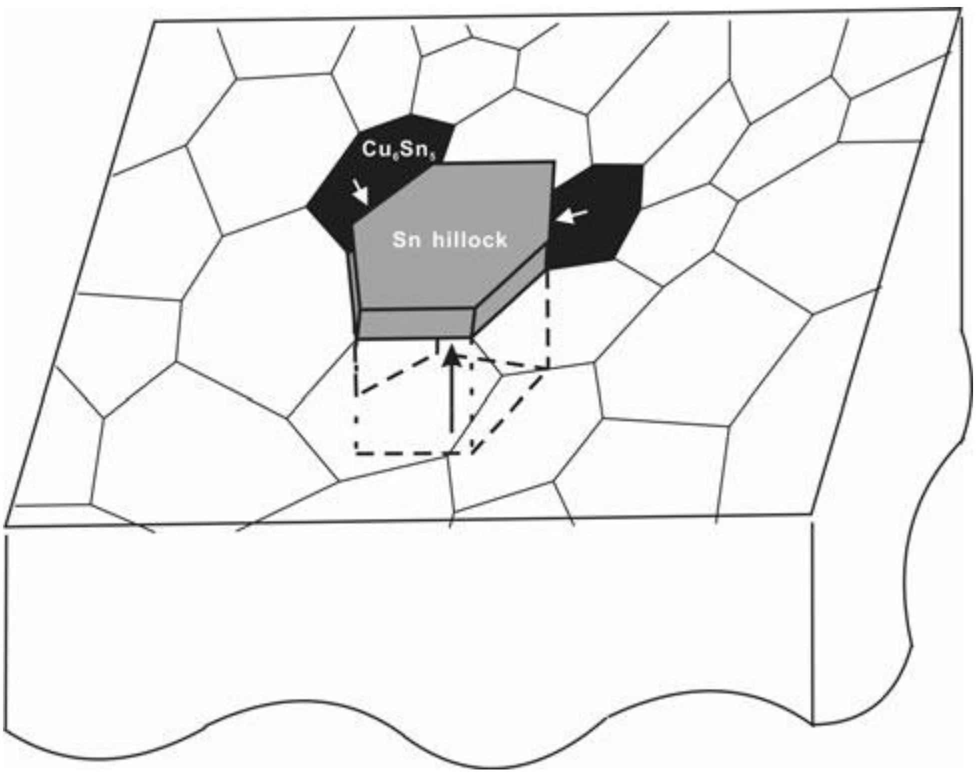

Fig.10 Schematic diagram of Sn hillock growth under in-plane compressive stress from Cu6Sn5 segregation [26].

1.2.6 Summary of Causes of whisker growth

Metallic whisker growth has grown by variable driving source. In particular, tin whisker is prone to grow on electroplating surface and Sn-based solder by various environments. The IMC growth drives the compressive stress on plating layer and solders by volume expansion, hence, the whiskers grow to relive the accumulated compressive stress under room temperature and or EM process. The oxidation induces similarly volume expansion in and on Sn and grain boundaries. These volume expansions result a compressive stress to grow tin whisker for reliving the stress. Thermal stress by inducing thermal cycling is one of important driving source of Sn whisker growth. Thermal cycling makes mismatch of CTEs between the plating layer and substrate. Tensile and compressive stress is forced on plated surface repeatedly during thermal cycling. The accumulated stress is relaxed by whisker growth.

The causes of whisker growth are based on a compressive stress in all cases. In particular, it is prone to generate compressive stress on lead-free electroplating and solder alloys under various environments. Therefore, to relaxing compressive stress is a key understanding for whisker mitigation under various conditions.

1.3 Previous research on whisker mitigation

Many researches about whisker growth model have been reported for a few decades as explained in chapter 1.2. On the base of the models, many efforts of whisker mitigation have been also researched. The compressive stress in plating layer has been a major cause of Sn whisker growth. Furthermore, in Sn electro plating, IMC growth is prone to follow the grain boundaries. The concentration on grain boundary growth disturbs the mobility of Sn grain boundary. Therefore, the Sn whisker has been grown to relieve the accumulated compressive stress. The IMC growth control is one of the effective methods to relaxing compressive stress on the Sn plating layer and solders. Annealing by heat treatment at 150 ℃ for longer than 30 min is typical for reduce whiskers at ambient storage. The heat treatment creates a uniform IMC layer at the interface between Sn plating and Cu substrate, and the uniform IMC layer hampers further IMC growth particularly along the Sn grain boundaries because of the decreased Cu diffusion rate [11-12, 14]. This heat treatment also, called "post-bake" in literature [28-29].

Film thickness (electro plating thickness) is also deeply related to the relaxation on compressive stress. Thickening the plating layer relaxes the compressive stress in tin plating to reduce the whisker density [30]. As increasing the film thickness (Fig. 11 a to c), the grain sizes are also increased as shown in Fig.11 d to f. Overall in the Fig.11, The thicker plating layer has more IMC volume with large grain. The compressive stress is lowest in 5.8 μm (see Fig.11 l), causing a minimum whisker density. The thickening plating layer effect is apparent in their reports for whisker suppression.

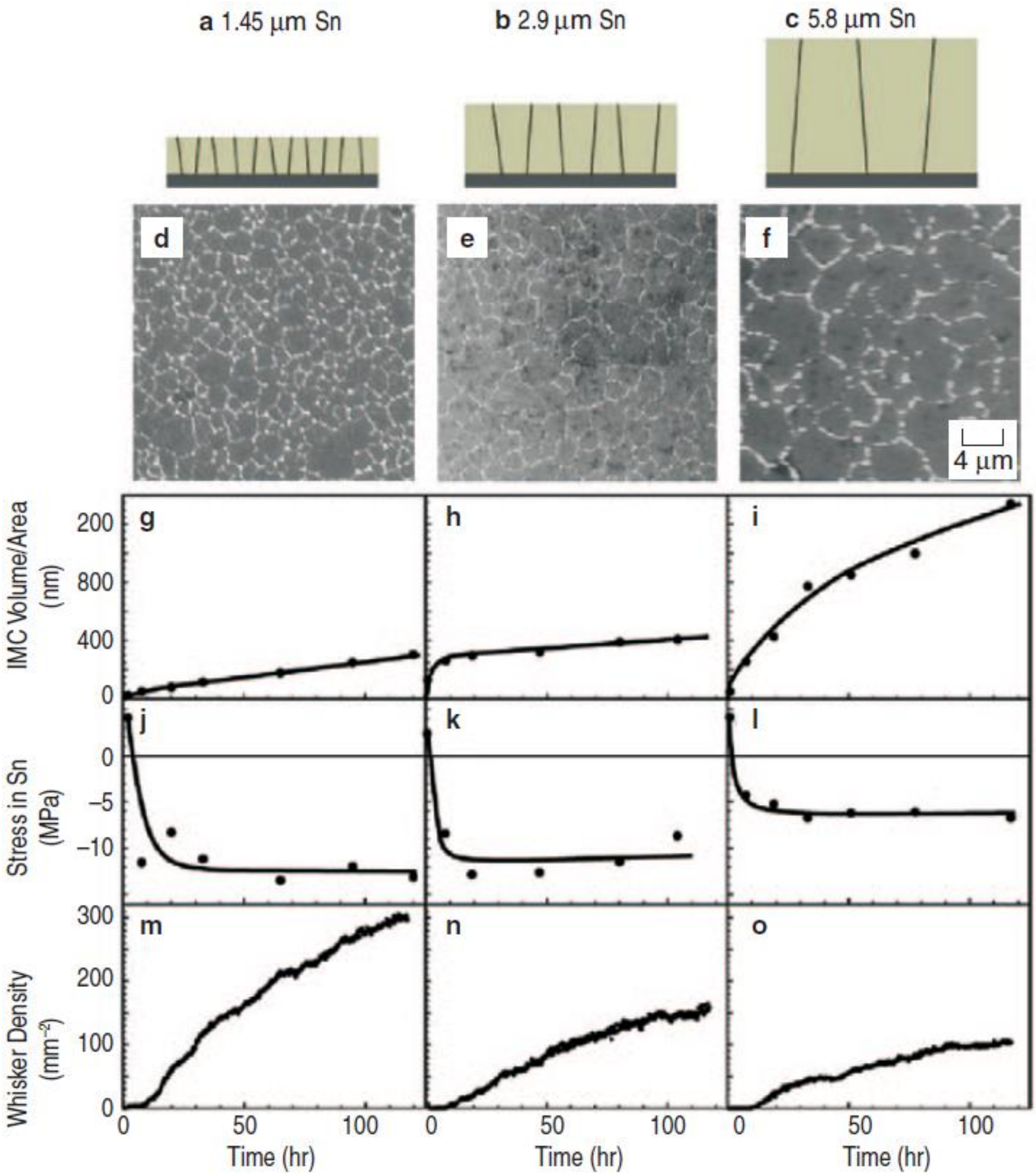

Fig.11 Simultaneous measurements of the evolution of IMC volume (g–i), in plan stress in Sn layer (j–l), and whisker density (m–o) are shown for three different Sn layer thickness [30].

Alloying with a various lead-free metal also challenges on whisker mitigation for a decade. Representatively, alloying Bi with Sn has been examined in the literature, where the columnar grains of the films were changed to equiaxed grains [31]. In their reports, the measured stress of 7.5 μm Sn films with 2.5-10 wt.% Bi content under thermal cycling has shown a relaxation similar to that in the Sn-Pb plating. Pure Sn, Sn-Pb and Sn-Bi have been compared by stress in plating layer during thermal cycling. Fig.12 and Fig.13 shows each results of stress comparing of pure Sn Sn-Pb and Sn-Bi with composition respectively. Comparing the Fig.12 (b) and Fig.13 (f), a similar stress development can be confirmed on the Sn-Pb and Sn-10Bi plating layer. Even the stress development of Sn-2.5Bi plating is lower than that of pure Sn (compare Fig.12 (a) and Fig.13 (b)). It is note that the compressive stress can be relieved by Bi alloying on Sn film with whisker suppression.

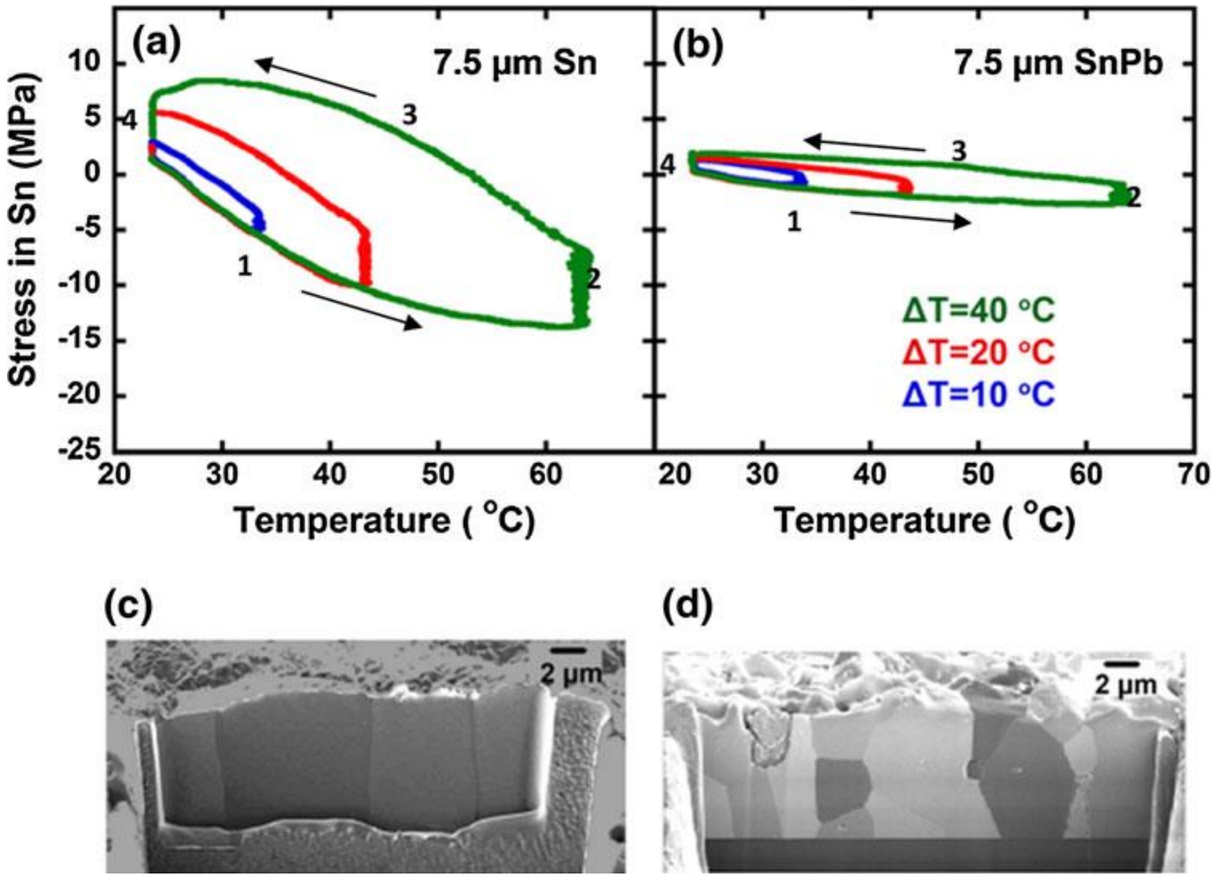

Fig.12 The stress comparison of (a) 7.5 μm Sn layer and (b) 7.5 μm Sn-Pb alloy layer Stress as to time variation: cross section view of (c) Sn and (d) Sn-Pb [31].

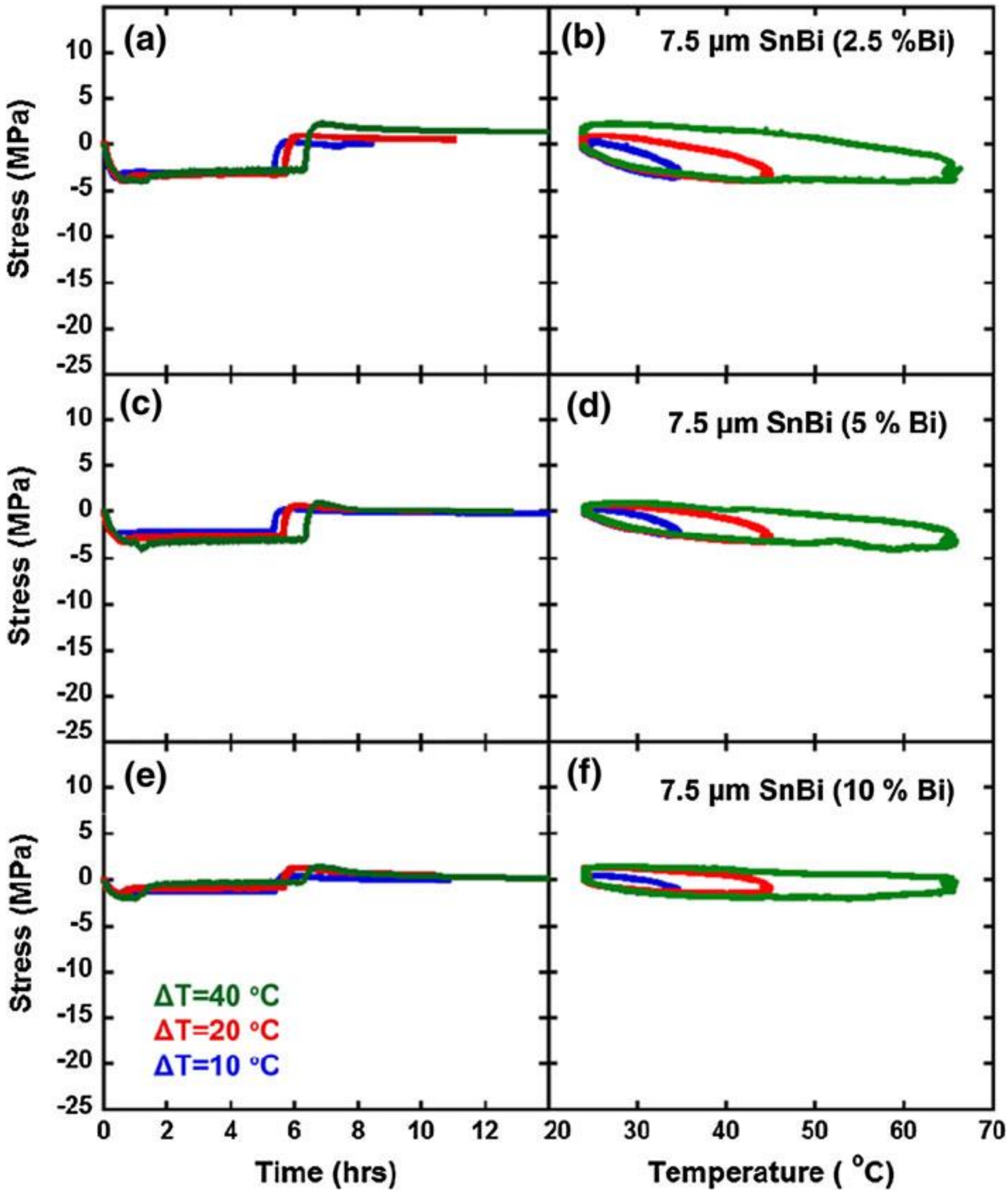

Fig. 13 Stress development as time variation: Sn-Bi alloy films with (a, b) 2.5 wt.% Bi, (c, d) 5 wt.% Bi, and (e, f) 10 wt.% Bi [31].

1.4 Objective and motivation of this thesis

Electronic devices are now being developed without lead since the restriction of hazardous substances (ROHS) directive for electronic equipment a decade ago. Hence, electroplating for electro-packaging is also being developed to be lead free. Sn-Pb alloys are superior materials for electro-packaging having properties such as good soldering ability, good wettability, a low meting point for soldering and especially a good tolerability of tin whisker generation under various environments. A challenge for lead-free electro-devices is the risk of failure from the growth of metal whiskers. Tin whiskers can grow up to a few millimeters during operation and can cause a short circuit failure in electronic components. For example, a whisker less than 100 µm in length can create a short circuit in fine pitch systems following the miniaturization trend of electronic devices. Thus, many approaches for mitigating tin whisker formation have been proposed using various methods. The various metallurgical investigations have been also reported to understand the growth mechanism of Sn whisker for their mitigations. Even though many approaches and reports about whisker growth mechanism and mitigation, the mechanisms are not sufficient for conclusive understands of Sn whiskers and the fundamental mitigation for long term whisker growth are not clear.

Consequently, in this thesis, the fundamental mechanism of Sn whisker growth has been proposed by understanding of Sn-Pb alloying. No whiskers have been confirmed on Sn-Pb plating under ambient temperature storage. Therefore, the understanding of whisker suppression effect in Sn-Pb alloying rolls inversely, a key comprehension of whisker growth mechanism.

Whisker problem in the vacuum environment has been nearly studied though many whisker failures have been reported about space applications during their operation in the vacuum such as satellite. So, in this thesis, the vacuum whisker is compared with air whisker by their characterizations under thermal cycling. The different plating thickness also, compared by thermal cycling test. The different thermal stress by induced thermal cycling has been investigated for the understanding whisker growth mechanism in the vacuum and air environments.

Finally, this research suggests whisker mitigation for various environments by a small amount of Bi addition. The alloying effect on whisker suppression has already been proposed in the literature, this thesis concludes that the minimum requirement of Bi addition necessary for whisker mitigation can be less than or equal to 0.5 wt. %. This mechanism of whisker mitigation would help the further investigation on metal whisker suppressions in particular, in the fields of lead-free applications.

References

1. K. G. Compton, A. Mendizza, and S. M. Arnold, “Filamentary growths on metal surfaces – “Whisker””, Corrosion-National association of corrosion engineers, 7, pp.327-334. (1951)

2. K. J. Puttlitz, G. T. Galyon, “Impact of the ROHS Directive on high-performance electronic systems”, J. Mater. Sci. Mater. Electron., 18, pp.347-365 (2007)

3. H.P. Howard, J. Cheng, P.T. Vianco, J.C.M. Li, “Interface flow mechanism for tin whisker growth”, Acta Mater., 59(10), pp.1957-1963 (2011)

4. G.T. Galyon, “A History of Tin Whisker Theory: 1946 to 2004 “, in SMTAI U.S.A (2004), September 26-30, on SMTAI International conference (SMTAI): Chicago

5. H.L. Cobb, “Cadmium whiskers”, Monthly Rev. Amer. Electroplaters Soc. 33(28), pp.28–30 (1946)

6. H. Leidecker, L.Panashchenko and J. Brusse, “Electrical Failure of an Accelerator Pedal Position Sensor Caused by a Tin Whisker and Discussion of Investigative Techniques Used for Whisker Detection”, in University of Maryland, U.S.A (2011), September 14-15, on the 5th International Symposium on Tin Whiskers

7. NASA homepage : Whisker failures, http://nepp.nasa.gov/whisker/failures/

8. P. Oberndorff, M. Dittes, P. Crema, P. Su, and E. Yu, “Humidity Effects on Sn Whisker Formation”, IEEE Trans. Electron. Packaging Manuf., 29(4), pp.239-245 (2006)

9. C. F. Li, Z. Q. Liu, and J. K. Shang, “The effects of temperature and humidity on

the growth of tin whisker and hillock from Sn5Nd alloy", Journal of Alloys and Compounds, 550, pp.231-238 (2013)

10. J-L. Jo, K-S. Kim, T. Sugahara, S. Nagao, K. Hamasaki, M. Tsujimoto, K. Suganuma, "Least lead addition to mitigate tin whisker for ambient storage", J. Mater. Sci. Mater. Electron., (2013) doi: 10.1007/s10854-013-1218-y

11. K. N. Tu, J. C. M. Li, "Spontaneous whisker growth on lead-free solder finishes", Materials Science and Engineering: A 409(1-2), pp.131-139 (2005)

12. J. W. Osenbach, R. L. Shook, B. T. Vaccaro, B. D. Potteiger, A. N. Amin, K. N. Hooghan, P. Suratkar, and P. Ruengsinsub, "Sn whiskers: Material, design, processing, and post-plate reflow effects and development of an overall phenomenological theory. IEEE Trans. Electron. Packaging Manuf. 28(1), pp.36-62 (2005)

13. Lee BZ, Lee DN, "Spontaneous growth mechanism of tin whiskers", Acta. Mater., 46, pp.3701-3714 (1998)

14. W. J. Boettinger, C. E. Johnson, L.A. Bendersky, K.-W. Moon, M. E. Williams, and G. R. Stafford, "Whisker and hillock formation on Sn, Sn-Cu and Sn-Pb electrodeposits", Acta. Mater., 53, pp.5033-5050 (2005)

15. T. Kato, H. Akahoshi, M. Nakamura, T. Terasaki, T. Iwasaki, T. Hashimoto and A. Nishimura, "Correlation Between Whisker Initiation and Compressive Stress in Electrodeposited Tin–Copper Coating on Copper Leadframes", IEEE Trans. Electron. Packaging Manuf., 33(3), pp.165-176 (2010)

16. T. Terasaki, T. Iwasaki, T. Okura, Y. Suzuki, T. Kato, M. Nakamura, and T. Hashimoto, "Evaluation of Tin-whisker Growth During Thermal-cycle Testing Using

Stress- and Mass-diffusion Analysis," 59th Electronic Components & Technology Conference, San Diego, CA, May 26-29, 2009, pp. 277-284

17. S.-K. Lin, Y. Yorikado, J. Jiang, K.-S. Kim, K. Suganuma, S.-W. Chen, M. Tsujimoto, and I. Yanada, “Microstructure Development of Mechanical-Deformation Induced Sn Whiskers”, J. Electron. Mater. 36, pp.1732-1734 (2007).

18. T. Shibutani, Q. Yu, M. Shiratori, and M.G. Pechtand, “Pressure-induced tin whisker formation”, Microelectron. Reliab. 48, pp.1033-1039 (2008).

19. T. Shibutani, Q. Yu, T. Yamashita, and M. Shiratori, “Stress-Induced Tin Whisker Initiation Under Contact Loading”, IEEE Trans. Electron. Packaging Manuf., 29, pp.259-264 (2006)

20. K.N. Tu, “Interdiffusion and reaction in bimetallic Cu-Sn thin films. Interdiffusion et reaction dans les films minces bimetalliques Cu-Sn. Interdiffusion und Reaktion in bimetallischen Cu-Sn-Schichten.”, Acta Mater. 21, pp.347-354 (1973).

21. R.M. Fisher, L.S. Darken, and K.G. Carroll, “Accelerated Growth of Tin Whiskers”, Acta Metall., 2(3), pp.368-373 (1954).

22. Y. Mizuguchi, Y. Murakami, S. Tomiya, T. Asai, T. Kiga, and K. Suganuma, “Effect of Crystal Orientation on Mechanically Induced Sn Whiskers on Sn-Cu Plating”, J. Electron. Mater., 41(7), pp.1859-1867 (2012)

23. K. Suganuma, A. Baated, K.-S. Kim, K. Hamasaki, N. Nemoto, T. Nakagawa, and T. Yamada, “Sn whisker growth during thermal cycling”, Acta. Mater., 59, pp.7255-7267 (2011)

24. J. W. Shin, and E. Chason, “Stress behavior of electroplated Sn films during thermal

cycling", J. Mater. Res., 24(4), pp.1522-1528 (2009)

25. J.-L. Jo, S. Nagao, T. Sugahara, M. Tsujimoto, and K. Suganuma, "Thermal stress driven Sn whisker growth: in air and in vacuum", J. Mater. Sci. - Mater. Electron., (2013) doi : 10.1007/s10854-013-1336-6

26. Q.S. Zhu, H.Y. Liu, Z.G. Wang, and J.K. Shang, "Surface Morphology of Sn-Rich Solder Interconnects After Electrical Loading", J. Electron. Mater., 41(4), pp.741-747 (2012)

27. F. Guo, G. Xu, H. He, M. Zhao, J. Sun, and C. H. Wang, "Effect of Electromigration and Isothermal Aging on the Formation of Metal Whiskers and Hillocks in Eutectic Sn-Bi Solder Joints and Reaction Films", J. Electron. Mater., 38(12), pp.2647-2658 (2009)

28. L. Sauter, A. Seekamp, Y. Shibata, Y. Kanameda, H. Yamashita, "Whisker mitigation measures for Sn-plated Cu for different stress tests", MICROELECTRON. RELIAB., 50, pp.1631-1635 (2010)

29. JEDEC STANDARD, JESD201A, "Environmental Acceptance, Requirements for Tin Whisker, Susceptibility of Tin and Tin Alloy, Surface Finishes, Revision of JESD201, March 2006 (2008)

30. E. Chason, N. Jadhav, F. Pei, "Effect of layer properties on stress evolution, intermetallic volume, and density during tin whisker formation", JOM 63(10), pp.62–68 (2011)

31. N. Jadhav, M. Williams, F. Pei, G. Stafford, E. Chason, "Altering the Mechanical Properties of Sn Films by Alloying with Bi: Mimicking the Effect of Pb to Suppress

Whiskers”, J. Electron. Mater. 42(2), 312-318 (2013)

Chapter 1

Introduction

Chapter 2.

Least lead addition to mitigate tin whisker for ambient storage

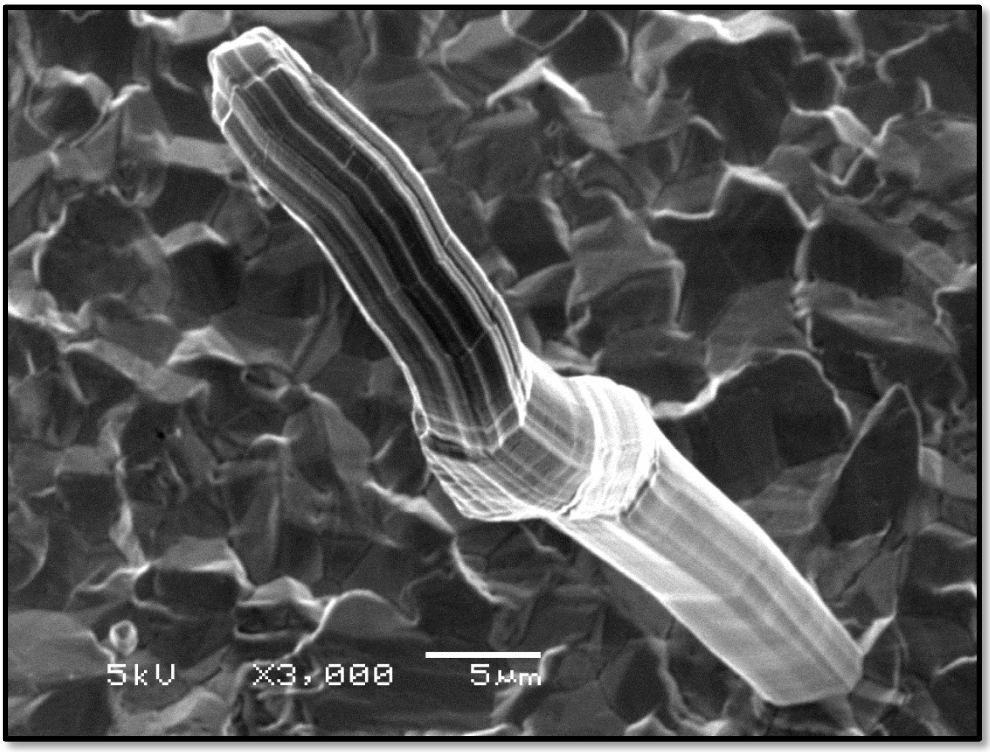

Tin whisker under room temperature storage (Jung-Lae Jo, 2013)

Abstract

In this chapter, long term surface evolution of matte tin electroplating has been investigated under room temperature to understand the tin whisker mitigation by a trace amount of lead addition. No whisker growth has been observed on all the Sn-xPb samples ($1 \leq x \leq 10$ wt.%), while at least 3 wt.% of Pb addition is required to alter the columnar grain structure of pure Sn plating to equiaxed grains. The mitigation mechanism by such a trace amount of Pb is not caused by the grain texture control, but is due to the less inter-metallic composite (IMC) growth; the segregated Pb at the columnar grain boundaries disrupts the IMC growth, and releases Sn grain boundary migrations to relax the internal stress. This mechanism of stress relaxation and whisker growth suppression suggests that lead-free Sn plating without whisker growth can be realized by co-plating Sn with a Pb-like metal element that precipitates at the grain boundary to interfere with the IMC growth.

2.1 Introduction

Electro or electro-less plating has been developed without lead following the recent movement for lead-free packaging of electronics devices. Lead-free plating of pure Sn, Sn-Bi, Sn-Ag and Sn-Cu have replaced the conventional Sn-Pb electro plating. However, such lead-free plating faces a risk of tin whisker growth. Tin whiskers that can grow up to a few millimeters often cause a short circuit failure in electronic components. Due to the miniaturization trend of electronic devices, a few ten micrometers length of whisker is enough to make a short circuit in fine-pitch packaging [1-4]. The tin whisker growth mechanism by internal or external mechanical stress has been reported frequently during the past decades. These reports have focused on: (i) the expansion of intermetallic compound (IMC) volume, (ii) Sn grain growth at room temperature by recrystallization or by grain migration, (iii) thermal stress caused by thermal expansion mismatch between plating and substrate, and (iv) oxidation on plating surface accelerated by high temperature and humidity [5-6]. To prevent tin whisker failure in electronic devices, various methods of whisker mitigation have been proposed. For example, annealing by heat treatment at 150 ℃ for longer than 30 minutes is typical for reduce whiskers at ambient storage. The heat treatment creates a uniform IMC layer at the interface between Sn plating and Cu substrate, and the uniform IMC layer hampers further IMC growth particularly along the Sn grain boundaries because of the decreased Cu diffusion rate [7-9]. Thickening the plating layer relaxes the compressive stress in tin plating to reduce the whisker density [10]. Recently, the stress relaxation mechanism of Sn-Pb alloying has been reported; the addition of lead in matte tin forms the equiaxed grain structure to reduce the residual stress of electroplating process, and is effective on Sn whisker incubation [11, 12]. And also, Sn-Pb plating eliminates Sn whisker by changing IMC growth [13]. However, the lead contents of examined in their reports were

5 wt. % to 40 wt. %, and the similar grain structure alternation from columnar to equiaxed was found in both the cases. Thus the necessary amount of Pb has been yet unknown, and the detailed role of Pb element in the Sn grain structure as well.

In this chapter, the role of small amount of Pb addition in matt tin plating has been explored in connection with whisker growth observations for one-year long storage under room temperature. Evolutions of the grain microstructure, surface texture, and IMC growths have frequently been observed during the storage experiment, and compared with various Pb concentrations of Sn-xPb co-electroplating where $0 \leq x \leq 10$ wt. %. The typical texture of electroplated pure Sn displays a vertical columnar structure that is prone to generate tin whiskers, while whisker mitigation has been confirmed in all the Pb added Sn plating specimens. However, our thin electro plating of Sn-xPb ($x \leq 3$ wt. %) displays a columnar grain structure similar to that of pure Sn, instead of the equiaxed grains that relieve compressive stress more effectively than the columnar grains [7] This means whisker suppression mechanism can be different when only 1 wt. % of lead is added in tin. The present experimental research aims to clarify the unidentified mechanism of tin whisker mitigation, seeking for further possibility to Pb-free whisker mitigation methods.

2.2 Experimental procedure

Matte Sn-*x*Pb (x = 1, 2, 3, 4, 5, 10 wt. %) were electroplated on a copper lead-frame for quad flat packaging (corresponding to CDA number C19400) sheets, using an electric current density of 5 A/cm2. The electroplating process was carried out in a 3 liter of 1 pH solution bath at 45 ℃ for 3 minutes and 10 seconds. After the electroplating, all the samples were cleaned with distilled water, and then dried for 20 seconds with a dry machine gun. Fig. 1 shows a typical electroplated lead-frame specimen. The plating thickness was about 5 μm for all the samples. These samples were stored at room temperature (25 ± 2 ^{o}C) for one year, and the growth behavior of Sn whiskers and surface changes were continuously observed by scanning electron microscopy (SEM, JSM-5510S, JEOL, Japan) during the test period.

The microstructure and crystal grain size of the coatings were determined by SEM observation on the surfaces, and on the cross-sections of the coatings (FE-SEM 2100, JEOL, Japan). Focused ion beam (FIB) microscope (Hitachi FB-2100, Japan) was utilized to fabricate cross-section samples of the coatings, whiskers, and hillocks, as well as FIB imaging. The distributions of Sn and Pb grains were determined at 1 μm depth from the topmost surface with using FIB. Cross section polisher (SM-09010, JEOL, Japan) of Ar ion etching was also used for cross-section sample preparations, and energy dispersive X-ray (EDX) analysis was performed. Finally, the Sn-*x*Pb plating layer was removed with using the etchant composed of hydrochloric acid (3 %) and nitric acid (5 %) in ethanol (92 %), and then the surface distributions of remaining IMCs were observed with field emission-scanning electron microscope (FE-SEM).

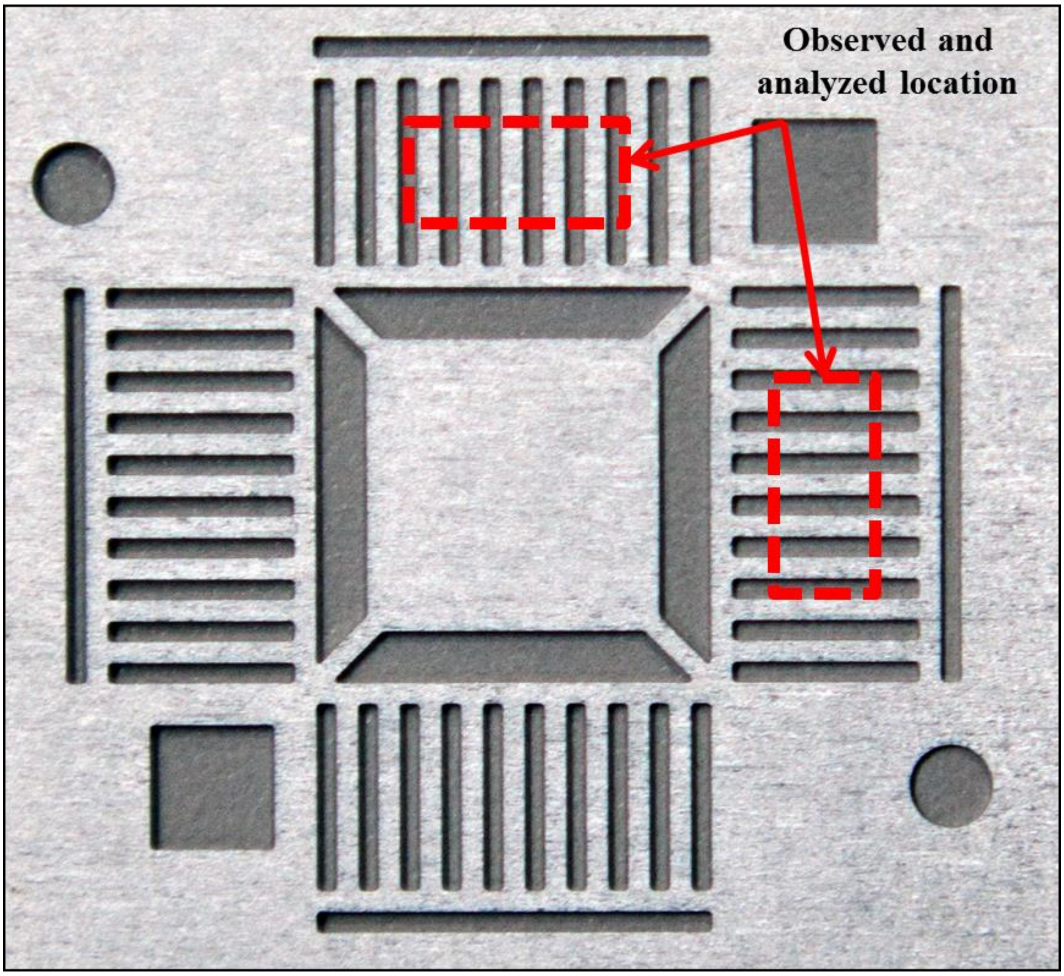

Fig. 1. Sn-Pb electro plating on copper lead frame sheet for quad flat package.

2.3 Results and discussion

2.3.1 Tin whisker generation at room temperature

The surface images of as-plated matte Sn and Sn-*x*Pb are presented in Fig. 2. All the fresh samples show flat surfaces without any whiskers or cracks. The morphologies of the topmost surfaces appear differently according to the amount of Pb addition. With increasing Pb content in Sn, the size of surface grains decreases. The small amount of Pb addition thus results in Sn grain refinement.

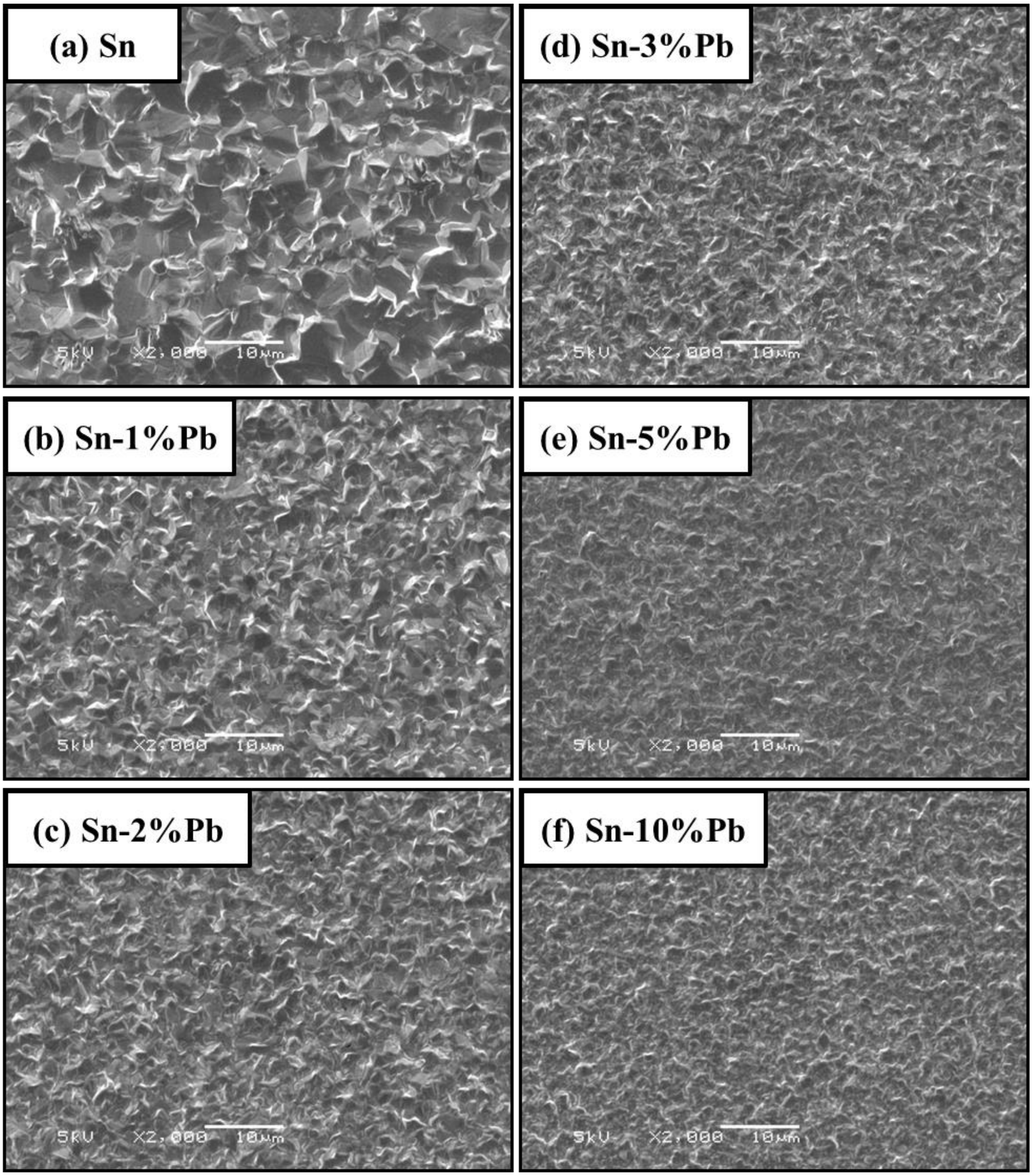

Fig. 2. Surface morphologies of the Sn-*x*Pb electro plating after as plated.

FIB images presented in Fig.3 display the Pb distributions under 1 μm from the top surface. The segregated Pb increases with increasing Pb content. Moreover, the average size of Sn grains is decreased with increasing Pb content as well. In particular, the grain sizes of Sn-1%Pb are smaller than those of the pure matte Sn as seen in Fig. 3 (a) and (b). This means that the grain refinement effect starts at only 1 wt. % of Pb addtion. The Pb grains are mainly located on Sn grain boundaries regardless of Pb content. Because of the negligible solubility of Pb in Sn at room temperature both the size and number of segregated Pb grains increases with increasing Pb content from 1 wt. % to 10 wt. %, being consistent with the report in the literature [7].

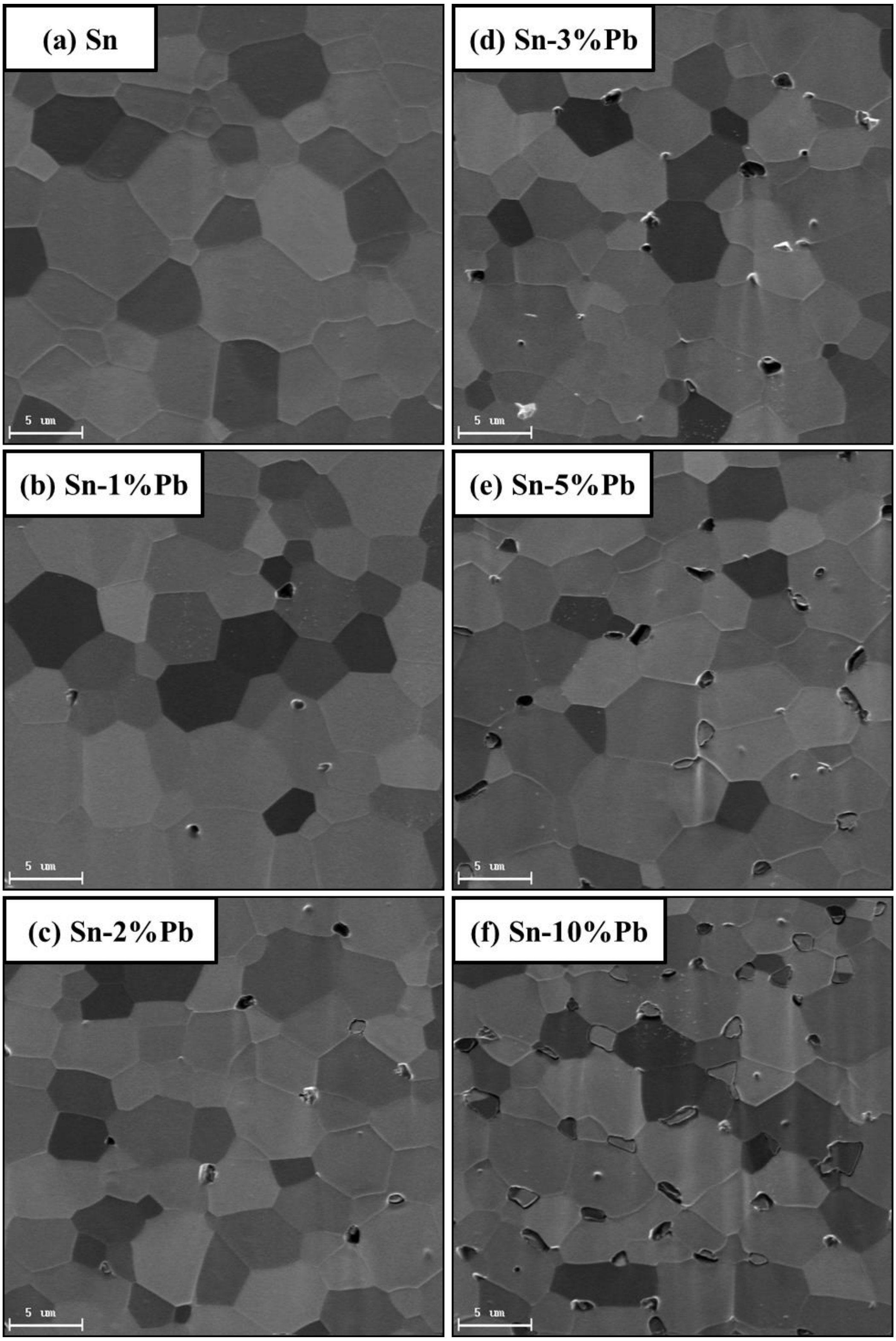

Fig. 3. Comparison with grain size and lead distribution of Sn-*x*Pb by FIB surface etching with gallium.

Fig. 4 shows the morphologies of all the plated samples after 24 hours on room temperature storage. Short tin whiskers have been confirmed only on the pure tin surface (see Fig.4a), while no morphological change on the plating with lead addition (Fig. 4b-4f). This indicates that only one day is enough to generate whiskers on pure Sn even under the room temperature to relieve the residual stress accumulated in the electroplating process. The surface images after the one year storage are presented in Fig. 5. These SEM images indicate that Sn whiskers can grow exclusively on the pure tin electroplated surface whereas hillocks are observed instead of whiskers on the Sn-*x*Pb plating surface irrespective of the lead content. The average density of Sn whiskers is about 2.28 counts/1000 μm^2 on pure Sn coating, while that of hillocks is less or equal to unity on all the Sn-*x*Pb samples (see Fig. 6). The maximum length and width among all the observed tin whiskers on the pure tin surface are about 52 μm and 5.8 μm, respectively. The hillocks found on Sn-*x*Pb plating surface have a witdth of 10.8 μm at maximum. Our frequent SEM observations have revealed that the continuous hillock growth is obvious during the first 10 days, but then gradually slows down to reach the saturation until the last observation after one year storage. All the lead added plating surfaces exhibit little change of surface and hillock morphology after the active growth found in the early days. This contrasts the unremitting whisker growth on pure Sn until the end of the storage tests. These observations lead us to the two possible explanations; (i) hillocks release the stress faster than tin whiskers; (ii) the stress accumulation continues for longer duration in pure Sn than lead added plating. It is not obvious to identify the reason directly from these surface observations. In any case, it is noteworthy that only 1 wt. % of lead addition drastically changes the stress relaxation mode from whisker growth to hillock creation.

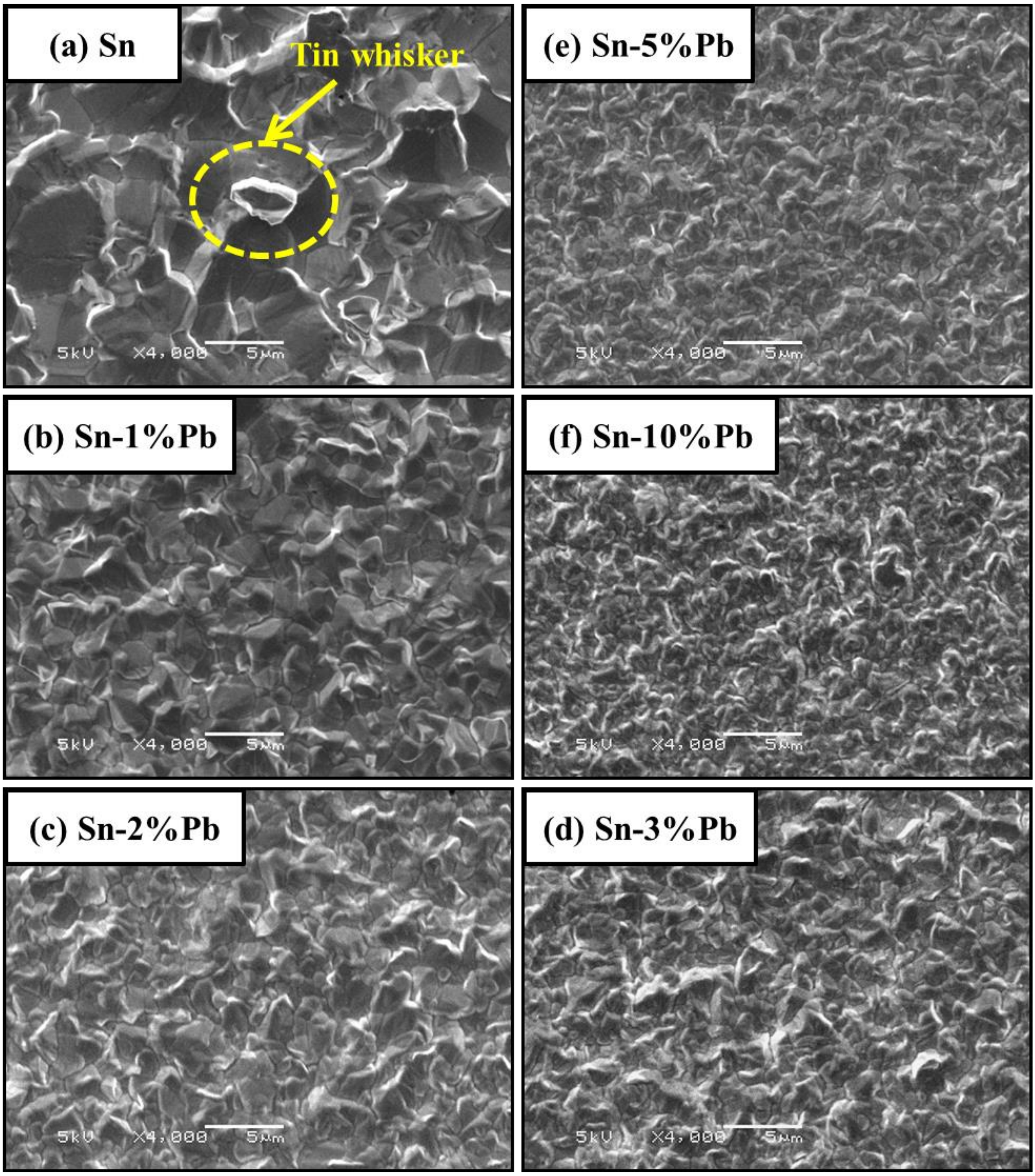

Fig. 4. The morphologies of electroplated Sn and Sn-*x*Pb after 24 hour on room temperature storage test.

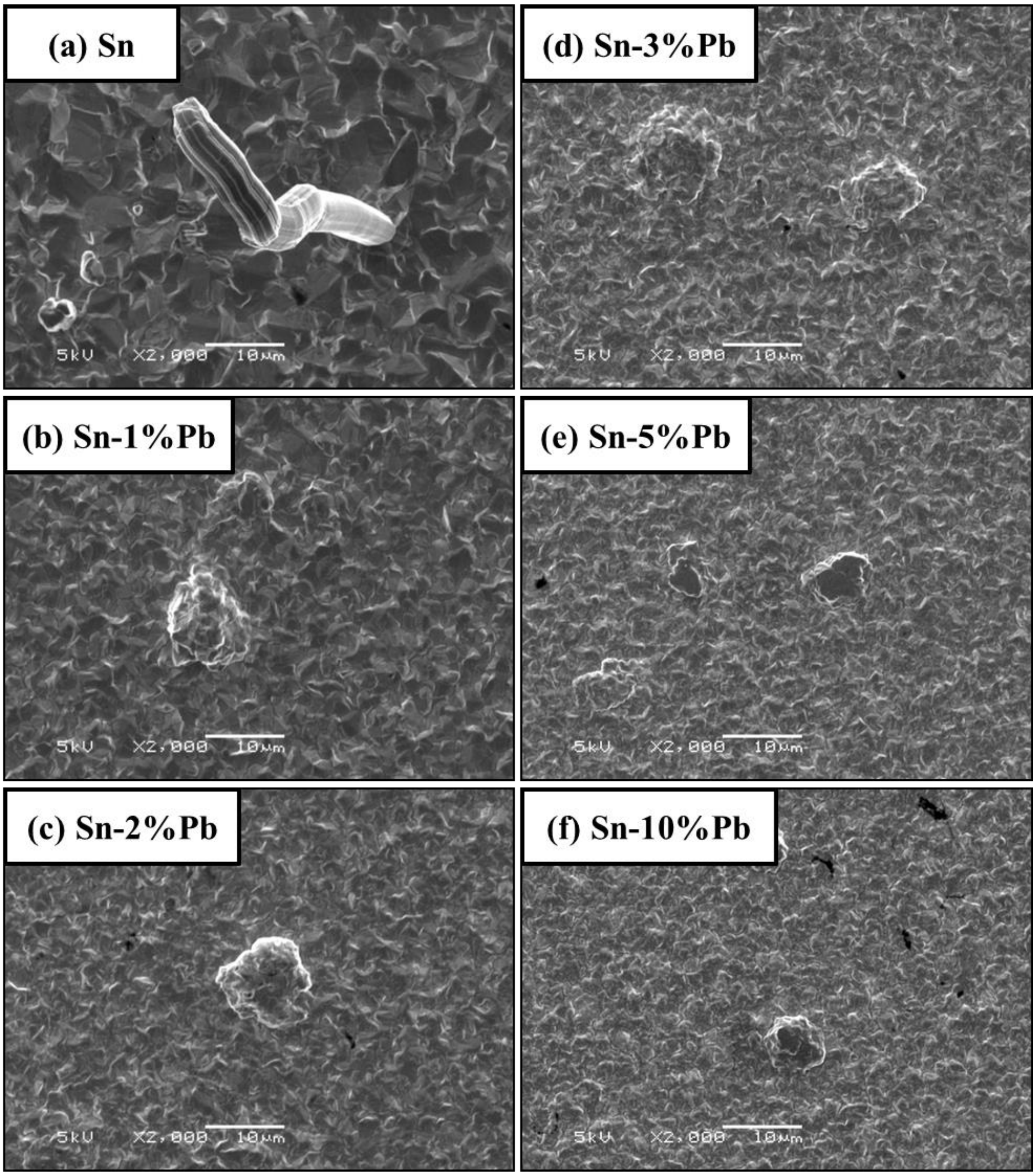

Fig. 5. The morphologies of electroplated Sn and Sn-*x*Pb after 1 year on room temperature storage test.

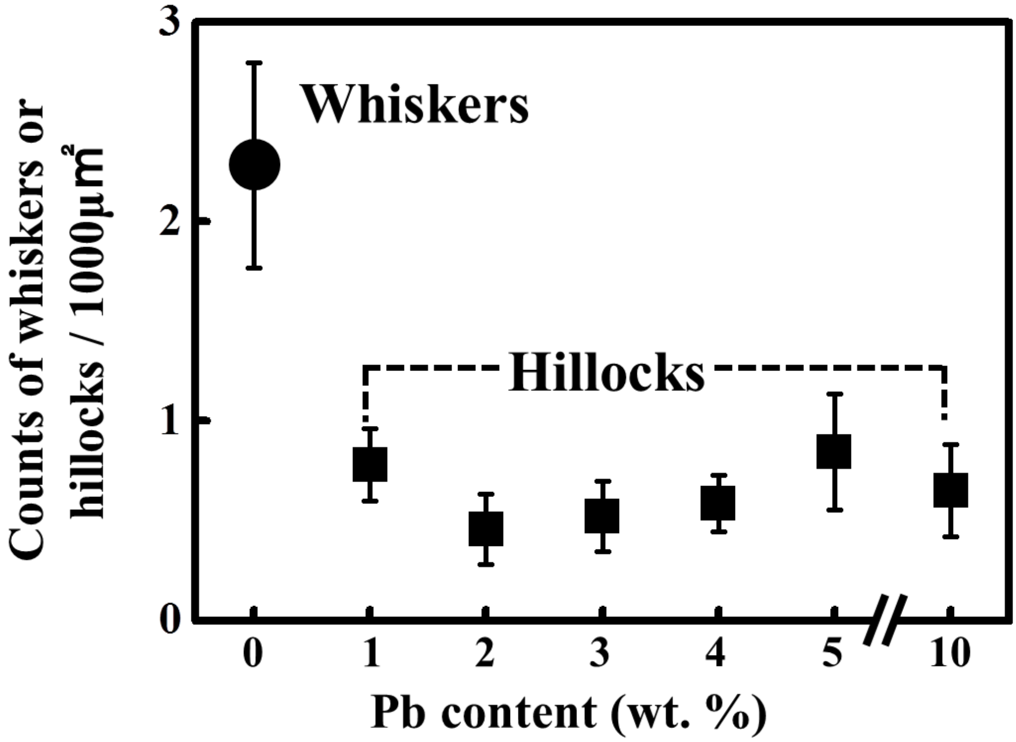

Fig. 6. Count of whiskers and hillocks on the each surface of Sn and Sn-*x*Pb after 1 year.

To investigate the source of internal compressive stress, cross-sectional observations have achieved by SEM. Fig. 7 shows the cross-sectional texture change during the long period storage tests: (a)-(d) as prepared, and (e)-(h) after one year at room temperature. At the beginning, pure Sn indicates a typical columnar structure in Fig. 7 (a). Both the structures of Sn-1Pb (b) and Sn-3Pb (c) appear to keep nearly columnar structure, but include some small Pb grains. In contrust, Sn-10Pb (d) exhibits a typical equiaxed grains including large Pb grains. More numbers of Sn grain boundaries becomes parallel to the substrate with increasing Pb content from 1 to 10 wt. %, since Pb co-deposition significantly reduces crystallographic texture orientation in Sn by preventing the columnar growth [7, 11]. All the

Sn grains found in Sn and Sn-*x*Pb samples have bulked up after one year without alternating the initial grain structures.

The IMCs at interface between Sn and Cu substrate continuously grow in all the samples during the one year at room temperature as shown in Fig. 7 (e-h). In the case of pure Sn plating, IMCs grow along Sn grain boundaries. Particularly large IMC growth can be observed at the boundaries of the root grain under the stemmed tin whisker (see Fig. 7e). Such a large IMC contributes to the increase of the compressive stress around the root Sn grain, and hence the whisker needs to grow at the surface to release the accumulated stress. In contrast, the volume of IMCs after one year in Pb added plating are smaller than that of pure Sn plating at Sn/Cu interface and at Sn grain boundaries. Moreover, the IMC growth in the Pb added Sn samples uniformly grew over the entire interface area during the one year of storage. These cross-section FIB observations in Fig. 7 reveal that tin whisker growth found only on pure Sn plating surface is due to the concentrated IMCs along the grain boundaries.

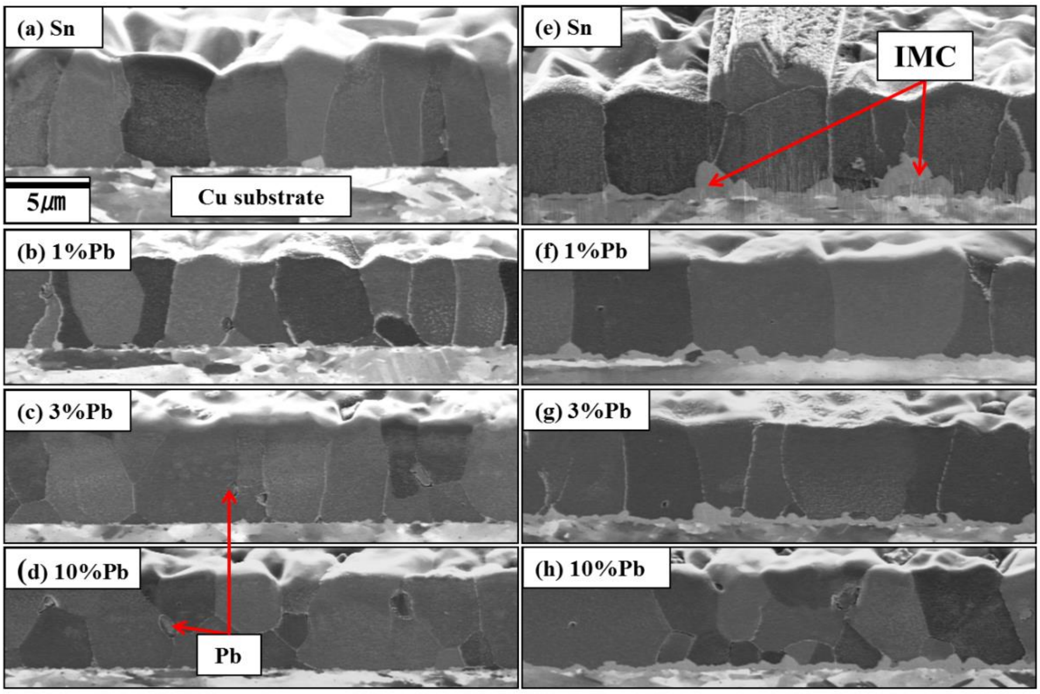

Fig. 7. Cross sectional views of Sn and Sn-*x*Pb (a) as state (b) after 1 year.

EDX results in Fig. 8 show the distributions of IMCs in pure Sn plating (a) and Sn-10Pb (b) on Cu substrate after one year. The determined composition is Cu_6Sn_5. The IMC growth patterns appear different in pure Sn and in Sn-10Pb samples. The IMCs of pure Sn grew to concentrate in grain boundaries which are consistent with the FIB cross-section analysis in Fig. 7, and the uniform growth pattern in Sn-10Pb as well. The IMC growth is faster and larger in pure Sn under room temperature than that in Sn-10Pb.

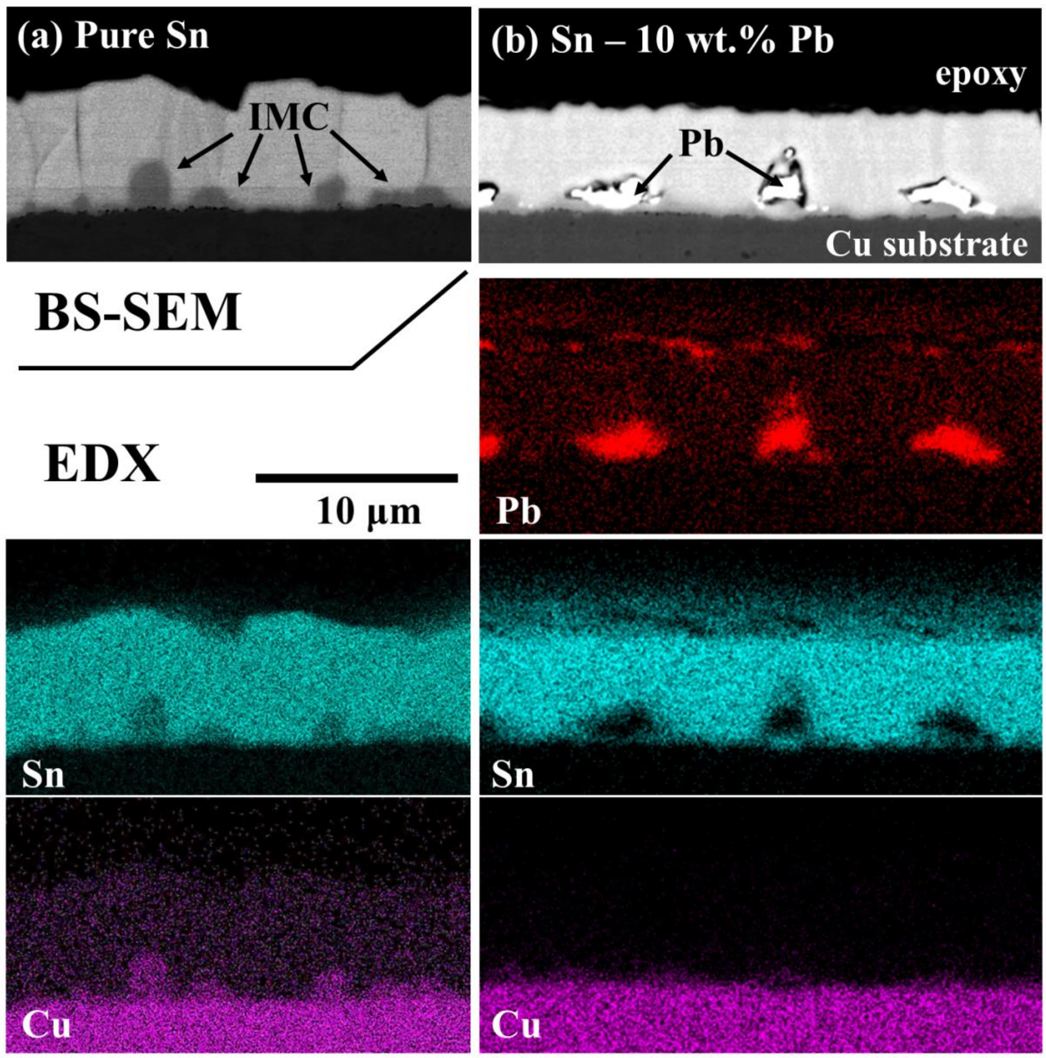

Fig.8. EDX analyses of Sn and Sn-10Pb after 1 year room temperature storage.

The back-scattered FE-SEM images in Fig. 9 display the final distributions of Sn grains, grown IMC, and segregated Pb in both pure Sn and Sn-10Pb plating samples after one year storage. The IMC growth along the Sn grain boundaries can be clearly seen in Fig. 9 (a)., while the Pb grains in Sn-10Pb appear to disturb the IMC growth at the grain boundaries (see Fig, 9 (b)). Consuming the diffused Cu atoms from the substrate, the IMC growth causes total volume increase of the plating. Larger the IMC volume, higher the compressive stress. Therefore, one can conclude that the compressive stress accumulated during the one year is higher in pure tin than in Sn-10Pb. This compressive stress due to the IMC growth changes the stress relaxation mode resulting in different surface morphologies such as whiskers or hillocks. This also implies that whisker needs higher compressive stress than hillocks to grow under the room temperature [5].

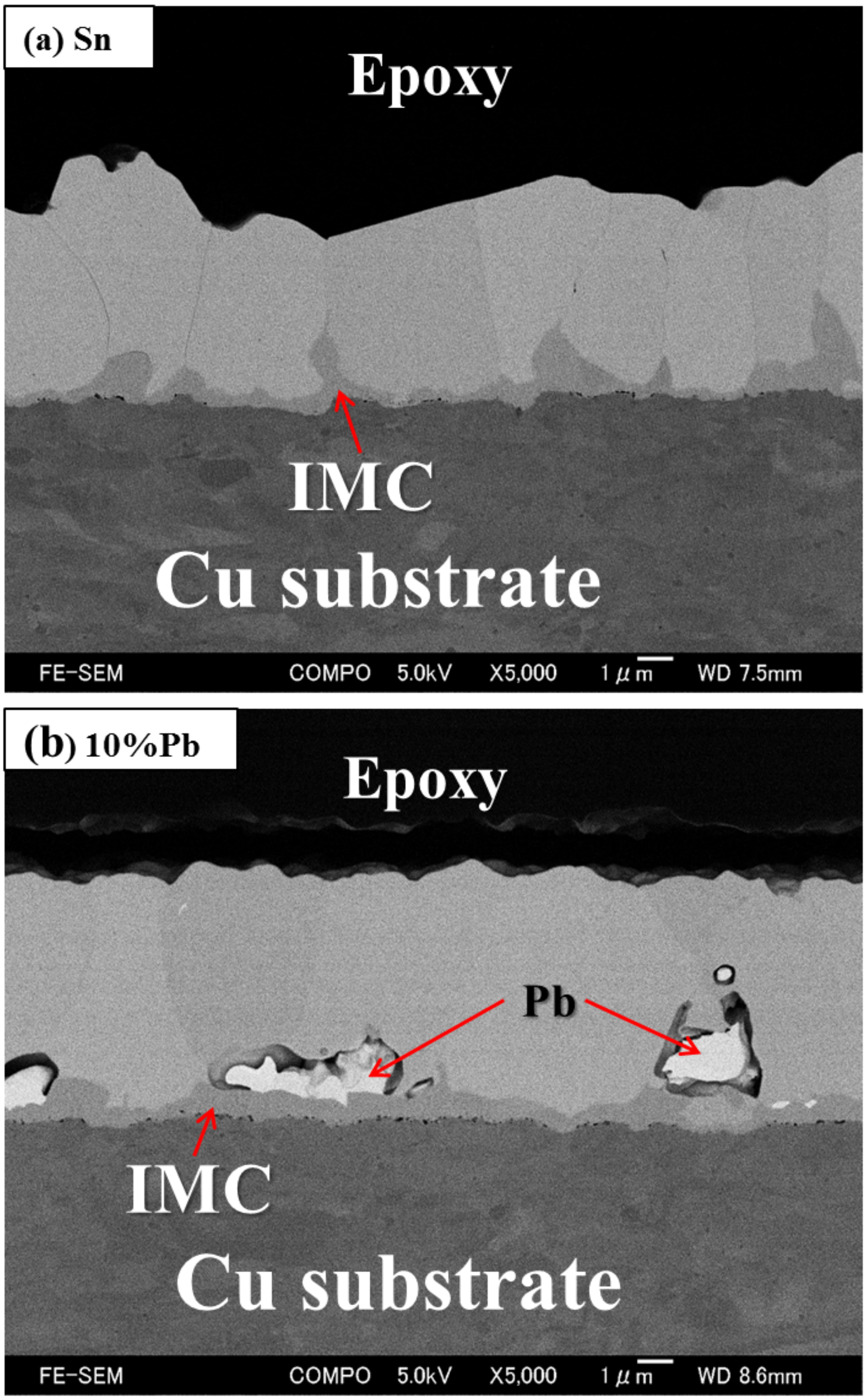

Fig. 9. IMC growth comparison of (a) Sn and (b) Sn-10Pb after 1 year room temperature torage.

The typical cross-sectional image of Sn hillock is presented in Fig. 10, observed on the Sn-1Pb sample surface after one year storage. The magnified image in Fig. 10 (b) displays that the Pb grain segregated at the Sn grain boundary blocks the IMC growth, particularly at the root of the hillock. W.J. Boettinger et al. proposed that such hillocks form due to the active mobility of more than one grains [7]. The considerably short IMC growth frees Sn grain boundary migration, and allows the grain growth to form the hillock. This hillock formation effectively releases the compressive stress without growing whiskers. It is noteworthy that this mechanism can be observed only 1 wt. % lead addition. Our observation proposes another whisker mitigation process without forming equiaxed grain structure.

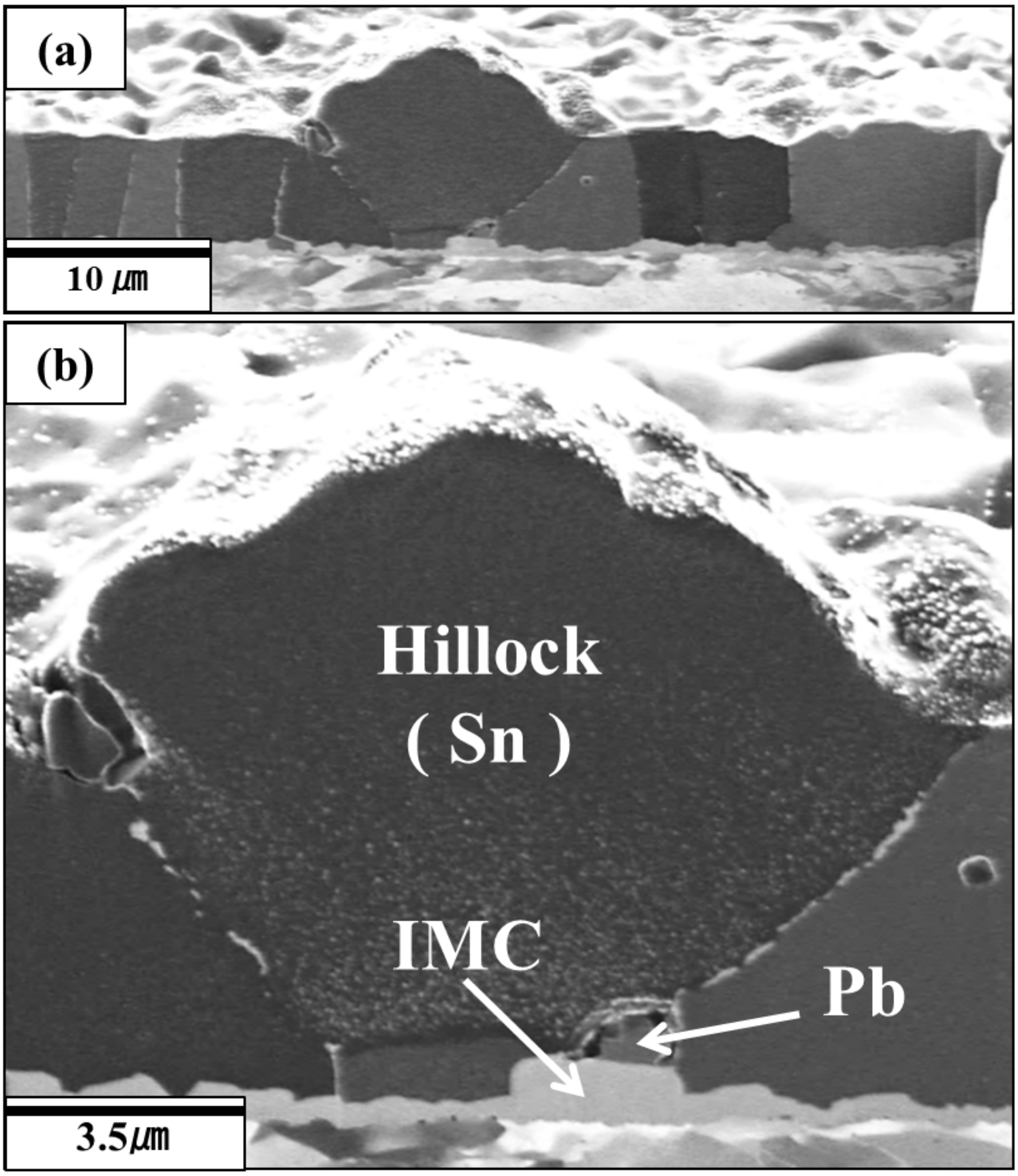

Fig. 10. Cross sectional views of Sn-1Pb (a) and magnification of hillock (b) after 1 year.

2.3.2 Intermetallic compound formation

The formation and growth of IMC formed under pure tin and Sn-1Pb plating after one year room temperature storage test are investigated by tin etching as shown in Fig. 11. The results of IMC dispersion also well supported the generation of whisker and hillock formation. In case of pure tin plating (Fig. 11 (a)), the IMC has mainly grown along the Sn grain boundaries, and forms a network structure covering the entire substrate surface. This network disturbs the grain boundary migration that relaxes the residual stress. As explained cross sectional analysis, therefore, the volume expansion from IMCs growth significantly contributes a compressive stress to tin plating layer, and then tin whisker generates to release the accumulated compressive stress. In the case of Sn-1Pb shown in Fig. 11 (b), the IMC forms more irregularly, and the volume is smaller than the case of pure tin plating. The different IMC growth is already reported by Jhang et al. [13]. They concluded that the lattice diffusion of Cu into Sn grains is enhanced with increasing Pb content in the deposits. However, the mechanism about higher lattice diffusion and hillock growth in the presence of Pb has not been reported [13].

The mobility of grain boundary is increased in Sn-*x*Pb due to the less IMC growth on grain boundary. That is the main reason of hillock formation instead of whisker for releasing the compressive stress under room temperature. It is noteworthy that a small amount addition of just 1 wt. % lead in tin changed the formation and growth of IMC during the room temperature storage. The ways of stress relaxation determined by the different IMC network formation are thus related to the growth of whiskers and hillocks.

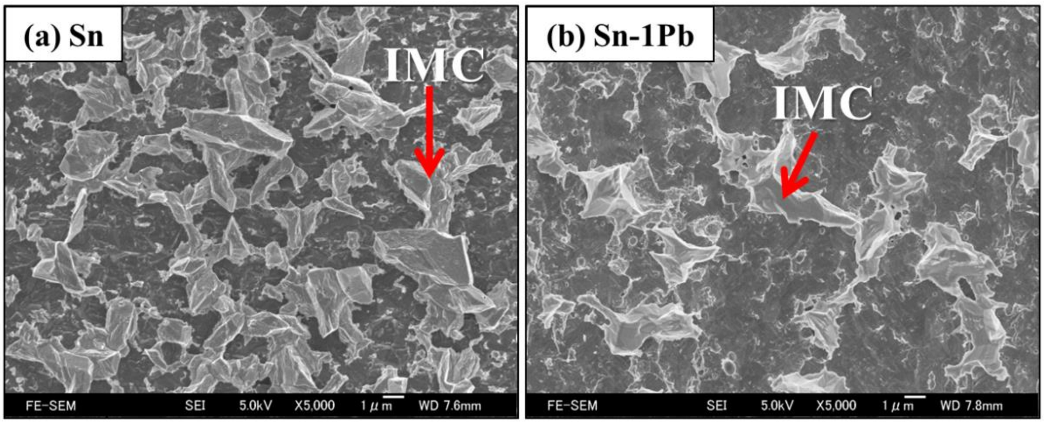

Fig. 11. The IMC dispersion of Sn (a) and Sn-1Pb plating after one year room temperature storage.

2.3.3 The formation mechanisms of tin whisker and hillock

The continuous process of accumulating and relieving compress stress during the one year storage are different in the pure tin plating and in that with 1 wt. % of lead addtion. Fig. 12 (a) illustrates the microstructure change in the pure Sn plating, from the initial as plated to the final state after one year. The grains of pure Sn and the IMC have been grown following to grain boundaries after one year. The grown IMC disturbs the mobility of Sn grain boundary. Therefore, the compressive stress caused by the volume expansion of IMC and grain growth of Sn can be relieved only by extrusion of Sn whiskers. That is a major cause of whisker generation in pure Sn under room temperature.

On the contrast, as-plated Sn-1Pb and after one year of Sn-1Pb are shown in Fig. 12 (b). The grain growth in Sn-1Pb is the same to that in pure Sn, but the IMCs growth are different. The Pb segregated between Sn grains interrupts the IMCs growth following to Sn grain boundaries. Thin IMC have uniformly formed on the interface. Therefore, the mobility of Sn grain boundary is not interfered during the one year. The dotted lines in Fig. 12 (b-2) indicate the grain boundary movement for one year. Hillock generation can effectively release the accumulated stress from volume expansion of grain and IMC. The columnar grain structure observed in Sn-1Pb is supposed to generate Sn whiskers in general, though 1 wt.% of lead addition into 5 μm plating is enough to mitigate Sn whisker up to one year of room temperature storage.

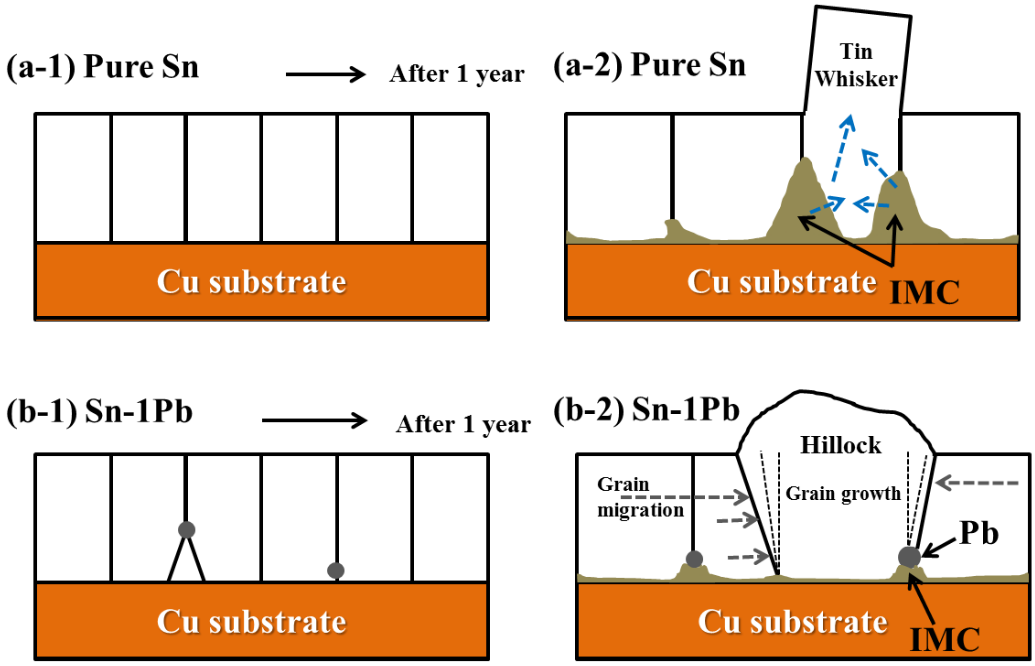

Fig. 12. The formation mechanisms of Sn whisker and (a) and hillock (b) under room temperature storage during one year.

2.4 Conclusion

Tin whisker mitigation process by lead addition has been investigated by comparing with pure matte Sn and Sn-*x*Pb electro plating with 5 μm thickness on Cu substrate. Tin whiskers have been observed only on pure Sn surface, and no whisker but hillocks on the lead added plating during the one year of room temperature storage test. In the tests, whisker growth is efficiently suppressed by only 1 wt. % of lead addition without altering the columnar to equiaxed grain structure. The whisker mitigation by such a small amount of lead addition is due to the suppressed IMC growth at the Sn grain boundaries, and freed grain boundary migration. Less obvious pinning of grain boundary migrations results in hillock growth that enough to release the compressive stress in the plating. Our results of higher lead content of 10 wt. % agree with the report in the literature [7], though the required amount of lead for whisker mitigation can be less or equal to 1 wt. %. The revealed mechanism of whisker mitigation by the least amount of lead addition would indicate the required properties of metal additives that can suppress whiskers like lead. Considering the low solubility of Pb in Sn, we would suggest that Bi can be a replacement candidate of lead for tin whisker mitigation.

References

1. H.P. Howard, J. Cheng, P.T. Vianco, J.C.M. Li, "Interface flow mechanism for tin whisker growth", Acta Mater., 59(10), pp.1957-1963 (2011)
2. G.T. Galyon, "A History of Tin Whisker Theory: 1946 to 2004 ", in SMTAI U.S.A (2004), September 26-30, on SMTAI International conference (SMTAI): Chicago
3. H.L. Cobb, "Cadmium whiskers", Monthly Rev. Amer. Electroplaters Soc. 33(28), pp.28–30 (1946)
4. K. G. Compton, A. Mendizza, and S. M. Arnold, "Filamentary growths on metal surfaces – "Whisker"", Corrosion-National association of corrosion engineers, 7, pp.327-334. (1951)
5. B. Horváth, B. Illés, T. Shinohara, G. Harsányi, "Whisker growth on annealed and recrystallized tin platings", Thin solid films, 520(17), pp.5733-5740 (2012)
6. K. Suganuma, A. Baated, K.S. Kim, K. Hamasaki, N. Nemoto, T. Nakagawa, T. Yamada, "Sn whisker growth during thermal cycling", Acta Mater. 59, pp.7255-7267 (2011)
7. W.J. Boettinger, C.E. Johnson, L.A. Bendersky, K.-W. Moon, M.E. Williams, G.R. Stafford, "Whisker and Hillock formation on Sn, Sn–Cu and Sn–Pb electrodeposits", Acta Mater. 53, pp.5033-5050 (2005)
8. K.N. Tu, J.C.M. Li, "Spontaneous whisker growth on lead-free solder finishes", Mater. Sci. Eng. A, 409, 131-139 (2005)
9. J.W. Osenbach, R.L. Shook, B.T. Vaccaro, B.D. Potteiger, A.N. Amin, K.N. Hooghan, P.Suratkar, and P. Ruengsinsub, "Sn whiskers: material, design, processing, and post-plate reflow effects and development of an overall phenomenological theory", IEEE Trans Electron Pack Manuf 28, 36 (2005)

10. E. Chason, N. Jadhav, F. Pei, “Effect of layer properties on stress evolution, intermetallic volume, and density during tin whisker formation”, JOM 63(10), 62-68 (2011)
11. N. Jadhav, J. Wasserman, F. Pei, E. Chason, “Stress Relaxation in Sn-Based Films: Effects of Pb Alloying, Grain Size, and Microstructure”, J. Electron. Mater. 41(3), 588-595 (2012)
12. M. Sobiech, J. Teufel, U. Welzel, E.J. Mittemeijer, W. Hugel, “Stress Relaxation Mechanisms of Sn and SnPb Coatings Electrodeposited on Cu: Avoidance of Whiskering”, J. Electron. Mater. 40, 2300-2313 (2011)
13. W. Zhang, F. Schwager, “Effects of Lead on Tin Whisker Elimination”, J. Elctrochem. Soc. 153(5), C337-C343 (2006)

Chapter2

Least lead addition to mitigate tin whisker for ambient storage

Chapter 3

Thermal stress driven Sn whisker growth: in air and in vacuum

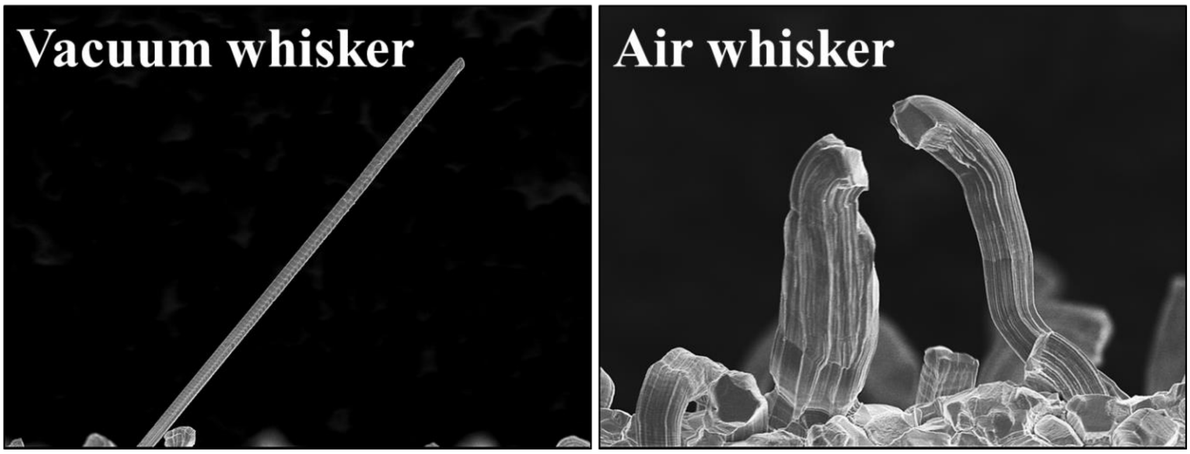

Thermal cycling whisker in vacuum and air (Jung-Lae Jo, 2013)

Abstract

In this chapter, whisker growths from matte tin electroplating have been observed during thermal cycling up to 1000 cycles either in air or in vacuum. The density, length, and width of thermal stress whiskers depend on the plating thickness of 2 μm and 5 μm in the present study. Whiskers grown on the 2 μm plating are longer and thinner than those on 5 μm plating. In both cases, whiskers grow thinner and faster in vacuum than in air. These apparent variations come from the grain sizes and the thermal stress distributions in the electroplating, intrinsically different in 2 μm and 5 μm thick films. The grain structure of whisker root, particularly grain boundary cracks oxidized in air, determines the stress concentration to drive the whisker growth. Cracking caused by oxidation was rarely observed in vacuum hence causes thin and strait whiskers even from thick plating. These results indicate that the stress concentration at whisker root grain is essential for controlling whisker growth morphology, and has a critical impact on various electronic applications. The present work also, establishes the fundamental understanding of whisker growth mechanism in air and vacuum.

3.1 Introduction

The thermal stress in plating is caused by mismatching coefficients of thermal expansion (CTE) between tin and substrate under varying temperature. Severe thermal cycling, i.e. stress cycling of compression and tension, is often unavoidable in electronic applications [1-5]. Typical and severe thermal conditions can be in auto vehicles and in satellites [6-7]. The operation temperature in the former case easily exceeds the limit of Si-based semiconductors. In the latter case, the electronic components permanently face to the thermal cycling in vacuum, and have to survive for long period without any maintenance. Nevertheless the reliability of electronic components is critical in both the cases, the severe thermal stress cycles – with or without surface oxidation – lead to the risk of Sn whisker growth [8].

In this chapter, hence focuses on the tin whisker growth driven by thermal stress, tested with severe thermal cycling in either air or in vacuum. Furthermore, two different thickness of Sn plating are examined for stress variation. The film thickness effect on the whisker growth from Sn films deposited on a Cu layer has been examined in the literature [9]. The study concluded that thicker plating effectively relaxed the compressive stress, and was more advantageous for reducing whisker density [9]. However, the Sn plating on Cu layer was severely affected by the interface IMCs, and the whisker growth too.

This present work, the influence of interface IMC is carefully eliminated by using 42 alloy as a substrate since the IMC growth rate is sufficiently slow and negligible within the period of our thermal cycling tests. We have then found that all the growth properties of the density, the maximum length, and the width of thermal whiskers are dependent on the thickness of the tin plating, i.e. thermal stress, in both the air and vacuum conditions. The thermal cycling in vacuum generally grows longer and thinner whiskers than those in air, and the similar tendency is confirmed for thinner plating films. These findings imply that the morphological properties of thermal whiskers are determined by the stress concentration on whisker root grain. Understanding the stress caused by thermal cycling in Sn films is hence the key for whisker risk managements in the electronics, particularly for aerospace applications.

3.2 Experimental

Matte tin films were electroplated with the electric current of 5 A/dm^2, on a 300 μm thick lead-frame sheet made of 42 alloy (42%Ni-57%Fe). The electroplating process time was 48 seconds for 2 μm thick films, and 136 seconds for 5 μm. All the specimens were cleaned with distilled water after the plating. A part of typical electroplated lead-frame sample is presented in Fig. 1(a).

The thermal cycling tests have been performed in a specially-designed vacuum chamber (ULVAC, Inc, Japan), which can maintain a high vacuum at the order of 10-4 Pa during the thermal cycling from 80 ℃ to -20 ℃. The temperature of the specimens was controlled by a *Peltier* thermoelectric device (UTC200A; Ampere Co. Ltd, Japan) built in the vacuum system. The thermal and stress cycling tests were continued up to 1000 cycles either in air or in vacuum. We adopted the same thermal cycling profile for both the tests in air and in vacuum; The heating and cooling rate are about 22 ℃ / min and 11 ℃ / min, respectively. The dwell time was set to 15 minutes at both the high and low peak temperatures. Thus, one thermal cycling took about 45 minute, and the total testing time of 1000 thermal cycles was about 750 hour.

The growth behavior of tin whiskers and surfaces were frequently observed during the thermal cycling tests by field emission scanning electron microscopy (JSM-5510S, JEOL, Japan), and growth properties like whisker length, width, and density were recorded as a function of the number of thermal cycles.

In this study, cross-section observations of Sn films and whiskers were carried out using a focused ion beam microscope (FIB; Hitachi FB-2100). FIB machine was also used to study the Sn grain distributions of the plating microstructure, by etching the topmost surface of the film down to 500 nm depth. The ImageTool (UTHSCSA, U.S.A.) was utilized for microscope image analysis to obtain the whisker growth properties like length and width.

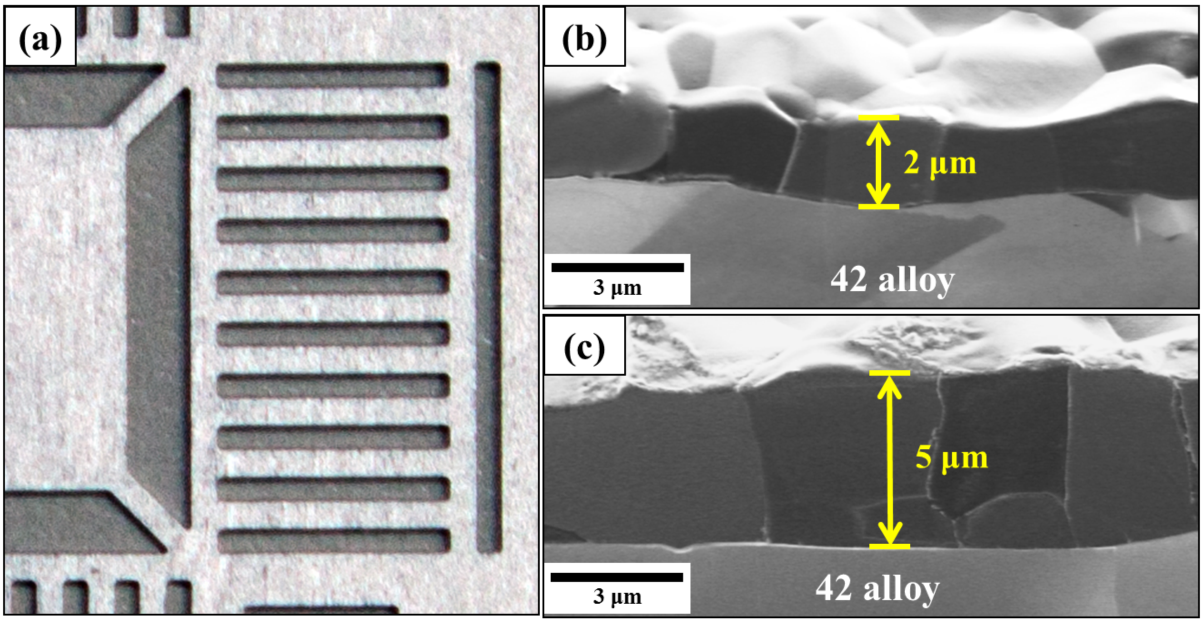

Fig. 1 Matte Sn electroplating on QFP lead frame; (a) a part of the frame sheet; (b) cross-section SEM observations of as-deposited films: (b) 2 µm, and (c) 5 µm thickness.

3.3 Results and discussion

3.3.1 Whisker growth after the thermal cycling in air

Cross sections of 2 μm and 5 μm as-plated films are presented in Fig. 1 (b)-(c). Both the films before thermal cycling tests have no crack at grain boundaries, and also no IMC at the interface between Sn films and 42-alloy substrate. The lack of interface IMC assures that the whisker growth is driven by thermal stress cycles in our present study. Fig. 2 displays typical whisker morphologies grown on 2 μm plating (a)-(b) and 5 μm plating (d)-(e) after 750 thermal cycles in air. Long and thin filament-like whiskers are observed on 2 μm plating, while short and thick winding whiskers, so-called nodule whiskers, on 5 μm film. The global distributions of whiskers on a part of the electroplated lead frame can be seen in Fig. 2 (c) and (f). Most of the whiskers exhibit winding nodule shape as shown in Fig.2 (e), typical for those grown by thermal cycles in air,. However, a considerable number of thin and straight whiskers can be found on 2 μm plating (See Fig. 2 (b)). The density of Sn whiskers is higher on 5 μm plating than that on the 2 μm (Compare Fig. 2 (c) and (f)).

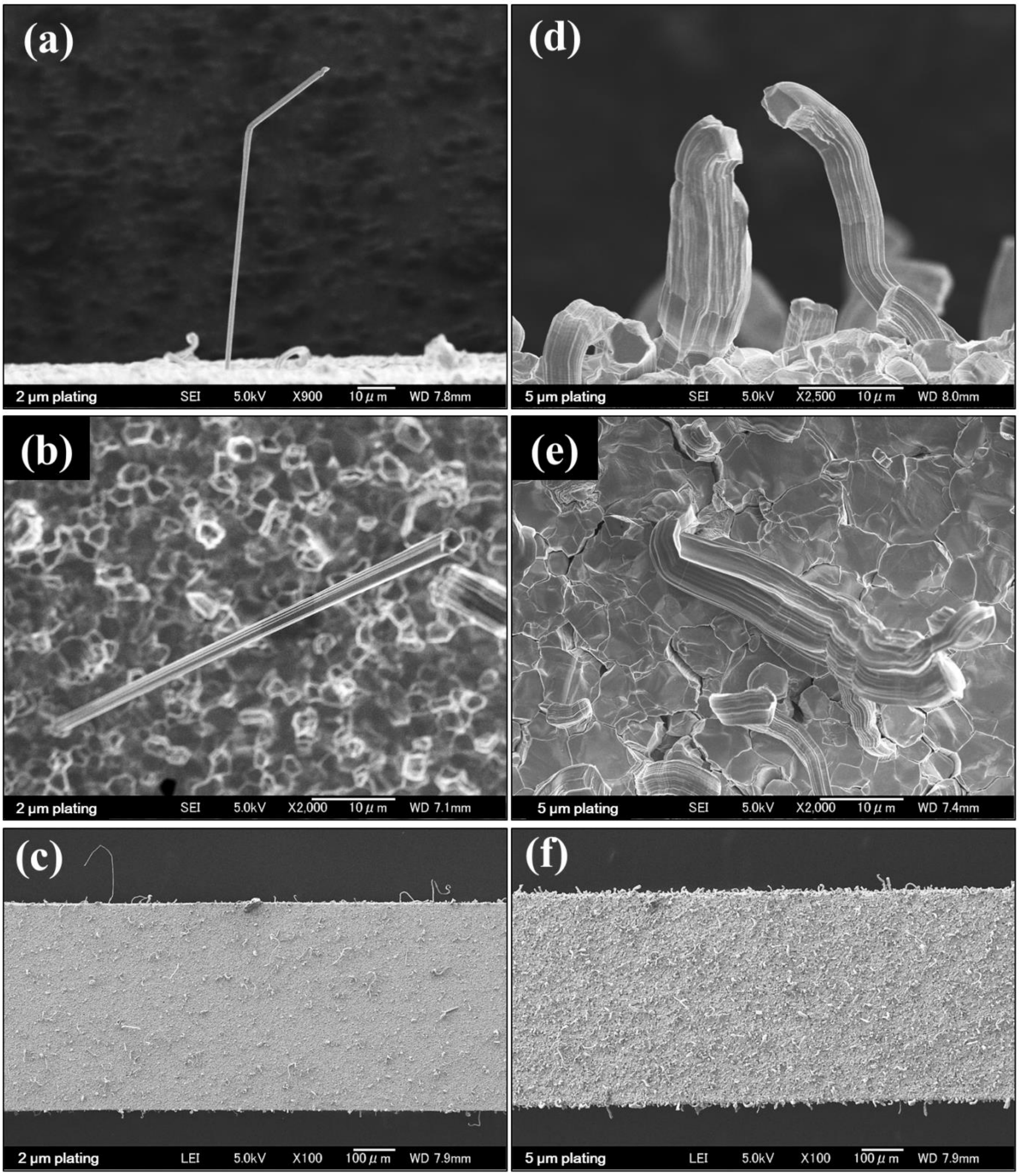

Figure 2 Typical Sn whiskers grown by thermal stress cycling in air; (a) on 2 µm plating after 750 cycles; (b)-(c) after 1000 cycles; (d) on 5 µm plating after 750 cycles, (e)-(f) after 1000 cycles.

The statistical characterization of the whisker growth properties on 2 μm and 5 μm thick films are summarized in Fig. 3. The count, density and maximum length of whiskers increases with increasing thermal cycles regardless of the plating thickness. The effect of plating thickness on whisker density described above is confirmed in Fig. 3 (a), as whiskers grow always denser on the thicker plating irrespective of the thermal cycles. The average width of whiskers on each plating thickness appears almost unchanged during the thermal cycles (see Fig.3 (b)), and thinner plating leads thinner whiskers. The maximum whisker length found on 2 μm plating is longer at any thermal cycle counts than that on 5 μm. These results from Fig. 2 and Fig. 3 indicate that the plating thickness has an obvious effect on the whisker growth morphology, i.e. the count density, average width, and maximum length during thermal cycling in air.

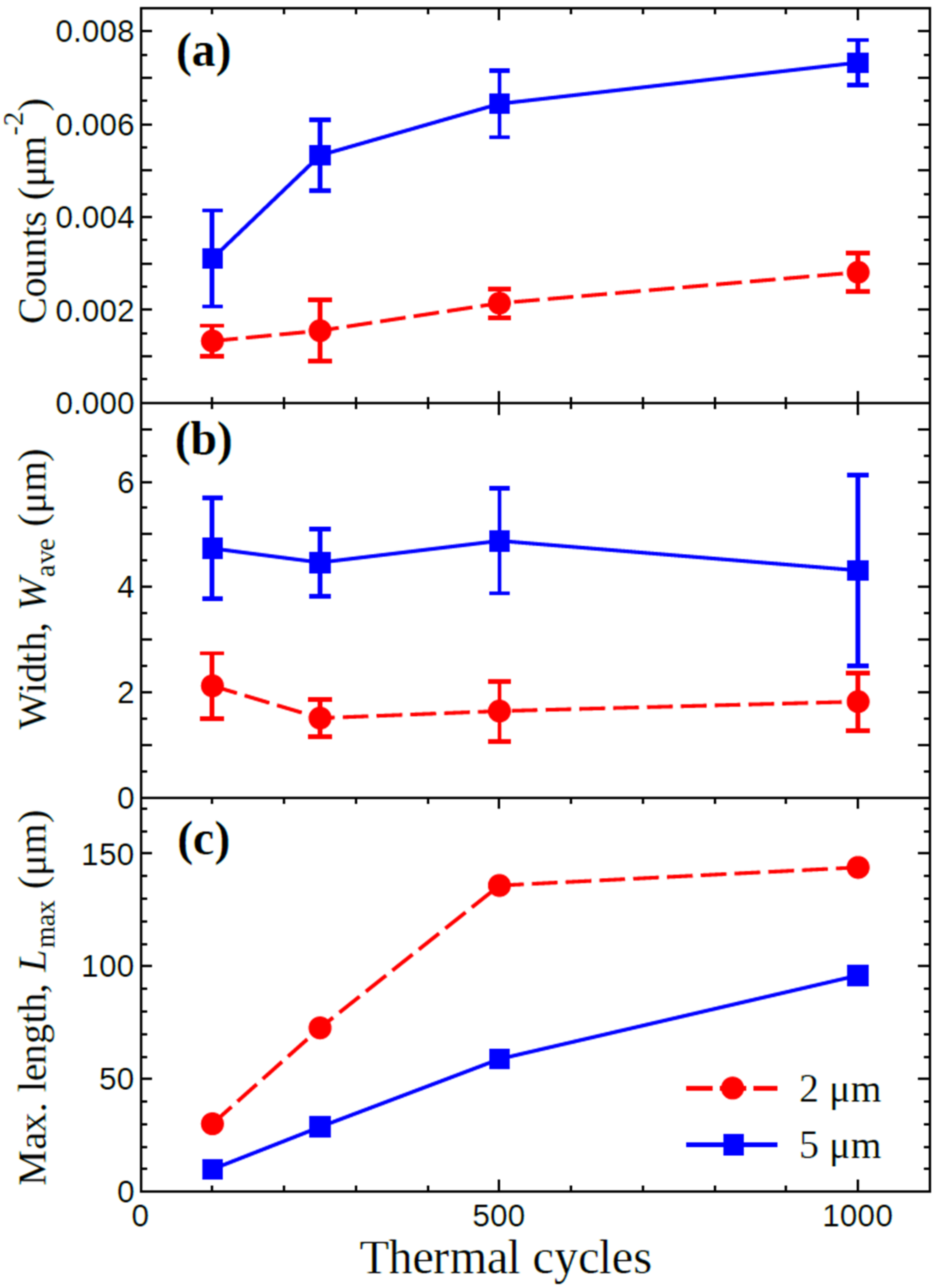

Fig. 3 Whisker growth characterization with increasing number of thermal stress cycles; (a) density, (b) width, and (c) maximum length of whiskers found on 2 μm and 5 μm thick plating.

These thickness effects may originate from the internal grain structures of the plating. FIB imaging can reveal the difference of macrostructures in as-deposited plating films with different thickness, as compared in Fig. 4 (a) and (b). The top most surface of 500 nm thck was etched out by gallium ion beam, and the microstructure images were taken by contrasting the crystal oriatiation of each Sn grain. From these FIB images, the average grain sizes of 2 μm plating and 5 μm plating were determined to about 2.0 μm and 5.2 μm, respectively. The grains in 5 μm plating were about two times larger than those in 2 μm plating. Since both the thickness and the grain size contributes to the internal stress distribution under the thermal cycling, the different film properties result in the variation of whisker morphologies.

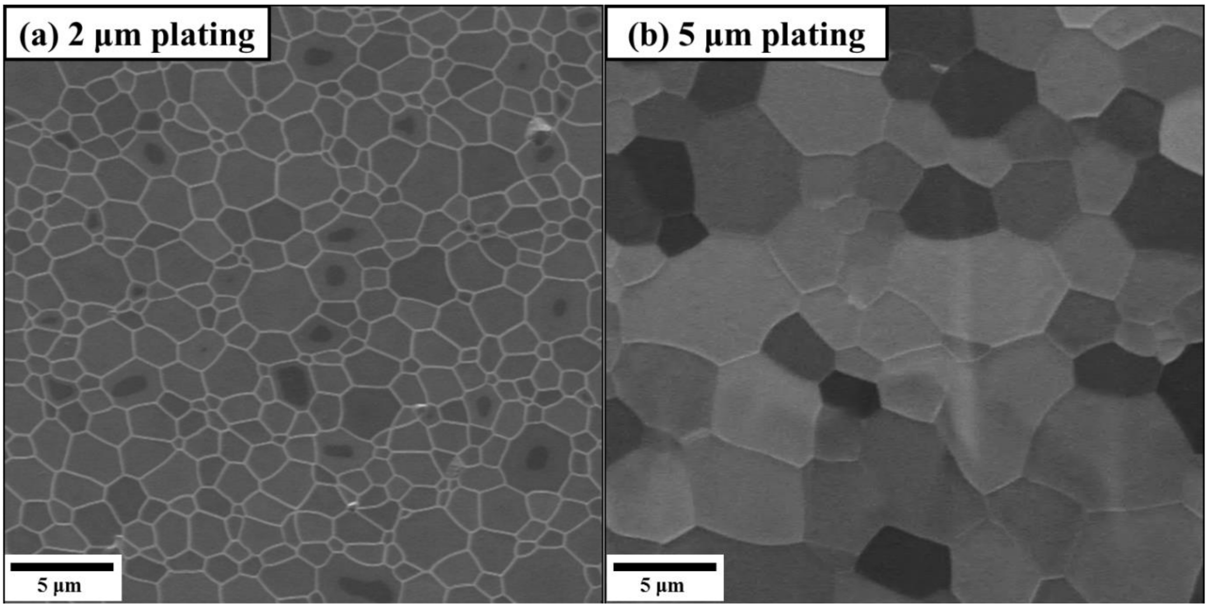

Fig. 4 FIB etching and imaging reveals that the grain sizes of as-deposited Sn electroplating are dependent on the film thickness: (a) 2 μm, and (b) 5 μm plating.

Another critical effect during the thermal cycling in air is the surface oxidation of Sn plating, which leads to grain boundary cracking. The back-scattered electron (BSE) microscopy images in Fig. 5 display grain boundary cracking on the plating surfaces after 1000 thermal cycles in air. These surface cracks mainly occur at Sn grain boundary are attributed to the thermal fatigue induced by oxidation [1]. On the 5 μm plating, a whisker is accompanied by well-developed cracks, i.e. grooves, around its root grain. In contrast, the cracks around the whisker on the 2 μm plating appear much narrower. These features of root cracks may affect the whisker growth; thick whiskers on 5 μm plating are developed with continuous bending during thermal cycling due to the large root grooves, as shown in Fig. 5(b), while those on 2 μm plating grow rather straight with shallow cracks around a whisker root (see Fig. 5(a)).

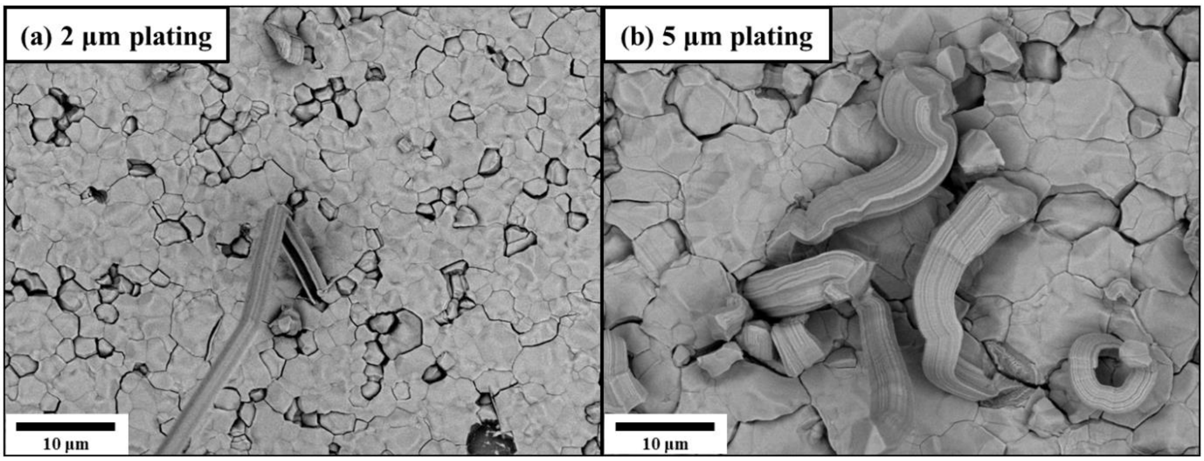

Fig. 5 Surface comparison of 2 μm (a) and 5 μm (b) plating after 1000 thermal stress cycles in air; Grain boundary cracks are clearly observed by back-scattering electron (BSE) microscope imaging.

The detailed grain structures at whisker root can be seen in Fig. 6. Typical whiskers on each plating thickness are observed by FIB cross section imaging in the figures. After the 500 thermal cycles in air, large and deep grooves have been developed on the 5 μm plating (see Fig. 6(d)). The yellow arrows in Fig. 6(d) indicate the deep root cracks around the thick whiskers almost reaching to the 42 alloy substrate. The cracks at the root of the thin and long whisker in Fig. 6(b) appear shallow, though the plating around the root grains is getting thinner. The cracking depth on 2 μm plating is thus limited presumably because of the atomic diffusion coming from surrounding grains. In this case, the limited cracking progress levels the remaining film thickness around the whisker. The Sn mass for whisker growth is supplied through this remained film channel; the well-balanced and continuous atom flows from the surrounding grains supports the straight whisker growth.

One can assume that concentrated stress at the root grain is the driving force of whisker growth. Fig. 6 shows that the deeper crack side, i.e. thinner remaining film, is coincident with the outer side of bending, indicating the whisker growth rate is faster than the other side. Since root cracking in thicker films may not progress equally, unbalanced cracking induces bending whisker. In thinner films, the limited cracking around a whisker increases the probability to grow straight whiskers. Thus the film thickness and stress concentration around whisker root is essential to determine the shape of whiskers grown by thermal stress cycling.

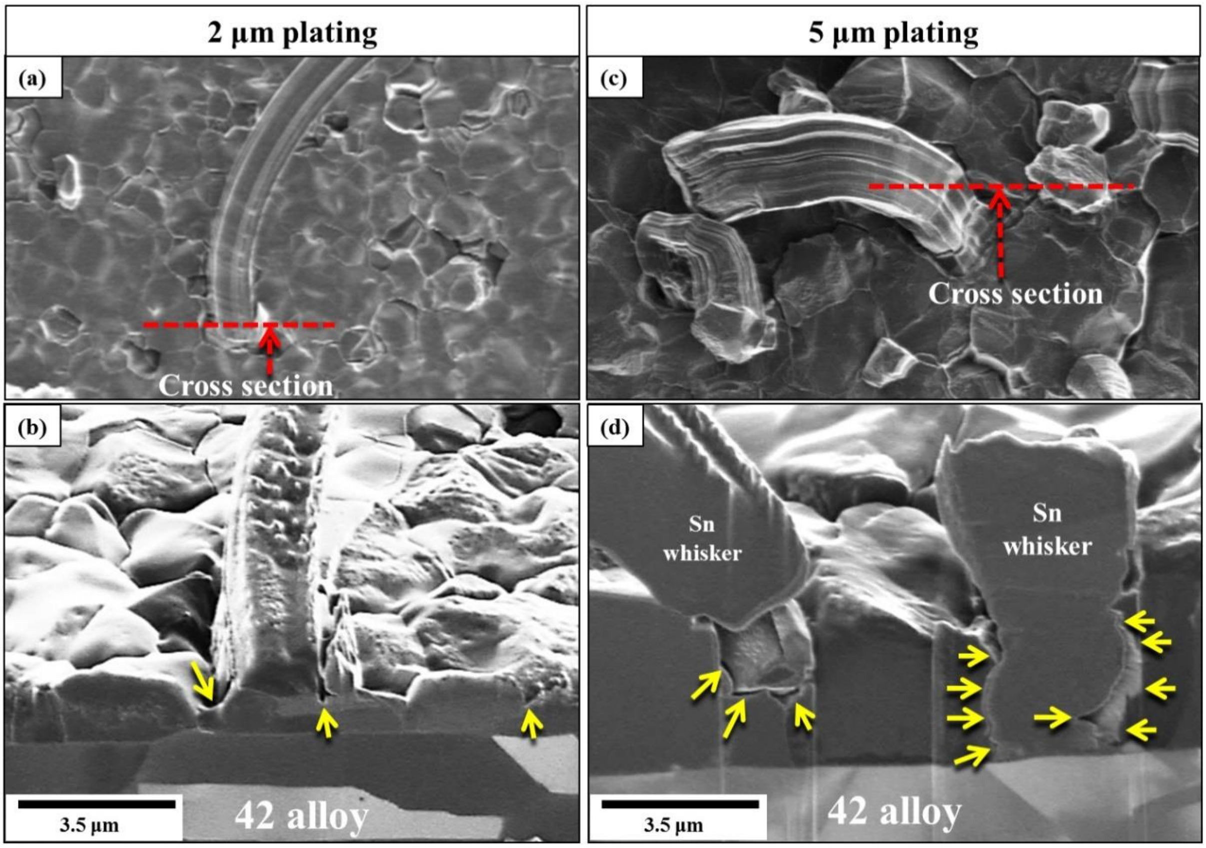

Fig. 6 Root grain structures and surrounding oxidation cracks of Sn whiskers grown by 500 thermal stress cycles in air: (a) on 2 μm plating, and (b) 5 μm plating. FIB imaging is used for the imaging, and also for cross-sectioning specimens shown in (c) and (d). Arrows in the figures indicate oxidation cracks.

3.3.2. Comparison of thermal cycling effect in air and vacuum

The thermal cycling of with 2 μm and 5 μm Sn plating has been tested in vacuum. The degree of vacuum was kept about 4×10^{-4} Pa during the thermal cycle tests. The maximum whisker length on each 2 μm and 5 μm plating has been recorded by FE-SEM observation with increasing thermal cycles (see Fig. 7). The similar tendency can be seen in air and in vacuum: whiskers grow longer on 2 μm plating than on 5 μm plating. Obvious difference is, however, that whiskers grow faster in vacuum than in air (compare with Fig. 7 and Fig. 3(c)). For example, the maximum length of the whiskers grown on 5 μm plating after 100 thermal cycles are 41 μm in vacuum, but only 10 μm in air. This agrees well with the results in previous reports by K. suganuma et.al. [1].

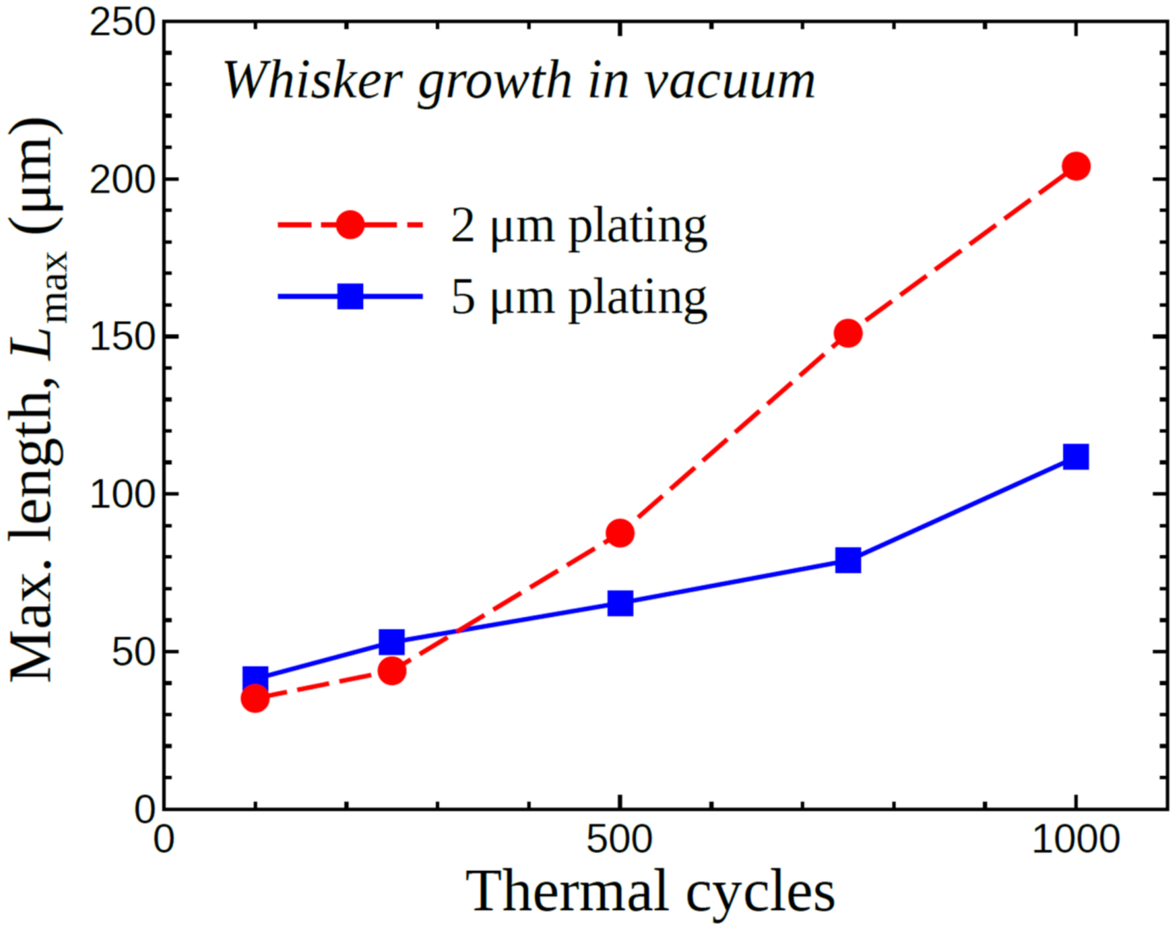

Fig. 7 Sn whisker length grown by thermal stress cycling in vacuum; comparison with the different thickness of electroplating.

The whisker growth features after 1000 thermal cycles in the overall testing conditions are summarized in Fig. 8. The longest whisker about 204 μm is observed on 2 μm plating in vacuum thermal cycling (see Fig. 8(c)). Sn whiskers in vacuum thermal cycling are longer than in air thermal cycling as compared with same plating thickness shown in Fig. 8 (c). However, whiskers on 2 μm plating are longer than all that on 5 μm plating irrespective of air and vacuum condition.

The count density and the whisker width in Fig.8 (a) and (b) display a tendency opposite to the whisker length. Whiskers on 5 μm plating exhibit thicker width and higher density than those on 2 μm plating regardless of atmospheric conditions. Both the largest width and the highest density are obtained in the case of 5 μm plating in air thermal cycling (see Fig. 8(a)). The averaged whisker width presented in Fig. 8(b) indicates that the whiskers in vacuum grow considerably thinner than those in air. There is an obvious correlation here; lower the whisker density, shorter the width. As we see in Fig. 3 and Fig. 4, the width of whiskers basically comes from the grain size in plating.

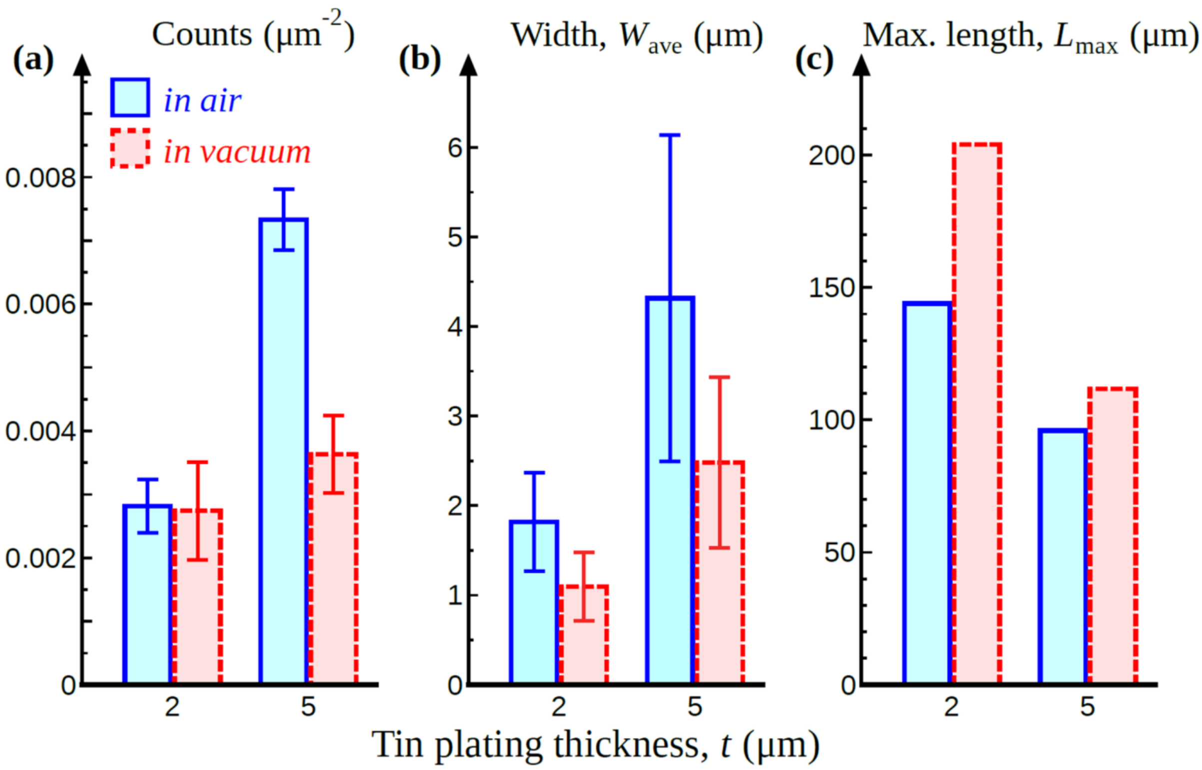

Fig. 8 Growth properties of thermal stress whiskers; comparison of the Sn electroplating thickness (2 μm and 5 μm) after 1000 thermal cycles either in air, and in vacuum.

To investigate the correlation between the whisker width and density, the grain size distributions of the FIB images in Fig. 4 are converted to the histogram plots in Fig. 9. The arrows in Fig.9 indicate the averaged width of thermal whiskers in air and in vacuum (see Fig. 8 (b)). In each case of the 5 um and 2 um films, the averaged whisker width in air is coincident with the averaged grain size in the plating. However, the width of whiskers is considerably thinner in vacuum as shown in Fig. 8 (b), and the different width is also indicated by the arrows in Fig. 9. The grain size corresponding to the whisker width in vacuum shows lower relative frequency than that at the average grain size in both the film thicknesses. This change of relative frequency in grain size agrees with the whisker density change found in Fig. 8 (a). The present statistical analysis implies that the whisker width is originated from the root grain size in our thermal cycling experiments, and thus the morphological properties of thermal whiskers are determined by grain structures in plating films.

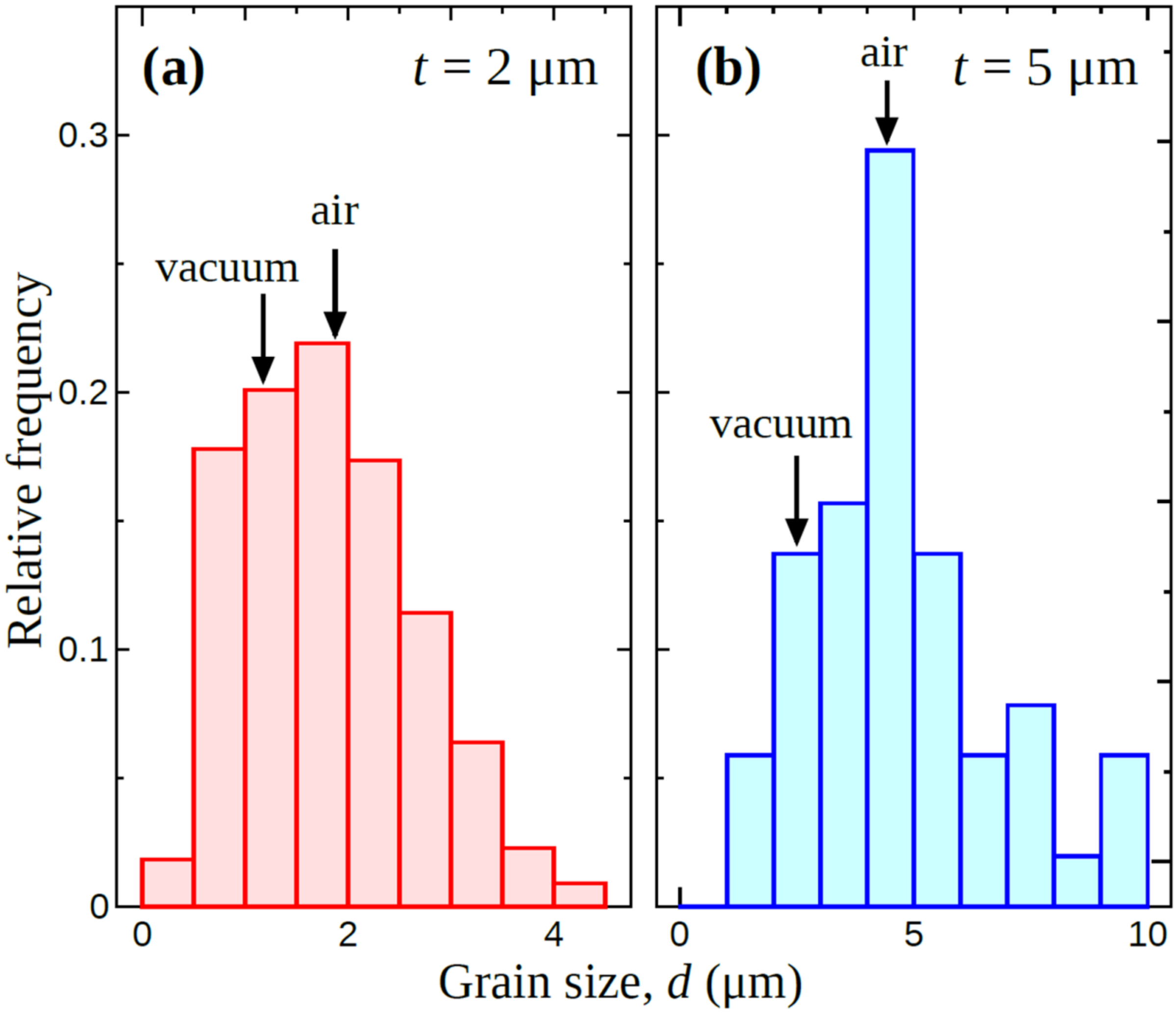

Fig. 9 Histogram of grain size distributions observed in Fig. 4: (a) 2 μm, and (b) 5 μm plating.

To clarify the effect of atmospheric environments, the 5 μm plating samples after the 100 thermal cycles either in air or in vacuum are compared in Fig. 10, focusing on the cross sections of whisker root grain structure. Even at the early stage of the thermal cycling, the grain boundary cracking has progressed deeply in air (see Fig.10 (a-b)), while no boundary cracking can be observed in vacuum as shown in Fig.10 (c-d). Thus the oxidation critically induces grain boundary cracking during thermal cycling. As seen in Fig.10 (a-b), the unbalanced cracking progress around the whisker root is the origin of bended whisker growth in air. In the vacuum, straight whiskers like a filament are grown because of the absence of grain boundary cracking. This is the source of different morphology of thermal stress whisker growth between in air and in vacuum.

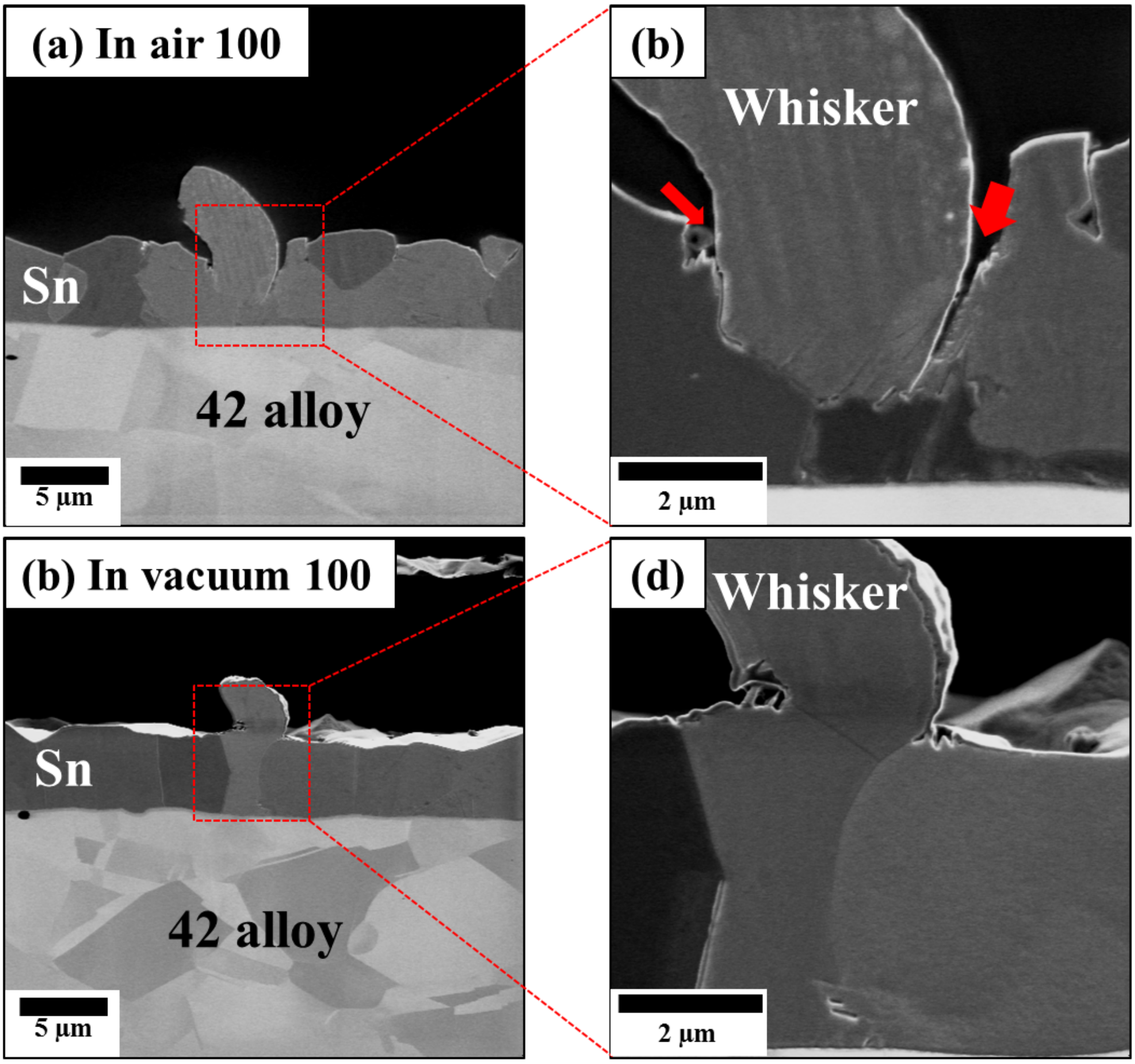

Fig. 10 Cross-sectional images of whisker-root grain in 5 μm thickness electroplating samples at an early stage of thermal stress cycling; (a) after 100 thermal cycles in air, and (b) in vacuum. Arrows in the figure indicate oxidation cracks at the root grain boundaries found only after thermal cycles in air.

FE-SEM images in Fig.11 certify the characteristic whisker growth comparison in air (a) and in vacuum (b). The whiskers shown in Fig. 11 are all on the 5 μm plating samples after 250 thermal cycling. In air, grain boundary cracking is obviously confirmed together with thick and bended whiskers. Moreover, large grooves can be seen near the whisker roots indicated by yellow arrows in the figure. In contrast, a thin and straight whisker is found in vacuum without any boundary cracking or groove near the whisker root (see Fig.11 (b)). Such a straight and long whisker on 5 μm plating can be obtained only in vacuum avoiding any oxidation cracking. The sound contacts at the grain boundary secure the Sn diffusion path toward the whisker, and enables strait and fast whisker growth. These characteristics difference in whisker growth morphology in air and in vacuum are consistent both with the cross section observation in Fig. 10, and with the statistical analysis in Fig. 8.

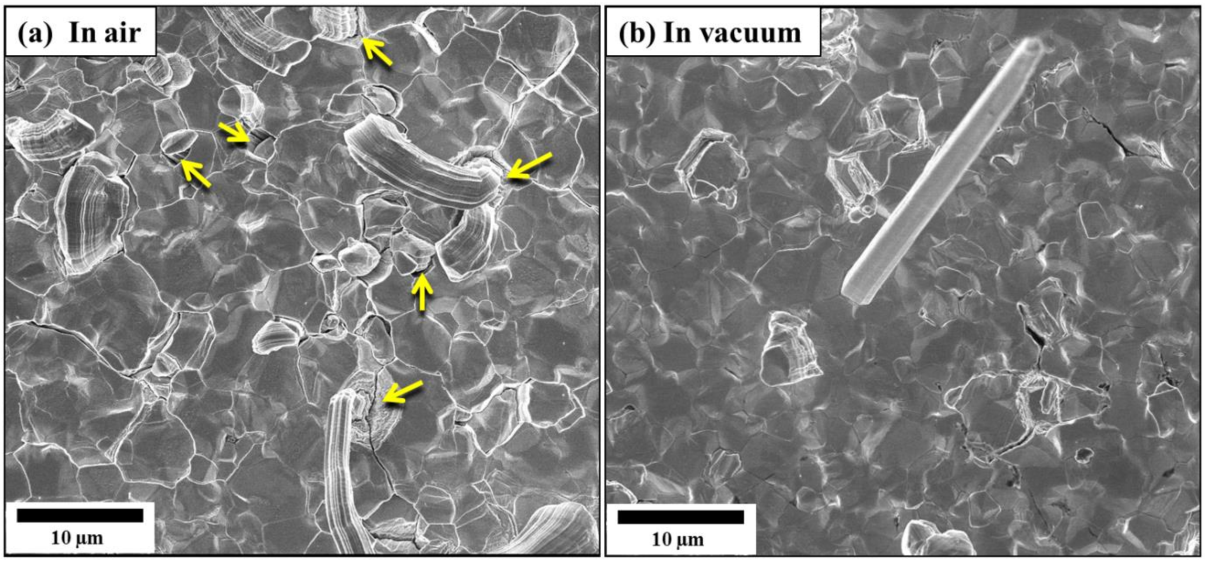

Fig. 11 Whiskers from 5 μm Sn electroplating found after 250 thermal stress cycles; (a) in air, and (b) in vacuum. On the thick Sn plating, thin and strait whiskers can be grown only in vacuum.

3.4 Conclusion

In this chapter, thermal stress driven whisker growth has been investigated on 2 μm and 5 μm matte Sn electroplating. In general, the thinner plating generates longer and thinner whiskers, but less dense than the thicker plating during thermal cycling. The whisker growth is deeply correlated to the grain size distributions in the plating, as well as the thickness. The atmospheric conditions during thermal cycling are critical, and determine the whisker shape – straight or bended – through grain boundary cracking induced by surface oxidation of Sn. The thermal whiskers in vacuum are hence longer and thinner than those in air. The average whisker width is related to the whisker density through the grain-size distribution in the as deposited plating. Overall, the thermal stress whiskers are dominated by the original grain structure in the electroplating, and the surface oxidation gives the variation of whisker morphologies. These investigations here would contribute to the whisker risk management in electronic packaging for critical applications like satellite and automobile, as well as toward the fundamental understanding of the growth mechanisms of Sn whiskers.

References

1. K. Suganuma, A. Baated, K.-S. Kim, K. Hamasaki, N. Nemoto, T. Nakagawa, and T. Yamada, “Sn whisker growth during thermal cycling”, Acta. Mater., 59, pp.7255-7267 (2011)

2. J. W. Shin, and E. Chason, “Stress behavior of electroplated Sn films during thermal cycling”, J. Mater. Res., 24(4), pp.1522-1528 (2009)

3. J.-L. Jo, S. Nagao, T. Sugahara, M. Tsujimoto, and K. Suganuma, “Thermal stress driven Sn whisker growth: in air and in vacuum”, J. Mater. Sci. - Mater. Electron., (2013) doi : 10.1007/s10854-013-1336-6

4. C. Xu, Y. Zhang, C. Fan, and J. A. Abys, “Driving Force for the Formation of Sn Whiskers: Compressive Stress—Pathways for Its Generation and Remedies for Its Elimination and Minimization”, IEEE Trans. Electron. Packag. Manuf., 28(1), pp.31-36 2005

5. B. Vandevelde, M. Gonzalez, P. Limaye, P. Ratchev, and E. Beyne, “Thermal cycling reliability of SnAgCu and SnPb solder joints: A comparison for several IC-packages”, Microelectron. Reliab., 47, pp.259-265 (2007)

6. H. Leidecker, L.Panashchenko and J. Brusse, “Electrical Failure of an Accelerator Pedal Position Sensor Caused by a Tin Whisker and Discussion of Investigative Techniques Used for Whisker Detection”, in University of Maryland, U.S.A (2011), September 14-15, on the 5th International Symposium on Tin Whiskers

7. NASA homepage : Whisker failures, http://nepp.nasa.gov/whisker/failures/

8. W. J. Boettinger, C. E. Johnson, L.A. Bendersky, K.-W. Moon, M. E. Williams, and G. R.

Stafford, "Whisker and hillock formation on Sn, Sn-Cu and Sn-Pb electrodeposits", Acta. Mater., 53, pp.5033-5050 (2005)

9. E. Chason, N. Jadhav, F. Pei, "Effect of layer properties on stress evolution, intermetallic volume, and density during tin whisker formation", JOM 63(10), pp.62–68 (2011)

Chapter3

Thermal stress driven Sn whisker growth: in air and in vacuum

Chapter 4

Mitigation of Sn whisker growth by small Bi additions

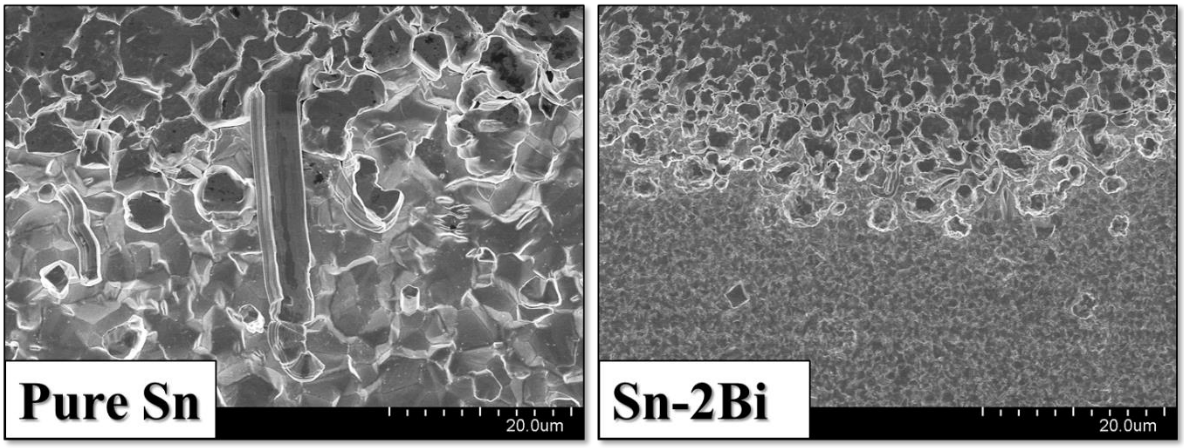

Surface of pure Sn and Sn-2Bi after 3days indentation (Jung-Lae Jo, 2013)

Abstract

In this study, the morphological development of electroplated matte Sn and Sn–*x*Bi (*x* = 0.5, 1.0, 2.0 wt. %) film surfaces was investigated under diverse testing conditions: one-year room-temperature storage, high temperature and humidity (HTH), mechanical loading by indentation, and thermal cycling. These small Bi additions prevented Sn whisker formation; no whisker growth was observed on any Sn–*x*Bi surface during either the room-temperature storage or HTH testing. In the indentation loading and thermal cycling tests, short surface extrusions (less than 5 μm) were occasionally observed, but only on *x* = 0.5 and 1.0 wt.% plated samples. In all test cases, Sn–2Bi plated samples exhibited excellent whisker mitigation, while pure Sn samples always generated many whiskers on the surface. We confirmed that the addition of Bi into Sn refined the grain size of the as-plated films and altered the columnar structure to form equiaxed grains. The storage conditions allowed the formation of intermetallic compounds between the plated layer and the substrate regardless of the Bi addition. However, the growth patterns became more uniform with increasing amounts of Bi. These microstructural improvements with Bi addition effectively released the internal stress from Sn plating, thus mitigating whisker formation on the surface under various environments.

4.1 Introduction

Eliminating the use of Pb in electronic device packaging has actively been pursued for the last decade due to the Restriction of Hazardous Substances directive for electronic equipment [1, 2]. Electroplating of the packaging is also expected to be Pb free, even though Sn–Pb alloys have ideal properties for soldering: excellent wettability, reasonably low melting points, and superior tolerance against Sn whisker formation under various environments. Sn whiskers can grow up to a few millimeters under usual operating conditions and may cause short-circuit failures and malfunctions in electronic components. For example, a whisker of length more than 100 µm easily forms a bridge in fine pitch wiring and electrode systems, which are becoming ever smaller with the trend of device miniaturization [3, 4]. Various methods for mitigating Sn whisker formation have hence been proposed. For instance, heat treatment at 150 ℃ for more than 30 min typically releases the residual stress in a material. Annealing creates a uniform intermetallic compound (IMC) layer at the interface between the Cu substrate and the plated layer and prevents further IMC growth along the grain boundaries by reducing the Cu diffusion rate [5-7]. The grain sizes in both the electroplated films and the interface IMC (Cu6Sn5) are related to the plating thickness [8]; thick plating is generally effective in relieving compressive stress. It has been observed that the thicker the plating, the lower the whisker density [9, 10].

Recently, we have revealed the whisker mitigation mechanism by adding a trace amount of Pb, which effectively suppressed whisker growth on Sn plating for over one year of ambient storage [11]. Even the addition of 1 wt. % Pb effectively suppressed Sn whiskers by inhibiting grain boundary IMC growth without altering the columnar grain structure.

In this study, we propose the addition of a small amount of Bi, instead of Pb, to avoid whisker growth on Sn electroplating surfaces [11]. When alloying Bi with Sn, the columnar grains of the films changed to equiaxed grains [12]. Under thermal cycling, the measured stress of 7.5-μm Sn with 2.5–10 wt. % Bi content showed a relaxation similar to that of Sn–Pb plating samples. Here we investigate the addition of smaller amounts of Bi, i.e., Sn–xBi (x ≤ 2 wt. %) electroplating, and demonstrate whisker mitigation under various environmental conditions. We also show that Bi addition achieves equiaxed grain structures in thinner as-plated Sn films (5 μm) as well as finer grain sizes. All Bi-doped samples exhibit excellent whisker mitigation in our tests: long-term ambient storage, high temperature and humidity (HTH), mechanical loading, and thermal cycling. The excellent results of these environmental tests prove that small Bi additions achieve a Pb-free whisker mitigation of Sn electroplating under relevant operating conditions for electronic devices.

4.2 Experimental

Matte Sn and Sn-*x*Bi (*x* = 0.5, 1.0, 2.0 wt. %) films were electroplated on a copper and 42 alloy (Fe-Ni) lead-frame sheet for quad flat packaging, using an electric current density of 2 A/dm^2. The electroplating process was carried out in a three-litter bath of solution with a pH of 1 at 25 ℃ for 310 s. After the electroplating, all the samples were cleaned with distilled water, and then dried for 20 s using a dry air gun. The film thickness was about 5 μm for all the samples. Table 1 shows the details of the electroplating conditions.

Table 1 Substrate types, plating thickness, and amount of Bi addition.

Substrate	Copper	42 alloy
Plating thickness	5 μm	5 μm
wt. % of Bi	0, 0.5, 1, 2	0, 0.5, 1, 2

All the samples were characterized by the four types of tests; ambient storage for one year, HTH, mechanical loading by ball indentation, and thermal cycling. We prepared 42 alloy lead-frame sheets for thermal cycle testing, because the coefficient of thermal expansion (CTE) mismatch is large in the combination of Sn plating and the substrate enough to accelerate thermal stress cycling. In addition, the effect of IMC growth during the thermal cycling can be eliminated because of the negligible diffusion of Fe/Ni into Sn plating. The details of the testing conditions are presented in Table 2.

Table 2 Variations of the tests, testing period, conditions, and substrate material.

Test type	*Period & cycles*	*Variables*	*Substrate*
Room temperature storage	**1 year**	**25±5 °C / 25 %**	**Copper**
High humidity/temperature	**1000 hours**	**85 °C / 85 RH %**	**Copper**
Indentation loading	**up to 3 days**	**300 g (*r* = 100 µm ball)**	**Copper**
Thermal cycling	**up to 100 cycles**	**-20 °C to 80 °C**	**42 alloy**

One year ambient storage tests at room temperature were carried out for all the samples. A custom indentation tool was used for the loading test with a ZrO_2 ball of 300 g. Thermal cycling tests were performed up to 100 cycles in a testing chamber (UTC200A, Ampere. Co. Ltd, Japan). HTH tests were carried out for 1000 h using a high humidity and high temperature chamber (SH-221, Espec, Japan). Fig.1 shows schematic diagrams of all the tests performed in this work.

The growth behavior of Sn whiskers and the evolution of the surface microstructure were observed by field emission scanning electron microscopy (FE-SEM 2100, JEOL, and SU0820, HITACHI, Japan.). A focused ion beam (FIB) microscope (Hitachi FB- 2100, Japan) was utilized to fabricate cross-sectional samples of the coatings, whiskers, and hillocks, and also to perform imaging. The grain sizes of Sn and Sn-*x*Bi films were determined at 1 µm depth from the upper surface using the FIB etching and microscopy.

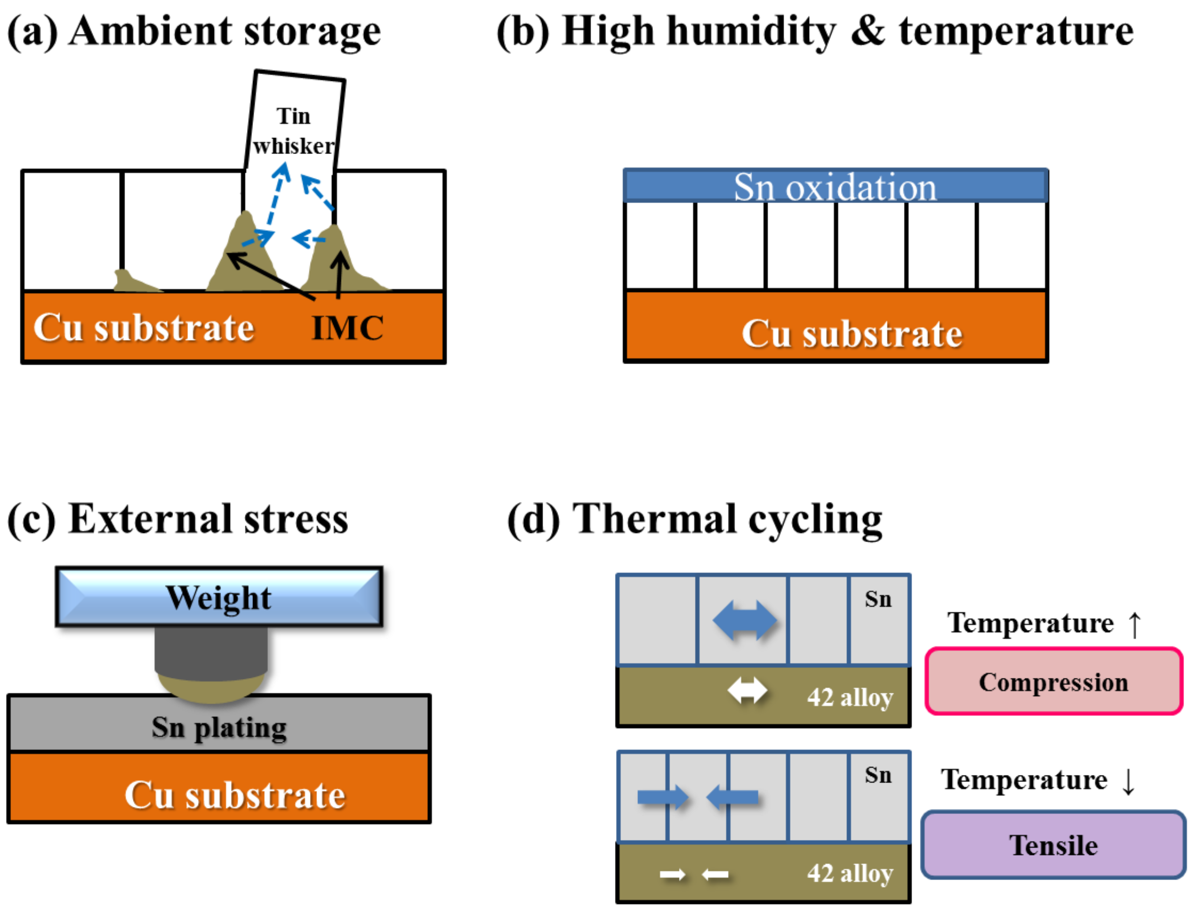

Fig. 1 Schematic diagram of (a) ambient storage test, (b) high humidity / temperature test, (c) loading test and (d) thermal cycling test.

4.3 Results and discussions

4.3.1 Surface evolution of Sn-*x*Bi electroplated films during environmental testing

Fig. 2 shows the results of the ambient storage tests (a) as-plated and (b) after one year. All the prepared samples appear to have flat surfaces without any whiskers or cracks, but the morphologies of the top-most surfaces are different according to the amount of Bi addition; the size of the surface grains decreased with increasing Bi content in the Sn, (see Fig. 2 (a)). The small amount of Bi addition thus results in Sn grain refinement. A similar effect by Sn-Pb alloying has been reported in the literature [11, 13-14]. As shown in Fig. 2(b), Sn whiskers can be observed only on the pure Sn surface during the one year ambient storage. Usually, Sn whiskers grow within 24 h after electroplating process on a pure Sn-plated surface [11]. Here in contrast no whisker is seen on the Sn-*x*Bi surfaces irrespective of the Bi content, while only hillocks are observed on the Sn-0.5Bi and Sn-1Bi surfaces. These results are similar to the results of Chapter 2 attempting to eliminate Sn whiskers during one year ambient storage by the small addition of lead in Sn [11]. The present results confirms that the addition of a trace amount of Bi, 0.5 wt.% in a 5 μm plated film, is sufficient to mitigate Sn whiskers as well for up to one year of ambient temperature storage.

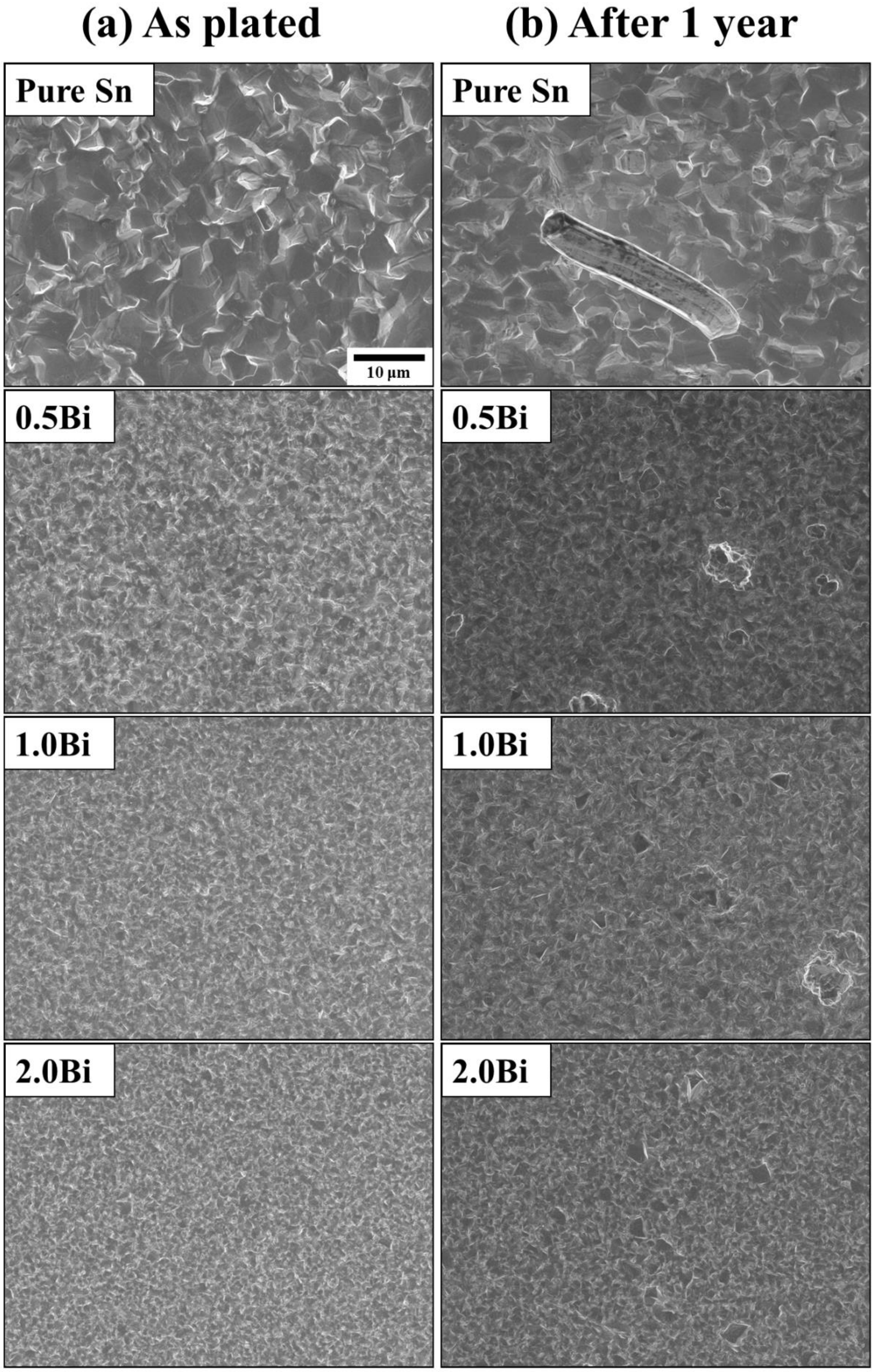

Fig. 2 Surface evolutions of matte Sn and Sn-*x*Bi: (a) as plated, (b) after one year ambient storage.

Fig. 3 shows the HTH test results exhibiting the similar tendencies to those in the ambient storage results. The dotted red circle in Fig. 3 (a) indicates a Sn whisker grown on the pure Sn surface during the 1000 h of HTH storage. Such whiskers can be developed on pure Sn under high humidity conditions [15-17]. Oxidation and corrosion of the metal induces a volume expansion into Sn plating layer during high humidity storage, and whiskers grow to relieve the accumulated compressive stresses from the volume expansion [16]. In our case of Bi addition, almost no morphological change is observed on any Sn-*x*Bi surfaces, as shown in Fig.3 (b)-(d). Thus only 0.5 wt.% Bi addition can effectively prevent Sn whiskers under high temperature and humidity storage, as well.

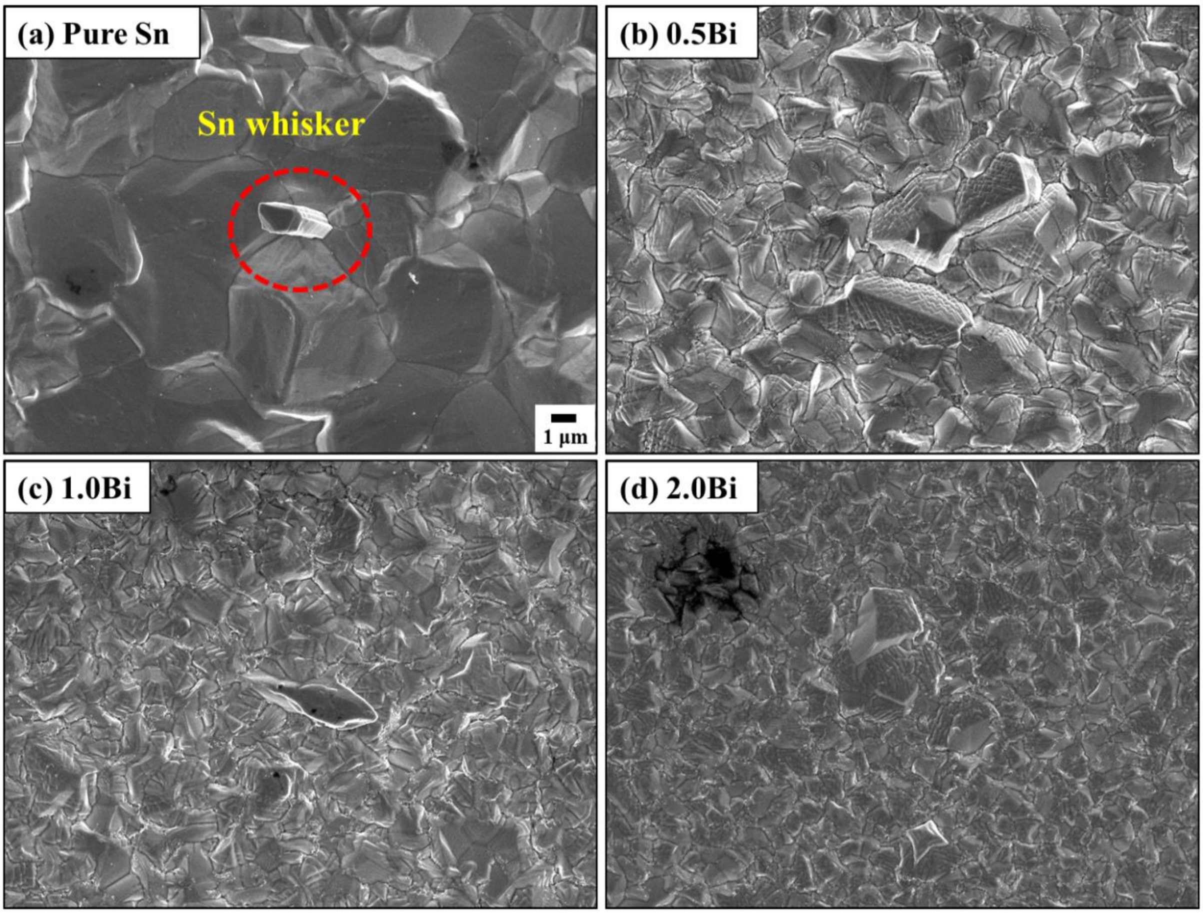

Fig. 3 The morphologies after 1000 h of high humidity / temperature storage: (a) pure Sn, (b) Sn-0.5Bi, (c) Sn-1Bi, and (d) Sn-2Bi.

Ball indentation tests have been performed to investigate whisker growth driven by external mechanical stress. Fig. 4 illustrates the surface evolutions of pure Sn and Sn-*x*Bi plating after 72 h of the mechanical loading. The indentation impression is shown in the lower magnitude microscope image of Fig.4 (a-1). After 24 h of loading, Sn whiskers are induced on pure Sn surfaces, while no whiskers are formed near the impression edge on the Sn-*x*Bi surfaces regardless of the Bi content. A long Sn whisker grew to about 35 μm in length near the indented area after 72 h of loading on a pure Sn surface, as shown in Fig.4 (a). In addition, the lengths of Sn whiskers on pure Sn surfaces are considerably shorter further away from the indentation as shown by the dotted red circles in Fig.4 (a). On the Sn-0.5Bi and Sn-1Bi surfaces in Fig. 4(b)-(c), however, a number of short extrusions like nodules or hillocks grow in the vicinity of indentation perimeter, although their lengths are less than 5 μm after the 72 h of loading. On the Sn-2Bi surface, no whiskers can be found near the indentation except small hillocks (see Fig.4 (d)). These results indicate that Bi addition, particularly 2 wt.% of Bi, is again efficient for whisker mitigation even under directly applied external mechanical stress.

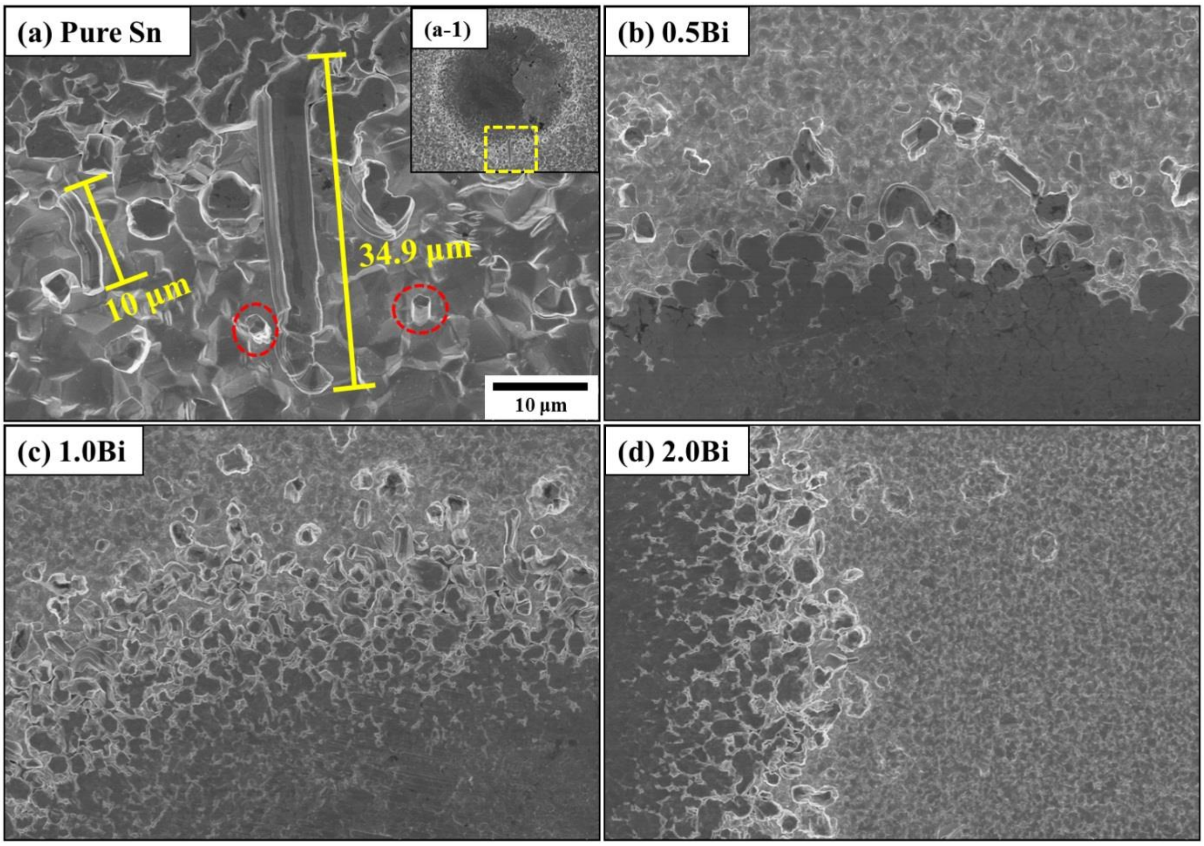

Fig. 4 The morphologies after 72 h loading test: (a) pure Sn, (b) Sn-0.5Bi, (c) Sn-1Bi, and (d) Sn-2Bi.

Thermal cycling tests were performed up to 100 cycles with pure Sn and Sn-*x*Bi plated films on 42 alloy substrates. The CTE mismatch between the plated layer and the substrate induces compressive and tensile stresses in the plating layer repeatedly during thermal cycling. Fig. 5 (a) presents a typical thermal-cycling whisker developed on a pure Sn surface often accompanied with large grooves around the whisker root marked by the yellow dotted arrows in the figure. As the red arrows in Fig. 5 indicate, there happens many grain boundary (GB) cracking, particularly on the pure Sn surface. These GB cracking and grooves are due to surface oxidation [18], but the density obviously decreases with increasing Bi content. Although hillocks can grow on these Sn-*x*Bi surfaces, no whiskers can be observed after the 100 thermal cycles. The maximum length/height of these hillocks or nodule features does not exceed 5 μm, while the length of the whiskers on pure Sn surface may reaches 30 μm (see Fig. 5a). The whisker mitigation effect by Bi addition is thus obvious in case of the severe thermal stress cycling.

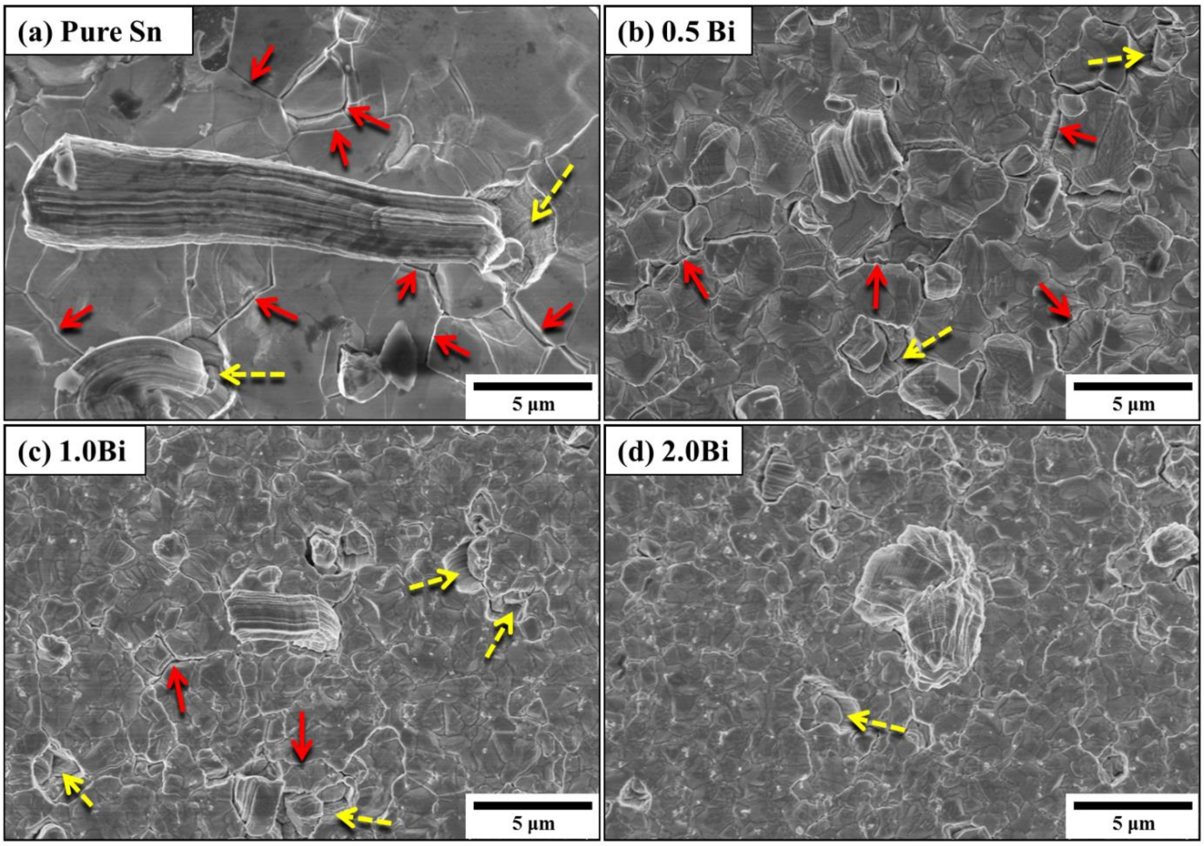

Fig. 5 The morphologies after 100 thermal cycles: (a) pure Sn, (b) Sn-0.5Bi, (c) Sn-1Bi, and (d) Sn-2Bi.

In summary, present work can conclude that small amount of Bi addition can mitigate Sn whisker growth in the four different environment tests. As little as 0.5 wt.% Bi addition exhibits obvious mitigation effect, and 2.0 wt.% addition appears to be sufficient to avoid the whiskers on the electroplating surface under ambient storage, at high humidity/temperature, subjected to mechanical loading, or exposed to thermal stress cycling.

4.3.2 Microstructure of Sn-*x*Bi films under ambient storage and different IMC growths

The grain textures of as-plated matte Sn and Sn-*x*Bi films have been investigated by FIB as shown in Fig.6. The average grain size decreases with increasing Bi content (see from (a) to (d) in Fig. 6). Surely the average grain size in Sn-2Bi plating is about the half of that in pure Sn. Hence, the small amount of Bi addition, even 0.5 wt. % of Bi in Sn refines the grain texture of electroplating.

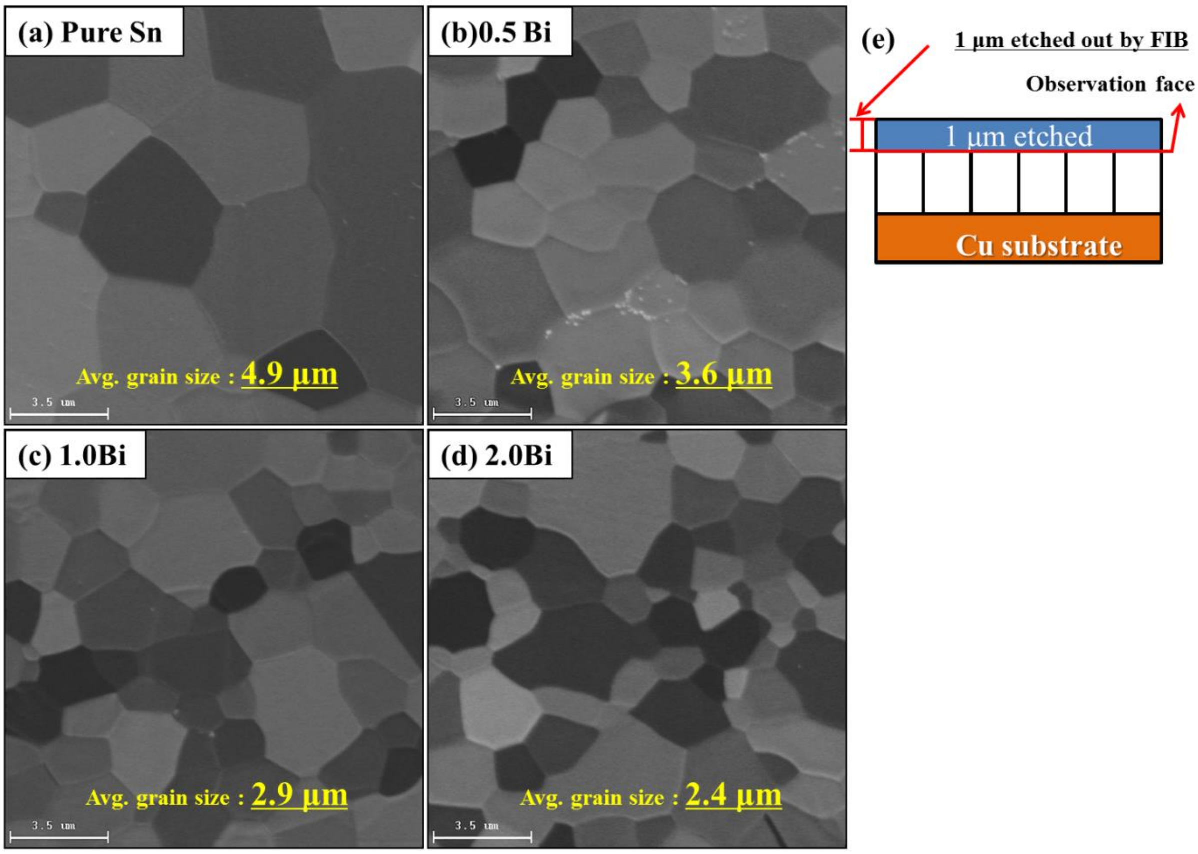

Fig. 6 Grain size observations of as-plated films using FIB microscopy: (a) pure Sn, (b) Sn-0.5Bi, (c) Sn-1Bi and (d) Sn-2Bi, and (e) schematic diagram of FIB etching.

Fig.7 compares the FIB cross section observations of Sn and Sn-*x*Bi: (a) as-plated, and (b) after one year of ambient storage. The columnar grain structure in pure Sn is altered to equiaxied grains because of the Bi addition of the content. These equiaxed grain structures effectively relieve the compressive stresses, and hence mitigate Sn whisker formation [5]. After the one year ambient temperature storage, Sn grains in the examined plating samples have bulked up as shown in Fig.7 (b). The columnar structure in pure Sn plating remains the same until after the one year storage, while the equiaxed grains in Sn-*x*Bi plating appears to be altered to columnar structure, probably because of the grain boundary movement caused by the observed grain expansion.

The IMC at the interface between Sn film and Cu substrate continuously grow in the samples during the one year ambient temperature storage, as confirmed by Fig.7 (b). However, the growth patterns are different in pure Sn and in Sn-*x*Bi. In the case of pure Sn, IMC mainly grows along Sn grain boundaries. Particularly large IMC growth can be observed at the boundaries around the root grain of whisker in pure Sn. Such a large IMC induces an compressive stress on the root grain, and drives the whisker growth to release the stress. In contrast, the volumes of the grown IMC under the Sn-*x*Bi films after one year are smaller than those in pure Sn samples, both at Sn/Cu interfaces and at Sn grain boundaries. Moreover, the IMC in the Sn-*x*Bi samples grows uniformly over the entire interface area during the storage tests. The cross sectional observations in Fig.7 indicate that room temperature whiskers, which can be found only on pure Sn surfaces, is driven by the concentrated IMC growth along the grain boundaries. The doping of Bi resulted in the refined and equiaxed grain structure due to partial and frequent crystal nucleation during electroplating. The refined grains provided additional diffusion paths at the interfaces between Sn and Cu substrates [19], and avoiding IMC growth concentrated on the grain boundaries.

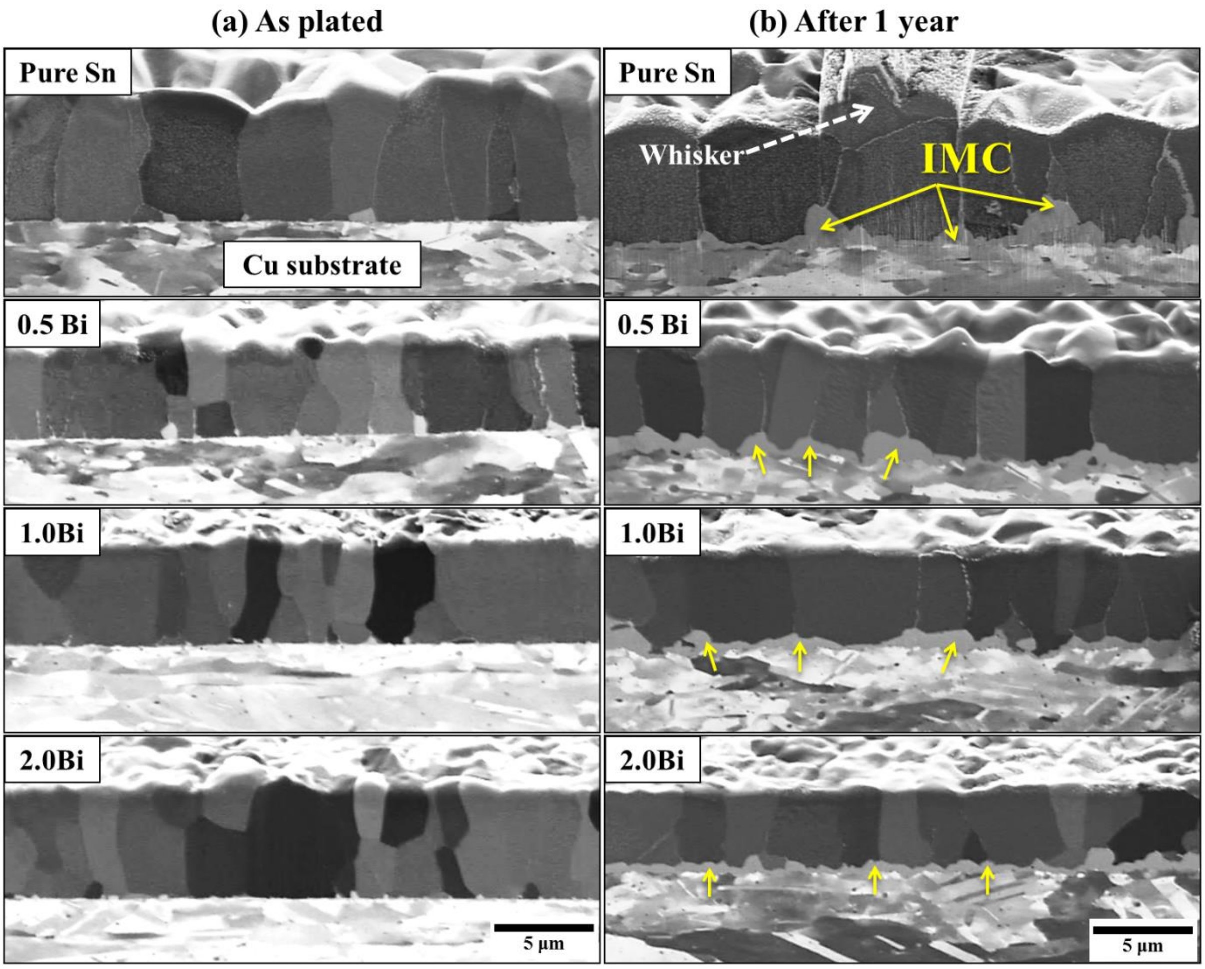

Fig. 7 Cross sectional views of pure Sn and Sn-*x*Bi plating: (a) as plated, and (b) after one year ambient storage.

Hillocks observed on all the Sn-*x*Bi plating surfaces are considered to relieve the accumulated compressive stresses during the storage. Such a hillock growth mainly occurs from grain boundary migration as reported in the literature [5, 11]. Fig. 8 shows a typical hillock on a Sn-0.5Bi: (a) surface top view, (b) cross-sectional, and (c) a magnified image of the cross-section. The considerably uniform IMC growth under the hillock helps the Sn grain boundary migration and allows the grain growth to form the hillock. The hillock growth effectively releases the compressive stresses without growing whiskers during the ambient storage. The small addition of Bi in our study eliminates any whisker formation during one year of ambient storage, by changing the IMC growth pattern from concentrated at grain boundaries to uniform distribution at the plating/substrate interface.

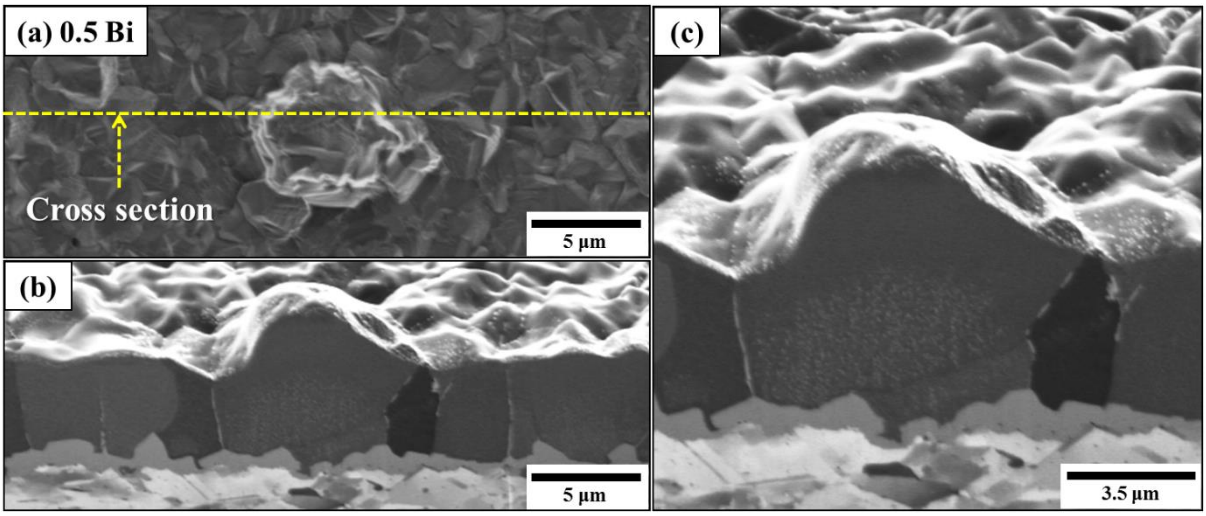

Fig. 8 A hillock found in Sn–0.5Bi plating after one year ambient storage: (a) top view of the hillock, (b) cross section observation, and (c) magnification image of the grain microstructure.

4.3.3 The whisker mitigation mechanism by least Bi addition

Sn whisker growth, in general, is caused by relieving accumulated stresses in the film. In our study, four different types of loading have been investigated to create stress inside of the electroplating films. During room temperature storage, compressive internal stress is generated by grain expansion and by IMC growth. The external loading added by directional indentation and CTE mismatch during thermal cycling resulted in accumulate compressive stress in and on the Sn layer. The compressive stress is effectively relieved by a small amount of Bi addition altering the columnar Sn grains to equiaxed structure. The IMC growth pattern is also changed to a uniform distribution at the interfaces between substrate and plated Sn layer. These effects of Bi doping are similar to those caused by Pb addition on IMC growth [11]. When Sn is alloyed with Pb, segregated Pb at Sn grain boundaries blocked the grain boundary IMC growth, while segregated Bi was not observed in the present study. The whisker mitigation mechanism by Bi doping is thus mainly related to the altered grain structure, i.e. columnar to equiaxed due to the grain refinement. The refined and equiaxed grain structure is superior to relieve compressive stress in any of our four environment test cases. Particularly on thermal cycling, the refined grain structure suppressed surface oxidation cracking along the grain boundaries, which is relevant to reduce whisker density [20]. It is remarkable that the obvious whisker mitigation effect starts from 0.5 wt. % of Bi addition even in the thin plating films of 5 μm thickness.

4.4 Conclusions

Sn whisker mitigation process by Bi addition has been investigated by comparing pure matte Sn and Sn–*x*Bi electroplating films with 5 μm thicknesses on either Cu or 42 alloy substrates using four different environmental tests. Tin whiskers are observed only on pure Sn surface, and no whisker (but some extrusions/hillocks) on the alloyed films during the one year of ambient temperature storage, HTH, loading and thermal cycling tests. In these tests, whisker growth is efficiently suppressed by Bi additions as low as 0.5 wt. %, which are shown to refine the grain size, and to alter the grain structure from columnar to equiaxed. The small amounts of Bi mitigate tin whisker growth by suppressing IMC growth at the Sn grain boundaries, allowing grain boundary migration, and resulting in hillock growth which can release the compressive stress during the ambient storage. These results nevertheless agree with the previous report on the higher Bi addition of 2.5 wt. % with thermal cycling [12]. The present achievements further conclude that the minimum requirement of Bi addition necessary for whisker mitigation can be less than or equal to 0.5 wt. %. The mechanisms of the whisker mitigation found in Sn-*x*Bi electroplating would guide further investigations of metal whisker suppression, in addition to realizing whisker-free Sn plating required for lead-free electronic devices.

Reference

1. K. J. Puttlitz, G. T. Galyon, "Impact of the ROHS Directive on high-performance electronic systems", J. Mater. Sci. Mater. Electron., 18, pp.347-365 (2007)

2. H. P. Howard, J. Cheng, P. T. Vianco, J. C. M. Li, "Interface flow mechanism for tin whisker growth", Acta Mater 59(10), pp.1957-1963 (2011)

3. K.G. Comptom, A. Mendizza, S.M. Arnold, "Filametary growths on metal surfaces – Whiskers", Corrosion 7(10), pp.327-334 (1951)

4. H.L. Cobb, "Cadmium whiskers", Monthly Rev. Amer. Electroplaters. Soc. 33(28), 28-30 (1946)

5. W. J. Boettinger, C. E. Johnson, L.A. Bendersky, K.-W. Moon, M. E. Williams, and G. R. Stafford, "Whisker and hillock formation on Sn, Sn-Cu and Sn-Pb electrodeposits", Acta. Mater., 53, pp.5033-5050 (2005)

6. K. N. Tu, J. C. M. Li, "Spontaneous whisker growth on lead-free solder finishes", Materials Science and Engineering: A 409(1-2), pp.131-139 (2005)

7. J.W. Osenbach, R.L. Shook, B.T. Vaccaro, B.D. Potteiger, A.N. Amin, K.N. Hooghan, P.Suratkar, and P. Ruengsinsub, "Sn whiskers: material, design, processing, and post-plate reflow effects and development of an overall phenomenological theory", IEEE Trans Electron Pack Manuf 28, 36 (2005)

8. M-H. Lu, K-C. Hsieh, "Sn-Cu Intermetallic Grain Morphology Related to Sn Layer Thickness", J. Electron. Mater., 36(11), pp.1448-1454 (2007)

9. E. Chason, N. Jadhav, F. Pei, "Effect of layer properties on stress evolution, intermetallic

volume, and density during tin whisker formation", JOM 63(10), pp.62–68 (2011)

10. J. Cheng, F. Yang, P. T. Vianco, B. Zhang, J. C. M. Li, "Optimum Thickness of Sn Film for Whisker Growth", J. Electron. Mater., 40(10), pp.2069-2075 (2011)

11. J-L. Jo, K-S. Kim, T. Sugahara, S. Nagao, K. Hamasaki, M. Tsujimoto, K. Suganuma, "Least lead addition to mitigate tin whisker for ambient storage", J. Mater. Sci. Mater. Electron. (2013) doi: 10.1007/s10854-013-1218-y

12. N. Jadhav, M. Williams, F. Pei, G. Stafford, E. Chason, "Altering the Mechanical Properties of Sn Films by Alloying with Bi: Mimicking the Effect of Pb to Suppress Whiskers", J. Electron. Mater. 42(2), 312-318 (2013)

13. J. Huaa, Y. Zhang, C. Wub, "Grain refinement of Sn–Pb alloy under a novel combined pulsed magnetic field during solidification", J. Mater. Process. Technol. 211(3), pp.463-466 (2011)

14. H.S. Betrabet, S.M. McGee, J.K. McKinlay, "Processing dispersion-strengthened Sn-Pb solders to achieve microstructural refinement and stability", Scripta Mater. 25, pp.2323-2328 (1991)

15. B. Horváth, B. Illés, T. Shinohara, G. Harsányi, "Effects of humidity on tin whisker growth — Investigated on Ni and Ag underplated layer construction", Thin Solid Films 520, pp.384-390 (2011)

16. P. Oberndorff, M. Dittes, P. Crema, P. Su, E. Yu, "Humidity Effects on Sn Whisker Formation", IEEE Trans. Electron. Packaging Manuf., 29(4), pp.239-245 (2006)

17. C-F. Li, Z-Q. Liu, J-K. Shang, "The effects of temperature and humidity on the growth of tin whisker and hillock from Sn5Nd alloy", J. Alloys Compd. 550, pp.231-238 (2013)

18. K. Suganuma, A. Baated, K-S. Kim, K. Hamasaki, N. Nemoto, T. Nakagawa, T. Yamada, "Sn whisker growth during thermal cycling", Acta Mater 59, pp.7255-7267 (2011)

19. E. Sandnes, M.E. Williams, M.D. Vaudin, G.R. Stafford, "Equi-Axed Grain Formation in Electrodeposited Sn-Bi", JEM 37(4), pp.490-497 (2008)

20. J-L. Jo, S. Nagao, T. Sugahara, M. Tsujimoto, K. Suganuma, "Thermal stress driven Sn whisker growth: in air and in vacuum", J. Mater. Sci. Mater. Electron. (2013) doi: 10.1007/s10854-013-1336-6

Chapter4

Mitigation of Sn whisker growth by small Bi additions

Chapter 5

Conclusions

5.1 conclusions

In this thesis, the Sn whisker growth mechanism and mitigation has been established for lead free electronic applications. To clarify the mechanism of Sn whisker growth, pure Sn and Sn-Pb addition have been compared with IMC growth under ambient storage. The whisker growths from different plating thickness and the atmosphere have been investigated for understanding of the driving force inducing whisker growth during thermal cycling. On the basis of the whisker growth mechanism, this thesis suggests the whisker mitigation by Bi doping in the Sn under various environments.

In chapter one, the history and the previous research of Sn whisker growth have been reviewed, and also, the efforts to eliminate the Sn whisker growth have been introduced by various method.

In chapter two, tin whisker mitigation process by lead addition has been investigated by comparing with pure matte Sn and Sn-*x*Pb electro plating with 5 μm thickness on Cu substrate. Tin whiskers have been observed only on pure Sn surface, and no whisker but hillocks on the lead added plating during the one year of room temperature storage test. Only 1 wt. % of Pb addition effectively eliminates Sn whisker growth to change without altering the columnar to equiaxed grain structure. The effective suppression of IMC growth at the grain boundaries results to mitigate Sn whisker growth cause, the segregated Pb grains on the grain boundaries interrupt IMC growth on grain boundary. Less obvious pinning of grain boundary migrations results in hillock growth that enough to release the compressive stress in the plating. These results also, indicate the required amount of lead for whisker mitigation can be less or equal to 1 wt. %. The revealed mechanism of whisker mitigation by the least amount of lead addition would indicate the required properties of metal additives that can suppress whiskers like lead. Considering the low solubility of Pb in Sn, chapter two suggest that Bi can be a replacement candidate of lead for tin whisker mitigation.

In chapter three, Thermal stress driven whisker growth has been investigated on 2 μm and 5 μm matte Sn electroplating. In the tests, longer and thinner whiskers were generated on the thinner platings, however, showing less density than the thicker plating during thermal cycling. The whisker growth is deeply correlated to the grain size distributions in the plating, as well as the thickness. The atmospheric conditions during thermal cycling are critical, and determine the whisker shape – straight or bended – through grain boundary cracking induced by surface oxidation of Sn. The thermal whiskers in vacuum are hence longer and thinner than those in air. The average whisker width is related to the whisker density through the grain-size distribution in the as deposited plating. Overall, the thermal stress whiskers are dominated by the original grain structure in the electroplating, and the surface oxidation affects the variation of whisker growth types. These findings here would contribute to the whisker risk management in electronic packaging for critical applications like satellite and automobile, as well as toward the fundamental understanding of the growth mechanisms of Sn whiskers along with the results of chapter two.

In chapter four, Sn whisker mitigation process by Bi addition has been established by comparing pure matte Sn and Sn–*x*Bi electroplating films with 5 μm thicknesses on either Cu or 42 alloy substrates using four different environmental tests. Tin whiskers are observed only on pure Sn surface, and no whisker (but some extrusions/hillocks) on the alloyed films during the one year of ambient temperature storage, HTH, loading and thermal cycling tests. In these tests, whisker growth is efficiently suppressed by Bi additions as low as 0.5 wt. %, which are shown to refine the grain size, and to alter the grain structure from columnar to equiaxed. The Bi doping completely mitigate tin whisker growth by suppressing IMC growth at the Sn grain boundaries, allowing grain boundary migration, and resulting in hillock growth which can release the compressive stress under one year of ambient storage. These achievements nevertheless agree with the previous report on the higher Bi addition of 2.5 wt. % with thermal cycling in the literature. In the remark, this thesis further conclude that the minimum requirement of Bi addition necessary for whisker mitigation can be less than or equal to 0.5 wt. %. Moreover, just 0.5 wt. % of Bi addition perfectly suppressed Sn whisker growth in four different severe environments.

Finally, the investigated whisker growth mechanisms in this thesis are expected to support a further fundamental research of metal whisker growth. In particular, the mechanisms of the whisker mitigation found in Sn-*x*Bi electroplating would guide further investigations of metal whisker suppression, in addition to realizing whisker-free Sn plating required for lead-free electronic devices.

A. List of published papers

1. **Jung-Lae Jo**, Shijo Nagao, Tohru Sugahara, Masanobu Tsujimoto, Katsuaki Suganuma; "Thermal stress driven Sn whisker growth: in air and in vacuum", **Journal of Materials Science: Materials in Electronics** (2013), DOI : 10.1007/s10854-013-1336-6

2. **Jung-Lae Jo**, Keun-Soo Kim, Tohru Sugahara, Shijo Nagao, Kyoko Hamasaki, Masanobu Tsujimoto, Katsuaki Suganuma; "Least lead addition to mitigate tin whisker for ambient storage", **Journal of Materials Science: Materials in Electronics,** (2013), DOI 10.1007/s10854-013-1218-y

3. **Jung-Lae Jo**, Shijo Nagao, Kyoko Hamasaki, Masanobu Tsujimoto, Tohru Sugahara, Katsuaki Suganuma; "Sn whisker relaxation by a small amount of Bi addition", Accepted on **Journal of Electronic Materials** (2013)

4. **Jung-Lae Jo**, Jong-Bum Lee, Jong-Min Kim, Young-Eui Shin, and Seung-Boo Jung*; "Reliability of Fine-pitch Flip-chip (COG) Bonding with Non-conductive Film Using Ultrasonic Energy"; **The Journal of Adhesion**, Vol. 86, Issue 5, 470

5. **Jung-Lae Jo**, Ja-Myeong Koo, Jong-Bum Lee, Jong-Gun Lee and Seung-Boo Jung*; "Effect of Atmospheric-Pressure Plasma Treatment on the Joint Strength between Au Flip Chip Bumps and Cu-Finished Si Wafer Substrates Bonded Using Ultrasonic Energy"; **Journal of the Korean Physical Society**, Vol. 54, No. 3, March 2009, pp. 1334_1338

6. **Jung-Lae Jo**, Jong-Bum Lee, Jong-Gun Lee, Sung-Ho Jeon, Jong-Min Kim, Young-Eui Shin, Jeong-Hoon Moon, Choong-Don Yoo, and Seung-Boo Jung*; "Effect of Surface Treatment on the Mechanical Strength of Ultrasonically Bonded Chip on Copper-Coated

Glass for Ultra-Fine Pitch Application in Microelectronics”; **Japanese Journal of Applied Physics** 48 (2009) 07GA07

7. Masanobu Tsujimoto, **Jung-Lae Jo**, Kyoko Hamasaki and Katsuaki Suganuma; “Effect of tin grain structure for tin whisker formation”, IEICE Transactions, (2011)

8. Ja-Myeong KOO, **Jung-Lae JO**, Jong-Bum LEE, Yu-Na KIM, Jong-Woong KIM, Bo-In NOH, Jeong-Hoon MOON, Dae-Up KIM, and Seung-Boo JUNG*; “Effect of atmospheric Pressure Plasma Treatment on Transverse Ultrasonic Bonding of Gold Flip-Chip Bump on Glass Substrate”; **Japanese Journal of Applied Physics** Vol. 47, No. 5, 2008, pp. 4309–4313

9. Bo-In Noh, **Jung-Lae Jo** and Seung-Boo Jung*; “Effect of Atmospheric-Pressure Plasma Treatment on the Adhesion Characteristics of a Flexible Copper Clad Laminate”; **Journal of the Korean Physical Society**, Vol. 54, No. 3, March 2009, pp. 1217_1222

10. Bo-In NOH, Ja-Myeong KOO, **Jung-Lae JO**, and Seung-Boo JUNG*; “Application of Underfill for Flip-Chip Package Using Ultrasonic Bonding”; **Japanese Journal of Applied Physics** Vol. 47, No. 5, 2008, pp. 4257–4261

11. Jong-Bum Lee, Jong-Gun Lee**, Jung-Lae Jo**, Ja-Myeong Koo, Chang-Keun Chun, and Seung-Boo Jung*; “Effect of Time and Pressure on Ultrasonic Bonding Strength of Flexible Printed Circuit Board to Glass with Nonconductive Film”; **Japanese Journal of Applied Physics** 48 (2009) 07GA08

B. Proceedings and International conference attended & presented

1. **"Effect of Sn whisker mitigation by addition of a small amount of Bi", Jung-Lae Jo**, Kyoko Hamasaki, Tohru Sugahara, Masanobu Tsujimoto and Katsuaki Suganuma, TMS, 142nd Annual meeting & Exhibition, Mar. 3-7, San Antonio, Texas, USA (2013)
2. **"Film thickness effect on tin whisker growth by thermal cycling"**, **Jung-Lae Jo**, Tohru Sugahara, Shijo Nagao and Katsuaki Suganuma, 16th Sanken International Symposium, Jan. 22-23, Osaka, Japan (2013)
3. **"Thermal Cycling Whiskers and Influence of Atmosphere"**, **Jung-Lae Jo**, Toru Sugahara, Shijo Nagao, Kyoko Hamasaki and Katsuaki Suganuma, 6th International Symposium on Tin Whiskers, Nov. 27-28, Leicestershire, UK (2012)
4. **"Influence of tin coating thickness on whisker growth during thermal cycling", Jung-Lae Jo**, Tohru Sugahara, Masanobu Tsujimoto and Katsuaki Suganuma, ESTC2012, Sep. 17-20, Amsterdam RAI, Netherland (2012)
5. **"SiC die‐attachment with minor elements addition pure Zn under formic acid reflow"**, S.W. Park, **J.L. Jo**, T. Sugahara, M. Ueshima, H. Iwamoto,and K. Suganuma, ESTC2012, Sep. 17-20, Amsterdam RAI, Netherland (2012)
6. **"Behaviors of Sn surface with whisker generation after thermal cycle"**, **Jung-Lae Jo**, Kiju Lee, Katsuaki Suganuma, ECO-MATES 2011, Nov. 28-30, Osaka, Japan (2011)
7. **"Growth mechanism of Sn whiskers in a vacuum and air with thermal cycling"**, **Jung-Lae Jo**, Keun-Soo Kim, Katsuaki Suganuma, MS&T'11Oct. 16-20, Columbus, Ohio, USA (2011)
8. **"Effect of thermal cycling on Sn whiskers growth"**, **Jung-Lae Jo**, and Katsuaki Suganuma, IUMRS-ICA, Sep. 19-22, Nangang, Taipei, Taiwan (2011)

9. Attended and presented the **MAM 2008** in Dressden, Germany during 2-5 March 2008 with “Mechanical and electrical properties of flip chip bump with Sn encapsulation after multiple reflows” (Poster)
10. Attended and presented **INTERFINISH 2008** in Pusan, Korea republic during 16-19 June 2008 with “Effect of Atmospheric pressure plasma treatment on Au Flip-chip bumps bonded with Cu Circuit on Glass using Ultrasonic Energy” (Oral)
11. Attended and presented **USE 2008** in Sendai, Japan during 11-13 November 2008 with “Effect of atmospheric plasma treatment on ultrasonic bump-less flip chip bonding” (Poster)
12. Attended and presented **ACE-X 2009** in Rome, Italy 22-23 June 2009 with “Reliability of Fine‐pitch flip‐Chip Bonding with Non‐conductive Film Using Ultrasonic Energy” (Oral)

C. Proceedings and Domestic conference attended & presented

1. **“Pb微量添加による室温Snウィスカ発生の抑制と組織的特徴”**、趙 亭來, 濱崎 恭子, 辻本 雅宣、菅沼克昭、日本金属学会 秋期大会、2011年11月7日、那覇、沖縄

2. K.S. Kim, K.J. Lee, S.S. Kim, **J.L. Jo**, K. Suganuma, H. Tanaka; “Microstructural Changes of Ag-Epoxy Conductive Adhesive Joints under High Humidity Environment”, MES2010(第20 回マイクロエレクトロニクスシンポジウム), 2010

Acknowledgments

Firstly, I am grateful to god for all this glory. I would like to thank Prof. Katsuaki Suganuma at the Institute of Science and Industrial Research (ISIR) in Osaka Univ. for his efficient and selfless help for my doctor's course. His wide and deep knowledge of material science can lead me to a wonderful experience and research. It is my great honor to study with Prof. Suganuma. I also, thank to Prof. Minamino, Prof. Nogi for their guidance my dissertation. I would like thank to Prof. Shijo Nagao patronized and also supported my publication activities. I deeply thank to Prof. Seung-Boo Jung at Sungkyunkwan University in Korea. It is possible to study at Osaka University for his recommend and warm instruction. In succession, I am grateful to Prof. Keun-Soo Kim in Hoseo University and those who help to me during my doctoral course. I would like thank to Masanobu Tsujimoto; Senior researcher of Uyemura, Japan. The electro plated sample has been supported by him.

I would like to mention and thank to my colleagues Dr. Sung-Jun Kim, Dr. Change Kim, Dr. Takehiro Tokuno, Dr. Sakamoto Soichi, Dr. Natsuki Komoda, Dr. Sung-Won Park, Dr. Ki-Joo Lee and Yung-Seok Kim, Mr. Araki Teppei, Chulmin Oh, Se-Min Park, Inui Tetsuzi, Uwataki Ryouji, Tonomura Eijii, Matsuo and Go Tenkyoku and research assistant Hamasaki.

I warmly special thanks to my all relatives for their kind encouragement, especially to my grandmother for her endless pray. Finally, I would like to thank my Father and Mother for supporting, waiting and praying the path for my scientific ambitions for long years.

Lastly, I am deeply grateful to my wife Ji-Young Ahn for her endless devotion and praying, last but not least, the same thank to my daughter Soo-Bin Jo.

감사의 글

먼저 이 모든 영광을 하나님께 드립니다.

박사과정 동안 지도해주신 수가누마 교수님께 깊은 감사를 드립니다. 교수님의 폭 넓은 지식과 격려는 학위과정 중 큰 힘이 되었으며, 학문적인 것 이외에도 생활적으로 인간적으로 많은 도움을 주셔서 다시한번 깊은 감사를 드립니다. 또한, 오사카 대학교에서 공부 할 수 있도록 도와주신 지도교수님인 성균관대학교 정승부 교수님께 깊은 감사를 드립니다. 정교수님의 가르침으로 다양한 분야를 접할 수 있었으며, 박사과정중에도 늘 많은 도움을 주셨습니다. 함께 논문투고를 위해 지도해주신, 나가오 교수님께 감사드립니다. 논문심사를 맡아주신 미나미노, 노기 선생님께도 깊은 감사의 말씀을 드립니다. 일본 항공 우주 연구센터 (JAXA)와의 공동연구를 통해 큰 경험을 하게 되었으며, 함게 연구를 진행했던 네모토, 나카가와 연구원님께도 감사의 말씀을 전합니다. 연구실의 다른 프로젝트를 함께 진행하며 고생한 스가하라 조교, 주식회사 우에무라의 쯔지모토님께도 깊은 감사를 드립니다. 짧은 기간이었지만, 열과 성의를 다해 지도해주신 호서대학교 김근수 교수님, 일본에 와서 아무것도 모르는 저를 물심양면으로 도와주신 삼성전자 김창재 박사님께 깊은 감사를 드립니다. 학위과정 중 함께 웃으며 동고동락 했던 한국, 일본, 중국, 몽고의 동료들인 삼성전자 이기주 박사, 오사카대학교 박성원 박사, 덴소 토쿠노 박사, 미쯔비시 사카모토 박사, 토팡홈즈 코모다 박사님께 감사를 드립니다. 연구실의 후배님들, 김영석, 오철민 형님, 박세민, 이누이, 우와타키, 마쯔오, 토노무라, 연구생 오군에게도 감사를 드립니다. 늘 조언을 아끼지 않았던 삼성전자 구자명박사님, 싱가폴의 이종범 박사님께도 깊은 감사의 말씀을 올립니다. 친구가 적은 저에게 늘 격려를 주었던 이지웅, 김의태, 이재훈 님께도 깊은 감사의 말씀을 드립니다. 이 밖에 좁은 지면에 감사한 분들의 존함을 다 언급하지 못한점 양해의 말씀을 드리며, 학위 과정 중 도와주신 모든 분들께 깊은 감사를 드립니다. 늘 기도해주신 모든 분들, 오금제일 교회 백용하, 김정화 목사님께 감사드리며, 저의 친 할머니이신 이분성 할머니께 감사의 말씀을 드립니다. 유년시절부터 지금까지 늘 함께해온 외가댁 모든 식두들께 깊은 감사를 드립니다. 특히, 6남매의 끈끈한 가족애가 있어 늘 웃을 수 있었기에 다시한번 깊은 감사를 드립니다. 또한, 늘 서울에서 기도해주신 장모님, 장인어른, 처제 처남에게도 감사의 말씀을 전합니다.

마지막으로, 못난 아들 믿음으로 끝까지 지켜봐 주시고, 기도해주신 사랑하는 아버지, 어머니께 감사 드립니다. 부모님의 기도와 믿음으로 오늘의 제가 있게 됨을 진심으로 감사 드립니다.

끝으로, 긴 시간 끊임없는 기도와 헌신으로 기다려준 아내 안지영에게 감사하며, 대학원 생활을할때 언제나 웃음을 준 딸 조수빈양에게도 감사를 표시하며, 이 기쁨을 함께 나누고 싶습니다.

2013년 7월 25일 조정래 드림.